

Technical Report Documentation Page

1. Report No. FHWA/TX-04/0-4098-4		2. Government Accession No.		3. Recipient's Catalog No.	
4. Title and Subtitle Evaluation of Alternative Materials to Control Drying- Shrinkage Cracking in Concrete Bridge Decks				5. Report Date October 2003	
				6. Performing Organization Code	
7. Author(s) Dr. Kevin Folliard, Cuyler Smith, Gregory Sellers, Michael Brown, Dr. John E. Breen				8. Performing Organization Report No. 0-4098-4	
9. Performing Organization Name and Address Center for Transportation Research The University of Texas at Austin 3208 Red River, Suite 200 Austin, TX 78705-2650				10. Work Unit No. (TRAIS)	
				11. Contract or Grant No. 0-4098	
12. Sponsoring Agency Name and Address Texas Department of Transportation Research and Technology Implementation Office P.O. Box 5080 Austin, TX 78763-5080				13. Type of Report and Period Covered Research Report 5/2001 - 8/2003	
				14. Sponsoring Agency Code	
15. Supplementary Notes Project conducted in cooperation with the U.S. Department of Transportation, Federal Highway Administration, and the Texas Department of Transportation.					
16. Abstract In the United States, restrained shrinkage cracking of concrete bridge decks is a significant durability problem. The issues affecting restrained shrinkage cracking arise from design and construction practices, as well as material properties. The mechanisms of drying, autogenous, and carbonation shrinkage are presented and discussed along with related creep issues. Thermal stresses also play a role in bridge deck cracking. These stresses result from the heat of hydration, diurnal temperature changes, and solar radiation. Current and proposed test methods are introduced and evaluated as they relate to evaluating a material's resistance to restrained drying shrinkage cracking. Both conventional and innovative methods of controlling drying shrinkage are presented. Some innovative materials are discussed, including: fibers, shrinkage-compensating concrete, shrinkage-reducing admixtures, and extensible concrete. The use of innovative materials combined with improved design and construction practices can eliminate restrained shrinkage cracking. Large-scale bridge decks are constructed that permit evaluation of drying shrinkage cracking in a more realistic exposure setup. It is determined that several innovative mixtures including extensible concrete perform well at resisting drying shrinkage cracking. The need for an implementation study is discussed as well.					
17. Key Words Drying Shrinkage, Concrete, Cracking, Bridge deck			18. Distribution Statement No restrictions. This document is available to the public through the National Technical Information Service, Springfield, Virginia 22161.		
19. Security Classif. (of report) Unclassified		20. Security Classif. (of this page) Unclassified		21. No. of pages 170	
				22. Price	

Evaluation of Alternative Materials to Control Drying-Shrinkage Cracking in Concrete Bridge Decks

Dr. Kevin Folliard
Cuyler Smith
Gregory Sellers
Michael Brown
Dr. John E. Breen

CTR Research Report: 0-4098-4
Report Date: October 2003
Research Project: 0-4098
Research Project Title: *Evaluation of Alternative Materials to Control Drying-Shrinkage Cracking in Concrete Bridge Decks*

Center for Transportation Research
The University of Texas at Austin
3208 Red River
Austin, TX 78705

www.utexas.edu/research/ctr

Copyright © 2004
Center for Transportation Research
The University of Texas at Austin

All rights reserved
Printed in the United States of America

Disclaimers

Authors' Disclaimer: The contents of this report reflect the views of the authors, who are responsible for the facts and the accuracy of the data presented herein. The contents do not necessarily reflect the official view or policies of the Federal Highway Administration or the Texas Department of Transportation. This report does not constitute a standard, specification, or regulation.

Patent Disclaimer: There was no invention or discovery conceived or first actually reduced to practice in the course of or under this contract, including any art, method, process, machine manufacture, design or composition of matter, or any new useful improvement thereof, or any variety of plant, which is or may be patentable under the patent laws of the United States of America or any foreign country.

Engineering Disclaimer

NOT INTENDED FOR CONSTRUCTION, BIDDING, OR PERMIT PURPOSES.

Project Engineer: Dr. Kevin J. Folliard
P. E. Designation: Research Supervisor

Acknowledgments

The authors wish to express sincere appreciation the TxDOT Project Director, members of the Project Monitoring Committee and their locations, and any others instrumental to the project. In addition, the authors would like to thank the laboratory staff at Building 18B for providing a helping hand as well as keeping the project on budget and on time.

Table of Contents

1. Introduction	1
1.1 Background.....	1
1.2 Scope of Project.....	1
1.3 Objectives of Project	2
1.4 Report Layout.....	3
2. State of the Art Review	5
2.1 Introduction	5
2.2 Restrained Shrinkage Cracking.....	7
2.2.1 Types of Shrinkage	7
2.2.2 Combined Effects of Creep and Drying Shrinkage	9
2.2.3 Thermal Stresses	9
2.3 Test Methods and Specifications.....	11
2.3.1 Fresh Concrete Tests.....	12
2.3.2 Hardened Concrete Tests	12
2.3.3 Modulus of Elasticity and Creep.....	13
2.3.4 Free and Restrained Shrinkage	15
2.3.5 Restrained Expansion of Shrinkage-Compensating Cement	17
2.3.6 Chloride Permeability	17
2.3.7 Additional Restrained Shrinkage Tests.....	18
2.3.8 Fracture Energy.....	19
2.3.9 Summary of Tests Methods	19
2.4 Bridge Deck Cracking.....	20
2.4.1 Stresses in Transverse Deck Cracking.....	20
2.4.2 Concrete Properties and Mix Proportions.....	24
2.4.3 Concrete Placement.....	29
2.5 Methods of Controlling Shrinkage Cracking	31
2.5.1 Conventional Methods	32
2.5.2 Innovative Methods.....	36
2.6 Conclusions	39
3. Laboratory Evaluations	41
3.1.1 Introduction.....	41
3.1.2 Mechanism of Drying Shrinkage.....	41
3.1.3 Innovative Methods Examined in the Study	42
3.1.4 Laboratory Testing.....	44
3.1.5 Experimental Program	52
3.1.6 Mix Designs.....	56
3.2 Experimental Procedures.....	57

3.3	Results and Discussion	58
3.3.1	Summary of Experimental Results	87
3.4	Conclusions	89
4.	Field Evaluations of Selected Bridge Decks in Texas	91
4.1	Introduction	91
4.2	Inspection Procedure	91
4.3	Louetta Road Overpass Inspection	92
4.3.1	Description of Louetta Bridge	92
4.3.2	Inspection Results	93
4.4	Dow Barge Canal Bridge Inspection	95
4.4.1	Description of Dow Bridge	95
4.4.2	Inspection Results	95
4.5	Conclusions	97
5.	Large-Scale Bridge Decks	101
5.1	Introduction	101
5.2	Design and Modeling of LSBDD	101
5.3	Phase I	108
5.3.1	Design and Construction	108
5.3.2	Columns	109
5.3.3	Formwork	110
5.3.4	Precast Concrete Panels (PCP)	110
5.3.5	Sources of Restraint	110
5.3.6	Concrete Mixtures	114
5.4	Results and Discussion	114
5.4.1	Fresh Properties	115
5.4.2	Hardened Properties	115
5.4.3	Instrumentation	121
5.4.4	Cracking	122
5.4.5	Conclusions	124
5.5	Phase II	125
5.5.2	Mixture Designs	126
5.5.3	Construction	130
5.5.4	Results and Discussion	130
5.5.5	Instrumentation	142
5.5.6	Cracking	144
5.5.7	Conclusions	145
6.	Conclusions and Recommendations for Future Research	147
6.1	Conclusions	147
6.2	Improvements in the Laboratory Program	148
6.3	Improvements in the Large-Scale Bridge Decks	148

6.4 Recommendation for Implementation.....	149
References.....	151

List of Figures

Figure 1.1 Various steps, in order of completion, used to investigate the use of innovative materials to control restrained shrinkage cracking in concrete bridge decks.	3
Figure 2.1 Causes of bridge deck cracking.....	6
Figure 2.2 Time dependence of restrained shrinkage and creep (Mehta 1993).....	9
Figure 2.3 Proposed tensile creep frame (Poston 1998).....	14
Figure 2.4 Diagrams of ring specimen (Shah 1997; Poston 1998).....	16
Figure 2.5 Cracking frame (Breitenbücher 1990).....	18
Figure 2.6 Transverse deck crack.....	23
Figure 2.7 Continuous moist curing (polyethylene film) (Kosmatka 1988).....	31
Figure 2.8 Polypropylene fibers.....	36
Figure 3.1 Time Dependence of Restrained Shrinkage on Creep (after Mehta and Monteiro 1993).....	41
Figure 3.2 Free Shrinkage Prism (ASTM C157).....	46
Figure 3.3 Mold and Restraining Cage for SCC Prism (ASTM C878).....	47
Figure 3.4 Creep Frame and Specimens (ASTM C512).....	48
Figure 3.5 Rapid Chloride Ion Penetration Test Setup (ASTM C1202).....	50
Figure 3.6 Schematic Drawing of AASHTO PP34 Specimen (Shah 1997; Poston 1998).....	51
Figure 3.7 Compressive strength for all mixtures at various ages.....	60
Figure 3.8 Elastic modulus for all mixtures at various ages.....	61
Figure 3.9 Split tensile strength of all mixtures for various ages.....	62
Figure 3.10 Coefficient as a function of time for Control IV mixture.....	63
Figure 3.11 Coefficient as a function of time for Control mixture.....	63
Figure 3.12 Coefficient as a function of time for Type K mixture.....	64
Figure 3.13 Coefficient as a function of time for FRC F-I mixture.....	64
Figure 3.14 Coefficient as a function of time for SRA mixture.....	65
Figure 3.15 Coefficient as a function of time for HPC mixture.....	65
Figure 3.16 Coefficient as a function of time for HPC II mixture.....	66
Figure 3.17 Coefficient as a function of time for HVFA mixture.....	66
Figure 3.18 Shrinkage Strain as a function of time for Control IV mixture.....	70

Figure 3.19 Shrinkage Strain as a function of time for Control mixture	70
Figure 3.20 Shrinkage Strain as a function of time for FRC F-I mixture.....	71
Figure 3.21 Shrinkage Strain as a function of time for SRA mixture.....	71
Figure 3.22 Shrinkage Strain as a function of time for HPC mixture.....	72
Figure 3.23 Shrinkage Strain as a function of time for HPC II mixture.....	72
Figure 3.24 Shrinkage Strain as a function of time for HVFA mixture	73
Figure 3.25 Shrinkage Strain as a function of time for FRC F-II mixture.....	73
Figure 3.26 Shrinkage responses for all mixtures.....	76
Figure 3.27 Restrained shrinkage results for Control mixture.....	77
Figure 3.28 Restrained shrinkage results for HPC II mixture	77
Figure 3.29 Restrained shrinkage results for HVFA mixture.....	78
Figure 3.30 Restrained shrinkage results for Type K mixture.....	78
Figure 3.31 Restrained shrinkage results for Control IV mixture	79
Figure 3.32 Restrained shrinkage results for FRC F-II mixture.....	79
Figure 3.33 Restrained shrinkage results for FRC F-I mixture	80
Figure 3.34 Restrained shrinkage results for SRA mixture	80
Figure 3.35 Restrained shrinkage results for Silica Fume mixture.....	81
Figure 3.36 Restrained shrinkage results for Control 7-day Cure mixture.....	81
Figure 3.37 Restrained shrinkage results for HVFA 7-day Cure mixture	82
Figure 3.38 Large Crack in Restrained Shrinkage Ring Specimen	83
Figure 3.39 Restrained Shrinkage at early age	86
Figure 4.1 Typical Precast, Prestressed Panel Details	92
Figure 4.2 Typical Stair Step Cracking.....	94
Figure 4.3 Stair-step Cracking on the Dow Bridge near Expansion Joint.....	96
Figure 4.4 Typical Transverse Cracking.....	97
Figure 4.5 Suspected Crack Locations.....	98
Figure 4.6 Section Through Panel to Panel Butt Joint.....	99
Figure 5.1 View of a typical precast concrete panel used as stay-in-place forms on the LSBDs.....	103
Figure 5.2 Detail of restrained end of LSBD using threaded reinforcing bar.....	104
Figure 5.3 A conceptual representation of “dog-bone” restraint setup so that cracking will most likely occur in the middle region of the bridge deck. Relative magnitude of shrinkage is represented by the arrows.....	105

Figure 5.4 Side view of end restraint. The end region beyond the PCP is heavily reinforced to encourage drying shrinkage to occur in the central portion of the deck.....	106
Figure 5.5 Meshing of LSBD for design purposes. Stresses in the girders and deck were determined to validate the preliminary design.....	107
Figure 5.6 Photograph of poured columns used to prevent differential settlement of the LSBDs.....	109
Figure 5.7 Photograph of actual PCP used in the construction of the LSBDs.....	110
Figure 5.8 Photograph of shear studs a day before the cast-in-place concrete was poured	111
Figure 5.9 Photograph of the end region showing two layers of threaded reinforcing bar as well as a bottom layer of deformed reinforcing bar	112
Figure 5.10 Photograph of 8 in. x 8 in. steel angle. The steel angle is bolted to the steel girder to provide a source of high restraint.	113
Figure 5.11 Compressive Strength of Phase I LSBDs: SRA and HPC	116
Figure 5.12 Tensile Strength of Phase I LSBDs: SRA and HPC.....	116
Figure 5.13 Modulus of Elasticity for Phase I LSBDs: SRA and HPC.....	117
Figure 5.14 Free shrinkage strain of HPC and SRA mixtures, both in the shrinkage room (solid line) and the field conditions (dashed line)	118
Figure 5.15 Restrained shrinkage strain gage output for SRA	120
Figure 5.16 Restrained shrinkage strain gage output for HPC	120
Figure 5.17 Initial internal temperature for HPC and SRA compared to the ambient temperature	122
Figure 5.18 Observed cracking on the HPC Phase I LSBD. Cracking initiated after five days and completely spread to either edge after eight days.	123
Figure 5.19 Photograph of drying shrinkage cracking on HPC Phase I LSBD after eight days. Crack is outlined in black for visual reference.....	124
Figure 5.20 Top view of Phase II LSBD before cast-in-place concrete (shows formwork)	126
Figure 5.21 Compressive strength of the Phase II mixtures	132
Figure 5.22 Tensile strength of Phase II mixtures	132
Figure 5.23 Modulus of Elasticity for Phase II mixtures.....	135
Figure 5.24 Free shrinkage strain for Phase II Control.....	137
Figure 5.25 Free shrinkage strain for Phase II HVFA	137
Figure 5.26 Free shrinkage strain for Phase II HPC	138
Figure 5.27 Free shrinkage strain for Phase II SRA	138

Figure 5.28 Free shrinkage strain for Phase II Fiber	139
Figure 5.29 Restrained shrinkage strain gage output for Control Phase II.....	141
Figure 5.30 Restrained shrinkage strain gage output for HPC Phase II	141
Figure 5.31 Internal deck temperature for Phase II LSBDs on the first day of pouring from 6:00 a.m. on the day of the pour to 6:00 a.m. the next day.....	143
Figure 5.32 Internal deck temperature for Phase II LSBDs on the second day of pouring from 6:00 a.m. on the day of the pour to 6:00 a.m. the next day	143
Figure 5.33 Observed cracking of Control LSBSD	144
Figure 5.34 Observed cracking for HPC LSBSD	144

List of Tables

Table 2.1 Laboratory test methods selected for study	12
Table 2.2 Factors affecting deck restraint (Krauss and Rogalla 1996).....	28
Table 2.3 Methods of controlling drying shrinkage.....	32
Table 2.4 Aggregate type related to drying shrinkage (Burrows 1998)	33
Table 3.1 Laboratory Test Methods.....	44
Table 3.2 Mixture Proportions.....	52
Table 3.3 Aggregate Properties.....	53
Table 3.4 Cement Chemistry (Brown and Sellers 2002)	54
Table 3.5 Fly Ash and Silica Fume Chemistry (Brown and Sellers 2002).....	55
Table 3.6 Mixture Proportions for Laboratory Specimens	56
Table 3.7 Laboratory Program Test Methods (Brown 2002)	58
Table 3.8 Fresh Concrete Properties.....	59
Table 3.9 Statistical regression parameters for creep using ACI 209.....	68
Table 3.10 Statistical regression parameters for shrinkage using ACI 209	74
Table 3.11 Restrained Ring Test Results (Brown 2002)	84
Table 4.1 Mixture Proportions for Louetta Deck Concretes.....	93
Table 5.1 Phase I Mixture Proportions	114
Table 5.2 Fresh Properties of Phase I Mixtures.....	115
Table 5.3 Mixture Proportions for Phase II LSBDs	127
Table 5.4 Fresh Properties for Phase II mixtures.....	131

1. Introduction

1.1 Background

With the release of ASCE's 2003 Progress Report, an update to the 2001 Report Card for America's Infrastructure in which the country's infrastructure received a grade of D+, it is obvious that the United States faces a growing epidemic of deteriorating infrastructure, and the problem is not getting any better. One of the weakest links in America's deteriorating infrastructure chain is its bridges, which often traverse otherwise impassible routes and consequently the bridge's presence is critical to the efficient flow of traffic and commerce. In fact, as of 2000, 27.5% of the nation's bridges (162,000) were structurally deficient or functionally obsolete (asce.org 2003). Furthermore, according to a survey conducted in 1996 from respondents in several state departments of transportation, more than 100,000 bridge decks in the United States have suffered from early age transverse cracking, a crack pattern that typically indicates the presence of drying shrinkage (Krauss and Rogalla 1996).

The presence of early age transverse cracking in concrete bridge decks is often what leads to the eventual structural deficiency of bridges in the long run because these cracks permit the ingress of harmful substances into concrete bridge decks. With the presence of cracks in concrete bridge decks, water, sulfates, chlorides, and other potentially corrosive agents are able to permeate to the interior of the bridge deck and cause further deterioration in the form of even larger cracks, spalling, potholes and eventually a loss of cross section of the bridge deck or reinforcing steel, which ultimately leads to an unsafe bridge. The repair of concrete bridge decks is often difficult and expensive because alternate routes are sometimes difficult or impossible to come by. To prevent deterioration from starting in the first place, concrete must not be allowed to crack, especially at an early age.

1.2 Scope of Project

Since the economics of an efficient bridge structure require a high degree of restraint in the bridge decks, the most feasible way to prevent early age transverse cracking is to approach the problem from the materials side. This means that the properties of concrete must either be manipulated through mixture proportion optimization (e.g., extensible

concrete) or through the use of innovative materials (fibers, shrinkage reducing admixture, etc.), which can be added to a concrete mixture to impart specific attributes, such as crack resistance. The understanding of how effective these options are at mitigating drying shrinkage cracking forms the basis of the project. The scope of the project as a whole is outlined below:

- Focus on concrete materials and mixture proportions as the most critical aspect to prevent transverse drying shrinkage cracks. Bridge design detailing and construction methods are not considered directly.
- Focus on drying shrinkage only. Ignore thermal, plastic, carbonation, and autogenous shrinkage.
- Optimize concrete mixture proportions to improve shrinkage crack resistance and determine the ideal properties for concrete to resist drying shrinkage cracking (extensible concrete).
- Use of innovative materials such as fibers, shrinkage reducing admixtures, shrinkage compensating cements, and high-volume fly ash to impart shrinkage cracking resistance to concrete.

1.3 Objectives of Project

Based on the scope of the project, the objectives of the project are defined below:

- Review the state of the art regarding restrained shrinkage cracking of bridge decks and identify the most promising mixtures for preventing or minimizing drying shrinkage cracking.
- Evaluate the potential benefits of using innovative materials to control shrinkage cracking, both in small- and large-scale laboratory testing.
- Recommend laboratory-based test methods that best assess shrinkage behavior.
- Recommend modifications to existing test methods, specifications, or design details, if necessary.

In order to accomplish these objectives, the project was divided into various steps outlined in Figure 1.1 below

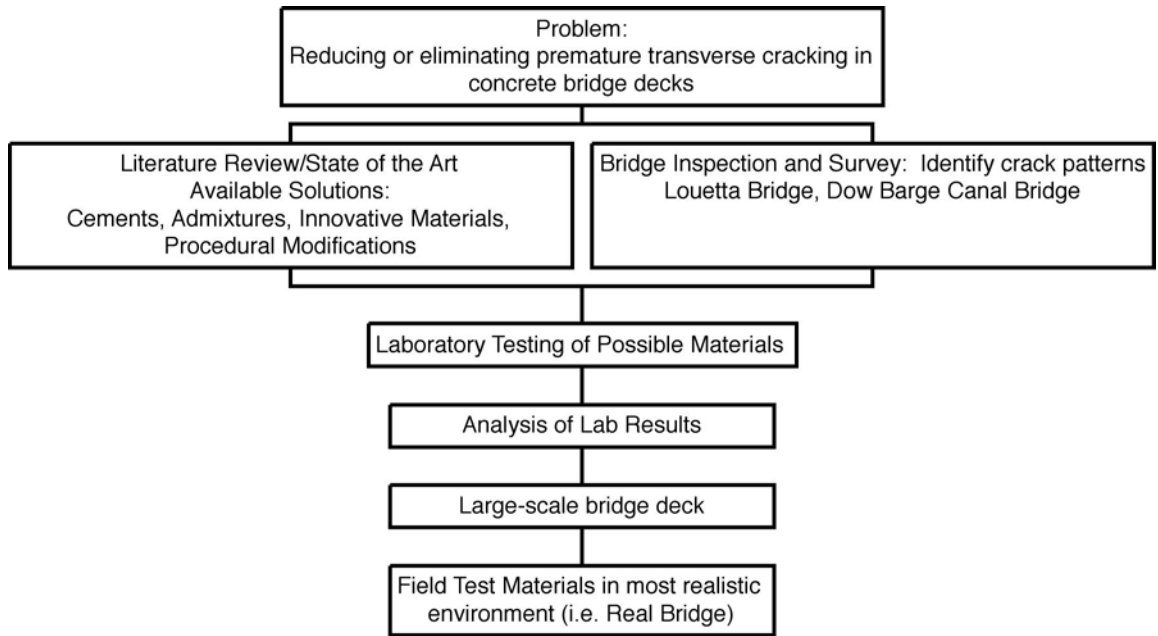


Figure 1.1 Various steps, in order of completion, used to investigate the use of innovative materials to control restrained shrinkage cracking in concrete bridge decks.

1.4 Report Layout

This report will be divided into six chapters, with each chapter covering a different facet of the project along with an introduction and a conclusion that identifies the need for future research. Chapter two presents an overview of the state of the art of using innovative materials to control restrained shrinkage cracking of concrete bridge decks. Chapter three covers the laboratory evaluations performed in order to determine various fresh and hardened concrete properties of innovative concrete materials. Chapter four presents a discussion of the field evaluations for selected bridge decks in Texas. Chapter five describes the design, construction, and results obtained from the large-scale bridge deck testing. Chapter six presents the conclusions and recommendations for future research, specifically the need to perform an implementation study of the most promising innovative materials in an actual bridge deck.

2. State of the Art Review

2.1 Introduction

Cracking in concrete is a major concern, particularly with bridge decks, because it can lead to premature deterioration. According to a recent survey from respondents in the state departments of transportation (DOTs), more than 100,000 bridge decks in the United States have suffered from early transverse cracking (Krauss and Rogalla 1996). This state-of-the-art review also found that the most important factors affecting the cracking in bridge decks are the concrete properties of decks. Other factors such as the girder type, span length, construction techniques (e.g., precast concrete panels), and detailing issues can also cause drying shrinkage cracking in bridge decks.

In order to determine the causes of transverse cracking problems that result from restrained shrinkage cracking, we must understand the actual mechanisms driving this type of cracking behavior. This chapter first discusses drying shrinkage and creep in detail, focusing on how one or both of these mechanisms can either contribute to or help reduce restrained shrinkage cracking. In addition to drying shrinkage, a number of different types of shrinkage can contribute to the development of cracking and durability concerns in concrete. These include plastic, autogenous, and carbonation shrinkage. Chapter two also explains how differences in the heat of hydration can subsequently lead to thermal stresses. Once the shrinkage of concrete occurs, external forces, such as adjoining structural members, will immediately restrain this shrinkage causing additional stresses to occur in the concrete. The shrinkage that concrete bridge decks undergo will be restrained at the ends by the supporting girders, placing large amounts of tensile stresses on these decks. The major causes of bridge deck cracking are illustrated in Figure 2.1.

Certain test methods must be administered in order to accurately describe concrete mixture proportions and the behavior of concrete when subjected to restrained shrinkage cracking. Included in this chapter are American Society of Testing and Materials (ASTM) and American Association of State Highway and Transportation Officials (AASHTO) test methods and specifications, which when implemented correctly in the laboratory, can be used to analyze the behavior of concrete as applied to shrinkage in structural applications. Réunion Internationale des Laboratoires d'Essais et de recherche sur les Matériaux et les

Constructions (RILEM) test methods are also mentioned, along with a variety of different restrained shrinkage tests that have been developed and have proven to be good predictors of restrained shrinkage cracking of different concrete mixture proportions. We also refer to two American Concrete Institute (ACI) committee reports that deal with some of the specific topics of restrained shrinkage cracking, including creep and shrinkage analysis, along with detailed descriptions regarding shrinkage-compensating concrete.

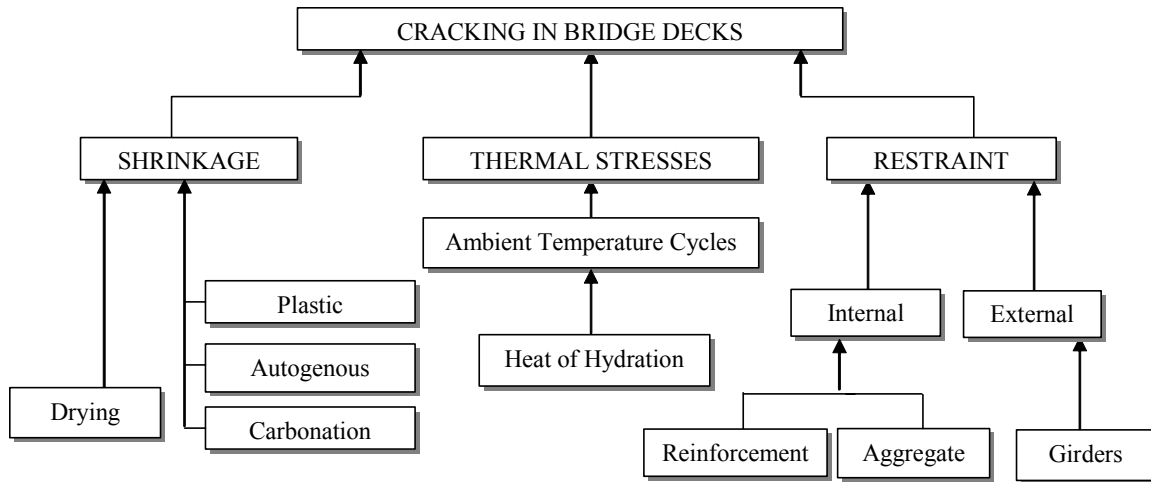


Figure 2.1 Causes of bridge deck cracking

Once the applicable test methods and specifications have been covered, the topic of bridge deck cracking is addressed. One of the topics deals with transverse deck cracking caused by stresses originating from a number of different sources. Design issues of the bridge decks are included, with the girder type and the support of the deck at the ends of the spans taken into consideration. The influence of different concrete properties and mixture proportions of the deck are subsequently described. This section includes a discussion of the increased use of high-performance concrete (HPC), specifically for bridge decks, which has been found to increase the frequency and severity of transverse cracking. It also covers construction techniques such as concrete placement and curing.

The last section of this chapter deals with the question of how to control shrinkage cracking. Two methods of control are presented: conventional and innovative. The conventional methods include proper selection of materials and concrete mixtures, along with good construction techniques. Because it is nearly impossible to control the conventional methods to produce a concrete mixture that will not crack, especially because

of the extreme number of variations that can occur, innovative methods must also be used to help reduce the amount of restrained shrinkage cracking. These methods include the use of fiber-reinforced concrete, the addition of shrinkage-reducing admixtures to concrete, the use of shrinkage-compensating cement, and the development of extensible concrete.

In the conclusion of this chapter, recommendations are made concerning the methods by which restrained shrinkage cracking in bridge decks can be tested and predicted.

2.2 Restrained Shrinkage Cracking

Restrained shrinkage cracking occurs when concrete is prevented from making volumetric changes by a source of restraint. Volumetric changes in concrete result from creep, shrinkage of the concrete or thermal loads.

2.2.1 Types of Shrinkage

Plastic Shrinkage

Plastic shrinkage occurs only in fresh concrete. The most common mechanism is the evaporation of water from the surface of the plastic concrete. However, the loss of water through the sub-base or formwork can exacerbate the effects of surface evaporation.

In the fresh concrete the particles are completely surrounded by water. If water is removed from the system, menisci are formed between particles. These menisci generate negative capillary pressure, which pulls the cement particles together. By pulling on the particles, the capillary stresses tend to reduce the volume of the cement paste. Capillary pressures continue to rise as water is lost at the surface of the concrete. When the pressures reach a critical value, the water that remains in the concrete rearranges to form discrete zones with voids between them. Plastic shrinkage cracking occurs at this point.

Autogenous Shrinkage

Autogenous shrinkage is a result of self-desiccation of the concrete. When no additional water is added to the concrete through curing, the concrete begins to chemically consume the water during hydration. Autogenous shrinkage is much more pronounced in concrete mixtures with a low water-cement ratio.

Autogenous shrinkage is significantly increased by the use of superfines such as silica fume. Paillere et al. (1989) tested a sealed concrete specimen in a restrained shrinkage apparatus. When a specimen with a 0.44-water-cement concrete was sealed, no failure resulting from shrinkage stresses occurred. However, when a specimen with high-range water-reducing admixture (HRWRA) and silica fume, but with the same cement content, was tested, cracking occurred in less than 4 days. In the second specimen the water-cement ratio had dropped to 0.26 because of the use of the HRWRA. Traditionally, autogenous shrinkage has been viewed as though it were of secondary importance. In more modern mixes containing HRWRA and superfines, this type of shrinkage can be a dominant influence on cracking.

Drying Shrinkage

There are three main mechanisms of drying shrinkage: capillary stress, disjoining pressure, and surface tension. Each of these mechanisms is dominant in a different range of relative humidity. The most relevant range of relative humidity for field conditions is 45% to 90%. In this range the capillary stress mechanism is the most dominant.

As water evaporates, the tensile stresses that were confined to the surface tension of the water are transferred to the walls of the capillary pores (<50 nm). The tension in the capillary walls results in shrinkage of the concrete.

Carbonation Shrinkage

Hardened cement paste will chemically react with carbon dioxide (CO₂). The amount present in the atmosphere is enough to cause considerable reaction over long periods of time. The extent to which concrete can react with the CO₂ is a function of relative humidity. At high relative humidity the concrete pores near the exposed surface are mostly filled with water; the water prevents the ingress of CO₂ and thus limits the reaction. Concrete exposed to CO₂ loses water and behaves as though it were exposed to drying conditions, in other words, the concrete will behave as though it were exposed to a lower atmospheric relative humidity than actually exists.

2.2.2 Combined Effects of Creep and Drying Shrinkage

The primary cause of both creep and drying shrinkage is the loss of adsorbed water, though the causes of the water loss are radically different. For drying shrinkage the driving force behind the water loss is the relative humidity, and for creep it is applied sustained stress. Restrained shrinkage induces tensile stresses in concrete. Creep causes the concrete to flow in small amounts and can serve to relax shrinkage stresses. Figure 2.2 illustrates the process described above and shows the delay in cracking that result from stress relaxation.

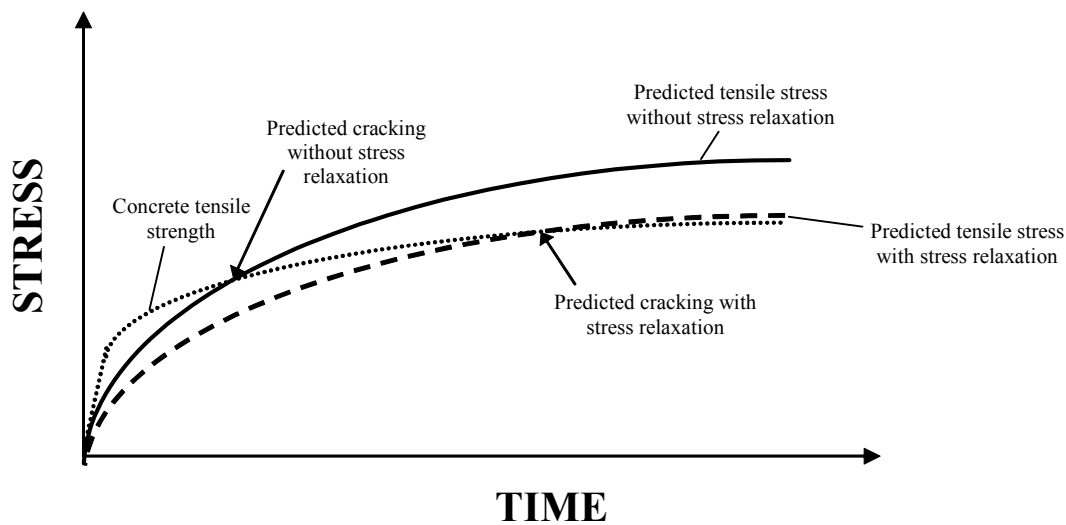


Figure 2.2 Time dependence of restrained shrinkage and creep (Mehta 1993)

2.2.3 Thermal Stresses

Under field conditions, a bridge will be subjected to temperature cycles. These cycles occur on a daily and seasonal cycle. Ambient temperature cycles are most important after the concrete has hardened. However, while the concrete is still plastic, the thermal loads will be applied from the heat of hydration produced within the concrete placement.

Heat of Hydration

The heat of hydration produces the first thermal load on the concrete member. As the fresh concrete hydrates and gains strength, the exothermic chemical reaction produces heat within the concrete placement. The temperature of the concrete slowly drops to match ambient conditions as hydration proceeds. This process is proportional to the size of the

concrete member; larger members take longer to cool to ambient temperatures. The plastic concrete can accommodate thermal loads without developing thermal stresses; after hardening, any thermal load restrained against length change will induce stresses. Thermal stresses will be the highest if the concrete hardens when it is at its highest temperature by forcing the stress-free state to be at an elevated temperature. As a result, the average temperature that the deck experiences will be lower than the environment in which the deck hardened, causing a volume contraction throughout the life of the deck.

Ambient Thermal Cycles

After hydration is complete, the weather determines the temperature and thermal stresses. The typical diurnal weather cycle begins with the coolest temperature occurring just before sunrise. The temperature then rises throughout the day and peaks a few hours before sunset. Cloud cover and precipitation affect this cycle and can cause dramatically different cooling and heating rates.

In addition to diurnal cycles, solar radiation is a large source of thermal loading. Concrete will absorb part of the solar radiation and reflect the rest. Asphalt overlays are typically darker in color than portland cement concretes (PCCs) and consequently absorb more solar radiation. However, the asphalt tends to insulate the concrete and reduce its thermal load.

Wind tends to reduce the temperature on the member by inducing heat transport with bulk fluid motion, or convection. Convection cools concrete surfaces, reducing the peak temperatures caused by the sun.

Restraint

Strain alone, caused by shrinkage, creep, or thermal loading, does not induce stresses. The forces and pressures provided by restraint cause stress. The restraint can be internal, from reinforcement and aggregate, or external, from the sub-base or superstructure of a bridge. If strains are not uniform throughout a member, as though produced by a thermal gradient, the member itself can serve as a restraint. If the concrete is subjected to shrinkage, the restraint will cause tensile stresses, which tend to create cracks.

Bridge decks are particularly susceptible to such restraint. Most bridge decks are composite with the girders that support them. This composite action can increase the

restraint if the girders do not undergo shrinkage and thermal strains that are identical to those of the deck. Dissimilar thermal strain characteristics will be more pronounced if steel girders support the concrete deck.

2.3 Test Methods and Specifications

In order to accurately measure the concrete properties affecting restrained shrinkage cracking, researchers must administer specific tests in accordance with ASTM/AASHTO specifications, along with possible additional tests from other governing bodies, such as RILEM. The necessary tests include basic concrete tests that must be conducted for quality control purposes. In addition to conducting the necessary tests, the researchers should examine procedures from ACI test reports, specifically for analysis of creep and shrinkage results, along with a report concerning shrinkage-compensating cement. Overall, these tests can be divided into two categories, fresh concrete properties and hardened concrete properties, which are summarized in Table 2.1 below.

Table 2.1 Laboratory test methods selected for study

Test Methods	Description
Fresh Concrete Properties	
AASHTO T119	Slump of Concrete
AASHTO T152	Air Content
ASTM C138	Unit Weight, Yield and Air Content
ASTM C1064	Temperature of Fresh Concrete
Hardened Concrete Properties	
AASHTO T22	Compressive Strength of Concrete
AASHTO T198	Splitting Tensile Strength of Concrete
AASHTO T97	Flexural Strength of Concrete
ASTM C1074	Estimating Concrete Strength by the Maturity Method
ASTM C469	Modulus of Elasticity of Concrete
ASTM C512	Creep of Concrete in Compression
AASHTO T160	Drying Shrinkage of Concrete (Free Shrinkage)
AASHTO PP34-99	Restrained Shrinkage Cracking of Concrete
ASTM C878	Restrained Expansion of Shrinkage-Compensating Concrete
AASHTO T277	Rapid Chloride Permeability

2.3.1 Fresh Concrete Tests

The fresh concrete tests are administered for quality control purposes to compare the concrete mixes when researchers are evaluating and testing for shrinkage cracking. The tests, listed below, also list in parentheses the specification number designated by ASTM and AASHTO:

- Slump of Concrete (AASHTO T119)
- Air Content (AASHTO T152)
- Unit Weight, Yield and Air Content (ASTM C138)
- Temperature of Fresh Concrete (ASTM C1064)

2.3.2 Hardened Concrete Tests

A number of hardened concrete tests must be administered for analysis of the drying shrinkage and cracking tendencies of a concrete specimen. The first four tests in the following list determine the strength of the concrete specimen, while the remaining tests are needed for modeling the shrinkage behavior of concrete and are described in detail. Included in the strength tests is the maturity method test, which establishes a relationship between strength and maturity while also determining the temperature history of the concrete for which strength is to be estimated. Once these tests have been administered and

the results have been analyzed, the drying shrinkage and cracking characteristics of the concrete specimens can be obtained. The hardened concrete tests include the following:

- Compressive Strength of Concrete (AASHTO T22)
- Splitting Tensile Strength of Concrete (AASHTO T198)
- Flexural Strength of Concrete (AASHTO T97)
- Estimating Concrete Strength by the Maturity Method (ASTM C1074)
- Modulus of Elasticity of Concrete (ASTM C469)
- Creep of Concrete in Compression (ASTM C512)
- Drying Shrinkage of Concrete (Free Shrinkage) (AASHTO T160)
- Restrained Shrinkage Cracking of Concrete (AASHTO PP34-99)
- Restrained Expansion of Shrinkage-Compensating Concrete (ASTM C878)
- Rapid Chloride Permeability (AASHTO T277)

2.3.3 Modulus of Elasticity and Creep

The modulus of elasticity is vital to our understanding and modeling of the shrinkage behavior of concrete. This test is administered by applying a specific stress at different times to a concrete cylinder and then measuring the strain at these stress values. Subsequently, the modulus of elasticity can be found by using the stress-strain relationship of concrete. In the National Cooperative Highway Research Program (NCHRP) Report 380 (Krauss and Rogalla 1996), the effective modulus of elasticity property of concrete is one of the three factors that control the cracking of bridge decks. The paper goes on to say that “the concrete effective modulus of elasticity significantly affects tensile stress in the deck and cracking” (pg. 39). As discussed earlier, restraint in bridge decks causes tensile stresses in the concrete, which in turn lead to shrinkage cracking.

In addition to the modulus of elasticity test, the creep of concrete in compression test is important. In this test, concrete cylinders are placed in a vertical loading frame as constant load is applied in direct compression over an extended amount of time. Strain readings are taken before and after loading, and subsequently the creep strain and creep rate can be obtained from these readings. In the same NCHRP report mentioned earlier, creep is defined as the one property of concrete that has the largest impact on long-term stresses and transverse cracking in bridge decks. Creep is closely related to the compressive strength of concrete by the fact that once the compressive strength of concrete increases, creep decreases by an amount greater than both the modulus of elasticity and the tensile strength increase. This is crucial to transverse bridge deck cracking because the tensile

stresses that are usually reduced by creep will now be greater than the tensile strength of concrete, leading to transverse cracking (see Figure 2.2).

Because the tensile stresses and strengths of concrete are of great significance for bridge decks, increasing interest has been directed toward the idea that concrete creeps in tension. Poston et al. (1998) developed a test in which concrete cylinders are loaded in direct tension by applying constant load acting across an adjustable lever arm. Because this frame did not provide accurate results, Poston et al. suggested a different type of tensile creep frame that, if conducted properly, should provide valuable information concerning creep in tension (see Figure 2.3).

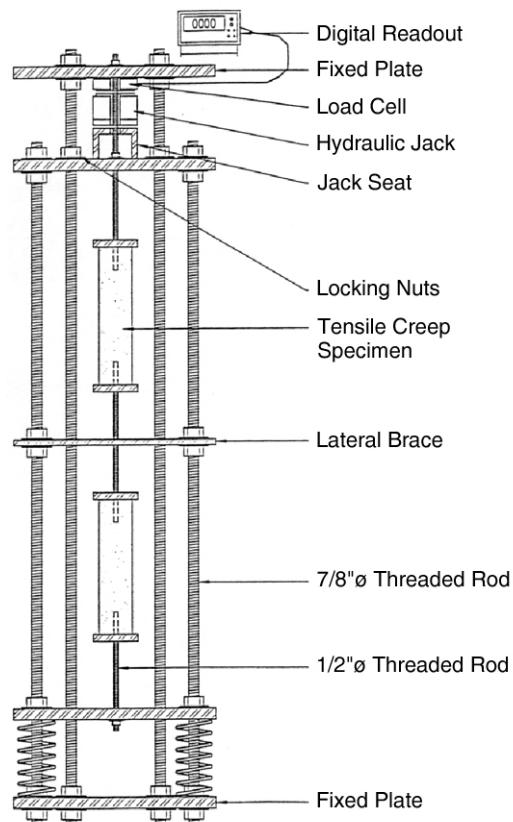


Figure 2.3 Proposed tensile creep frame (Poston 1998)

A source of information about the analysis and prediction of shrinkage cracking that takes into account the effects of creep is the ACI Committee 209 report (1999). This report presents recommendations regarding shrinkage and creep behavior analysis, taking into account a variety of factors dealing with the size of the concrete members, construction

techniques, and many other issues. This report should be followed and utilized in order to compare the predicted shrinkage cracking with the values obtained from the restrained shrinkage tests, described below.

2.3.4 Free and Restrained Shrinkage

The drying (free) shrinkage test should be administered to determine the actual shrinkage of the concrete without any restraint applied. The test consists of casting a concrete beam and measuring the displacement on two ends as a direct relation to the time elapsed after stripping the molds.

A relatively new test method known as the ring test has been designed to measure the tendency of concrete to undergo drying shrinkage cracking and has now been adopted by AASHTO as a provisional test method. The setup for the test and an illustration of the casting method can be seen in Figure 2.4. This restrained shrinkage test, which was utilized as part of the NCHRP Project C12-37, has been developed by a number of researchers in the past (Weiss et al. 1998, ref. 22; Folliard and Berke 1997) as an accurate method for predicting the length of time until the concrete cracks. Weiss et al. (1998, ref. 23) contend that this test solves the problem that arises when researchers perform a direct tensile test on a concrete specimen while analyzing the specimen for any tensile stresses being developed due to restraint.

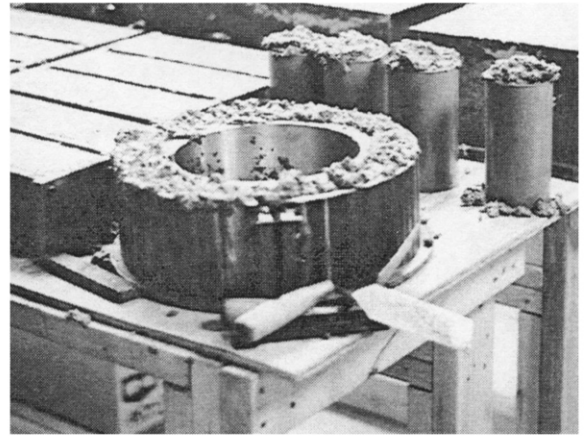
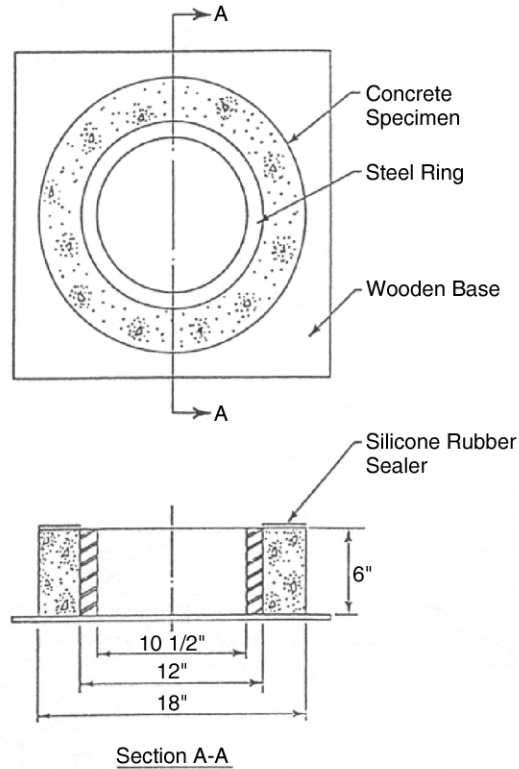


Figure 2.4 Diagrams of ring specimen (Shah 1997; Poston 1998)

The test method consists of casting a 3 in. thick concrete ring around the perimeter of a steel ring, then moist curing the specimen, and subsequently placing the rings in an environmentally controlled chamber at a temperature of 72 °F, with 50% relative humidity. The concrete is then subjected to extremely high levels of restraint against shrinkage, provided by the steel. Consequently, the ring test represents a worst-case scenario for concrete when dealing with shrinkage cracking. Weiss et al. (1998) notes that the test method avoids eccentricities being developed in the concrete specimen, creating a more realistic method of direct tensile restraint. Strain gages, attached to the inside of the steel ring, measure the amount of time that passes before the concrete breaks to relieve stress along the steel ring. In addition to measuring the amount of time until the concrete cracks, the procedure also allows for the total crack area of the concrete ring to be measured once the test has been concluded. Along with the free shrinkage test, the different concrete mixtures can be compared and analyzed for the actual restrained shrinkage tendencies of each mixture.

2.3.5 Restrained Expansion of Shrinkage-Compensating Cement

Shrinkage-compensating cement is an innovative material that has received considerable attention for its ability to control drying shrinkage in concrete. The restrained expansion test examines both the expansion and contraction of a concrete beam specimen containing shrinkage-compensating cement during moist-curing and dry storage phases. The specimen is restrained by a cage consisting of a steel-threaded rod running through the mold and secured to the ends of the beam by steel plates and bolts.

In addition to the restrained expansion test, the aforementioned ring test can be used to determine the cracking tendencies of shrinkage-compensating concrete by measuring the amount of time (in days) until the specimen cracks. A critical factor for this test is the placement of molds that are strong enough to confine the shrinkage-compensating concrete and initially place the specimen into compression. This method will provide insight into the behavior of shrinkage-compensating concrete as applied to recommended construction techniques for this material.

Along with these tests, the ACI Committee 223 Report (1998) is a standard practice that sets forth recommendations for proportioning, mixing, placing, finishing, curing, and testing shrinkage-compensating concrete in structures. It specifically mentions the topic of curing and applying adequate protection to the concrete during the early stages of hydration. This report can be a useful source of information for researchers testing shrinkage-compensating cement and interpreting the results.

2.3.6 Chloride Permeability

The permeability of concrete bridge decks is one of many concerns that have to do with transverse cracks developing and propagating throughout the depth of the decks themselves. Burrows (1998) states that “the rapid corrosion of reinforcing steel in concrete resulting from chloride ions is a pervasive worldwide problem” (pg. 48). Specifically, the overall durability of a bridge deck can be substantially damaged if transverse cracks develop and the deck is subjected to sources of chloride (e.g., sea water, deicing salt). The rapid chloride permeability test uses electricity that forces chloride ions to penetrate through the concrete; subsequently, the charge passed through the sample can be measured and correlated to the actual penetration water or other ions into the concrete. Accordingly,

this test allows for comparison of the durability of different concrete mix proportions, based on the permeability of the concrete.

2.3.7 Additional Restrained Shrinkage Tests

Numerous restrained shrinkage tests have been developed in addition to the provisional ring test described above. Springenschmid (1994) has performed extensive research and developed a cracking frame, as seen in Figure 2.5, to examine restrained shrinkage of concrete and RILEM has since adopted this test as a standard test, designated TC119. According to Breitenbücher (1990), the frame is able to restrain both contraction and expansion in the longitudinal direction of the concrete member, while restraint stresses are measured continuously. This restraint closely resembles restraint conditions imposed by girders to the concrete bridge decks. The actual test consists of insulating a concrete bar and surrounding the formwork with two steel bars running longitudinally and two steel cross-heads at each end. The concrete is allowed to cool to ambient temperature, and after four days, if the concrete has not cracked, it is cooled at a constant rate until cracking occurs. Thus, the temperature at which the concrete cracks indicates how well the concrete will resist cracking in practical applications, such as bridge decks. Concrete that cracks at higher temperatures in this test is prone to early cracking.

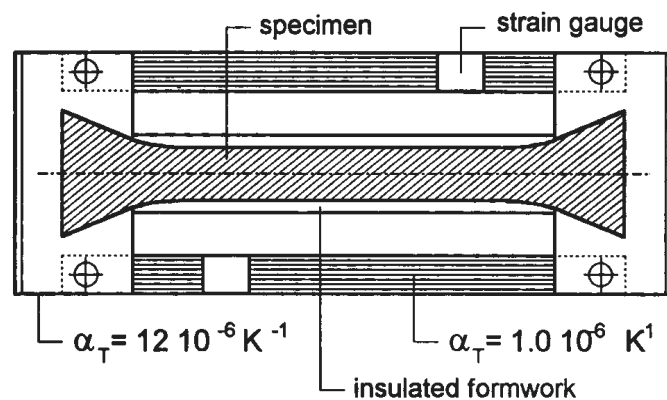


Figure 2.5 Cracking frame (Breitenbücher 1990)

Poston et al. (1998) has examined two additional tests that pertain to restrained shrinkage cracking in concrete. The first test involves casting a concrete beam specimen

against a thin steel plate on the bottom of the specimen. Under standard conditions, the beam deflects upward at the unrestrained end. This upward tip deflection is measured at three locations over a certain period of time. The interaction between the beam and the steel plate, which is impregnated with sand grit to improve the bond to the concrete, represents the restraint to the concrete specimen.

The German angle test was also investigated as a possible candidate for measuring restrained shrinkage. In this test, a steel angle, 39 in. in length and with cross-sectional dimensions of 1.5 x 2.75 in., is filled with concrete. The length of time until the concrete cracks, the number of cracks, and the average width of cracks are recorded.

2.3.8 Fracture Energy

An important test measuring the fracture energy, G_F , of a concrete specimen is RILEM TC-50. The fracture energy of concrete can be useful in analyzing shrinkage cracking behavior because it can be characterized as the actual amount of energy needed to create a crack of unit area or fracture surface (Guo and Gilbert 2000). The test consists of placing a notched beam in three-point bending and measuring the displacement, δ_f , and the applied load, P , throughout the test. Using these values and an equation for the amount of work done by the load P , the weight of the beam, and other testing equipment, we can calculate the fracture energy (Guo and Gilbert 2000).

2.3.9 Summary of Tests Methods

As seen above, researchers need to conduct tests in order to understand and model shrinkage behavior of concrete. A great deal of research has been directed toward developing an accurate and easy-to-implement test method to analyze restrained shrinkage cracking of concrete. AASHTO has adapted the ring test as a provisional test method, while RILEM has incorporated the cracking frame as a standard test. Currently, researchers are developing variations of the cracking frame by placing a vertical concrete beam under restraint at the ends through steel clamps. The end result of conducting the various tests is the selection of the best candidate mixtures for bridge decks.

2.4 Bridge Deck Cracking

In 1996, NCHRP Report 380, “Transverse Cracking in Newly Constructed Bridge Decks” (Krauss and Rogalla 1996), concluded that the transverse cracking was a result of a combination of thermal contraction, drying shrinkage, and concrete with a high modulus and little creep capacity. Bridge decks exhibit a high degree of restraint because of the composite nature of the deck and supporting girders. Forcing the deck and superstructure to act compositely means that no relative displacement can occur, thus restraining the concrete from shrinking.

2.4.1 Stresses in Transverse Deck Cracking

All concrete shrinks and undergoes volumetric change with temperature. However, shrinkage and thermal loading alone are not enough to cause cracking. Length change in concrete must be restrained from such movements to induce stresses. Cracking is caused by the tensile stresses that are induced by restrained shrinkage.

Restraint

Deck restraint can come from either internal sources, such as reinforcement or aggregate or external sources, such as supporting girders. Bridge decks are typically much longer in one direction than the other; because of this geometry, shrinkage tends to be more pronounced in the longitudinal direction. Again, the shrinkage is highly restrained and will develop stresses in the longitudinal direction of the deck. To relieve the shrinkage stresses, the deck will crack in the transverse direction, perpendicular to the stress.

Thermal Stresses

As described previously, thermal loads cause length change in concrete. Decks are particularly susceptible because they tend to be much longer in one direction. Length changes are more pronounced in that direction because thermal expansion is directly proportional to length. Thermal strains alone do not induce stresses; the deformation of the bridge deck must be restrained.

Restrained thermal contraction causes tensile stresses in deck elements and can compound the effects of shrinkage. However, thermal contraction usually occurs over a

relatively short period of time. Creep cannot effectively relax thermal contraction because of the time needed to develop creep strains.

The discussion above assumes that there is a uniform or linear thermal gradient through the thickness of the deck. If a non-uniform temperature gradient is present when the concrete hardens, any applied thermal gradient will induce stresses regardless of restraint. These stresses develop because of the difference in the applied thermal gradient and the stress-free gradient. The difference in gradient may produce a non-uniform strain.

Shrinkage Stresses

Shrinkage stresses develop in a manner similar to that of thermal stresses. Concrete decks will tend to shrink in the longitudinal direction, which is restrained, and cracks will develop in the transverse direction perpendicular to the stress. Shrinkage tends to occur over a period of time much longer than that of thermal contractions; because of this time effect, creep can help to relieve some of the shrinkage stresses.

Traffic Stresses

Many bridge decks were reported to have cracked in the transverse direction before traffic was allowed on the structure in NCHRP Report 380 (Krauss and Rogalla 1996). Accordingly, traffic-induced stresses are not considered to be a primary cause of transverse cracking. In simply supported structures, traffic loads will develop compressive stresses in the deck. Compressive stresses will not contribute to transverse cracks. In continuous bridges, traffic loads will induce tensile stresses in the deck over supports. However, transverse cracks in continuous bridges are not localized to areas near the support. Consequently, traffic is not likely to cause the cracks to form, but it will serve to open existing cracks.

Design Issues

As part of NCHRP Report 380 (Krauss and Rogalla 1996), a survey of bridges was performed to determine any relationships between design procedures and cracking in the field. During design, temperature and shrinkage stresses are rarely considered, and temperature and shrinkage reinforcement is generally considered to be sufficient to control cracking. Presented below is a summary of the report findings.

Span Support and Continuity

In simply supported spans, temperature and shrinkage stresses are almost uniform along the length of the span. Simple supports allow free rotation and can accommodate the curvature that results from deck shrinkage. Conversely, continuous spans restrain the curvature of the deck at interior supports. This restraint affects the stresses and increases cracking near the supports.

Girder Effects

As previously described, a bridge deck acts compositely with its supporting girders. Transverse cracking would not occur without such girder restraint. However, decks that are designed not to be composite will still have a great deal of friction between the underside of the deck and the girders. Unless this friction was reduced, it would still provide enough restraint to produce transverse cracking.

Krauss and Rogalla reported that bridges supported by steel girders are cracked more than decks supported by concrete beams. They attributed this effect to the inability of the steel to shrink with the concrete and the higher elastic modulus of steel. Also, there is a marked difference between the coefficients of thermal expansion for concrete and steel. Additionally, steel is more thermally conductive than concrete and will react faster to a changing environment.

Girder size and spacing also affect restraint. Larger girders provide more restraint and therefore induce more cracking. Longer span bridges will likely have larger girders; the higher incidence of cracking on longer span bridges may be the effect of girder size rather than span length. As one would expect, more closely spaced girders provide more restraint as well.

Deck Design

The longitudinal stresses that lead to transverse cracking, which can be seen in Figure 2.6, are influenced by deck thickness, reinforcement cover, reinforcement spacing and size, embedded studs, and concrete strength.



Figure 2.6 Transverse deck crack

Thicker decks often develop smaller shrinkage stresses for the same amount of shrinkage. However, thicker decks are more prone to develop non-uniform shrinkage stresses, which in turn induce bending.

Krauss and Rogalla found that the concrete cover has an inconsistent effect on cracking. Increasing the cover reduces the ability of the reinforcement to distribute the shrinkage stresses. A larger number of smaller bars at a closer spacing are believed to reduce cracking. Epoxy-coated bars were found to produce larger cracks but fewer of them. This was attributed to the lower bond-slip strength of epoxy-coated bars as opposed to black bars.

Transverse deck cracks tend to develop directly above the transverse reinforcement. This effect is compounded if the top and bottom layers of bars lie directly over one another, producing a weakened plane. There is also evidence that cracks often propagate from the corners of prestressed, precast deck panels. The panels add restraint to the cast-in-place concrete in which they are embedded.

Concrete Strength

Higher-strength concrete is more susceptible to transverse cracking than concrete of a moderate strength. Higher-strength concrete typically has a larger amount of cement, which increases the shrinkage potential and heat of hydration. Also, the modulus of elasticity of higher-strength concrete is larger so for the same amount of strain a higher-modulus material will experience more stress.

2.4.2 Concrete Properties and Mix Proportions

The concrete properties provide the designer with the most ability to control and prevent shrinkage cracking. Although the girder size is more influential on transverse cracking, the span length generally dictates the girder size, whereas the concrete properties can be modified without serious negative consequences.

Mixture Proportions

Reducing the cement content increases creep but decreases the heat of hydration and the associated thermal stress. Lower cement content will therefore result in a mix that is less prone to cracking. Little correlation, if any, was found between the amount of time that passed before cracking occurred and water content. Concrete with higher water content shrinks more, but an increase in creep tends to offset the increased shrinkage. Reducing the water-cement ratio increases strength and decreases free shrinkage. The increase in strength increases the modulus and, in turn, increases the cracking potential.

A minimum of cement paste should be recommended for bridge deck construction. A minimum amount of paste will decrease shrinkage because the paste is the component of concrete responsible for shrinkage. However, the decrease in paste volume will also decrease the creep, and there may be no net effect of minimizing the volume of paste. Consequently, there is no conclusive recommendation at this time.

Modulus of Elasticity and Creep

The combination of modulus and creep determines the stresses caused by the shrinkage strains. Both the modulus and the tensile strength of concrete are affected by the compressive strength. An increase in compressive strength will increase the tensile strength and the modulus of concrete. This increase means the concrete will have a greater resistance to cracking and a greater stress driving the cracking. Also, higher-strength

concrete tends to have a lower amount of creep. As mentioned before, creep serves to relax the stresses caused by shrinkage. The simplest way to decrease the concrete modulus is to decrease the compressive strength. To increase the creep potential, the volume of cement paste should be increased.

Concrete Strength

Creep is the controlling factor in resistance to shrinkage cracking. Compressive strength and creep are inversely proportional; higher-strength concrete tends to creep less. Increasing the compressive strength of concrete usually increases the stresses that result from restrained expansion more than it increases the tensile strength; the net effect is a higher cracking potential.

Aggregate

To reduce the thermal stresses produced by hydration, engineers should use a leaner concrete mix. Larger aggregate should be used to achieve this goal without sacrificing workability.

In addition, an aggregate with a low modulus, a low coefficient of thermal expansion, and high thermal conductivity should be used. The modulus of the aggregate is the most influential because the concrete is mostly aggregate. Accordingly, a low modulus aggregate will produce a low modulus concrete, which is crack resistant.

Cement Type

We recommend cement that will produce less heat of hydration, e.g., Type II or Type IV. Type III (high early strength) should be avoided because of the large increase in the heat of hydration it produces. If Type III is to be used, care should be taken to minimize the amount of cement.

Silica Fume

NCHRP Report 410, "Silica Fume Concrete for Bridge Decks," states that "Cracking tendency of concrete is influenced by the addition of silica fume only when the concrete is improperly cured" (pg. 17). The report also discusses an increase in compressive strength with the use of silica fume. This study did not focus on shrinkage cracking, so its results should not be accepted without question. An increase in elastic modulus is likely to

increase the probability of cracking. This effect was experimentally shown by Krauss and Rogalla. They noted that restrained shrinkage rings (AASHTO PP34-99) that contained silica fume cracked 5 to 6 days earlier than similar specimens without silica fume.

Admixtures

Admixtures can adversely affect the shrinkage potential of concrete. For instance, water reducers can be used to reduce the paste volume and thereby enhance the creep capacity without the loss of workability. Set retarders can be used to delay set and to decrease the amount of heat of hydration. A lower heat of hydration will decrease the thermal shock on the hydrating concrete. However, overly long retardations will increase the potential for plastic shrinkage cracking. Proper curing is necessary with the use of a set retarder. Conversely, set accelerators increase the heat of hydration and early-age shrinkage. This combination will increase transverse shrinkage and the resulting cracking.

Shrinkage-reducing admixtures (SRAs) are also available. These admixtures reduce the drying shrinkage by reducing the surface tension of the water in the capillary pores. If the surface tension of the water is reduced, there is less tension transferred to the capillary walls, and consequently less shrinkage. Laboratory evaluations (Folliard and Berke 1997) have shown a slight decrease in compressive strength when an SRA is used. Taking advantage of the water-reducing properties of SRAs can offset the decrease in strength.

Fiber Reinforcement

Steel Fibers

Steel fibers can affect the properties of concrete, but the reinforced properties depend on the percentage of fiber addition, the aspect ratio of the fibers, and the strength of the concrete paste. Longer fibers provide more strength but decrease workability. For this reason, fibers with an aspect ratio of less than 100 are commonly used.

Although there is considerable variation in the data, steel fiber reinforced concrete (SFRC) has been shown to increase the tensile strength, flexural strength, and compressive strength of concrete. Tests have shown that steel fibers do not affect the shrinkage strain of concrete, but the fibers can reduce the amount of cracking associated with the shrinkage strain.

Polypropylene Fibers

Low fiber volumes can significantly reduce the plastic shrinkage of concrete. For low-volume fiber reinforcement, fiber volume is typically 0.1%–0.3%. At low dosages such as these, the fibers have little, if any, effect on the properties of the hardened concrete. Some manufacturers of polypropylene fibers have claimed that the addition of a low volume of fibers significantly reduces shrinkage cracking. These claims have not been supported by laboratory evaluations, and such claims should be carefully examined.

However, high volumes of fiber, generally greater than 2%, can increase the ductility and toughness of concrete. At high volumes, polypropylene fibers can be used to prevent shrinkage cracking. The shrinkage stress produced in the concrete is transferred to the fibers, which can better withstand the tensile stresses than the concrete can.

High-Performance Concrete

High-performance concrete (HPC) is concrete with superior strength, durability, and dimensional stability. However, there is evidence that HPC bridge decks exhibit significantly more shrinkage cracking than traditional concrete decks. HPC has a higher paste volume; the increase in cracking is attributed to the increase in shrinkage without an increase in creep from the large paste volume. Additionally, HPC often contains silica fume to reduce permeability. Wiegrink et al. (1996) demonstrated that creep decreased with increasing amounts of silica fume.

HPC will have a higher tensile strength, but the elastic modulus of the HPC will also be higher. The combination of higher tensile strength and higher modulus will still produce shrinkage cracking. With a higher modulus, the tensile stresses for a given amount of deformation will be higher than in a traditional concrete.

Additionally, HPC often exhibits faster strength gain than traditional concrete. The faster strength gain amplifies the effects of the thermal shock resulting from heat of hydration. As described above, if the concrete hardens before it cools to ambient temperatures, the stress-free state will be at the higher temperature. Therefore, the temperature experienced by the bridge will be lower than that at the stress-free state, and a length contraction will occur and induce tension in the deck.

Table 2.2 summarizes the effects of the above factors on deck restraint.

Table 2.2 Factors affecting deck restraint (Krauss and Rogalla 1996)

Factors	Effect			
	Major	Moderate	Minor	None
DESIGN				
Restraint	✓			
Continuous/simple spans		✓		
Deck thickness		✓		
Girder type		✓		
Girder size		✓		
Alignment of top and bottom reinforcement steel		✓		
Form type			✓	
Concrete cover			✓	
Girder spacing			✓	
Quantity of reinforcement			✓	
Reinforcement bar sizes			✓	
Dead-load deflections during casting			✓	
Stud spacing			✓	
Span length			✓	
Bar type (epoxy-coated vs. black)			✓	
Skew			✓	
Traffic volume				✓
Frequency of traffic-induced vibrations				✓
MATERIALS				
Modulus of elasticity	✓			
Creep	✓			
Heat of hydration	✓			
Aggregate type	✓			
Cement content and type	✓			
Coefficient of thermal expansion		✓		
Paste volume — free shrinkage		✓		
Water-cement ratio		✓		
Shrinkage-compensating cement		✓		
Silica fume admixture		✓		
Early compressive strength			✓	
HRWRA			✓	
Accelerating admixtures			✓	
Retarding admixtures			✓	
Aggregate size			✓	
Diffusivity			✓	
Poisson's ratio			✓	
Fly ash				✓
Air content				✓
Water content				✓
Construction				
Weather	✓			
Time of casting	✓			
Curing period and method		✓		
Finishing procedures		✓		
Vibration of fresh concrete			✓	
Pour length and sequence			✓	
Construction loads				✓
Traffic-induced vibrations				✓

2.4.3 Concrete Placement

Construction practices can affect the cracking potential of a deck. Improper finishing as well as the environmental conditions at the time of placement can increase the effects of early transverse cracking.

Weather and Time of Placement

To reduce cracking, concrete should be placed during cool weather. Placing concrete in cool weather will slow the hydration reaction and reduce the heat produced by the exothermic hydration process. As discussed previously, it is advantageous to reduce the heat of hydration to minimize early and residual thermal stresses. Placing concrete during mild weather, when the temperature extremes associated with the diurnal cycle are less pronounced, will help to reduce any early thermal loading.

Wind speed should also be carefully monitored. If the winds are sufficiently high, they can cause an increase in the evaporation rate from the surface of the concrete. If the evaporation increases, the propensity for plastic shrinkage cracking will also increase. Construction specifications should specify windbreaks or fogging if the wind speed exceeds the accepted limit of 0.2 lb/ft²/hr. This value may need to be halved for more exotic concrete mixes containing silica, HRWRA, or any other components that may decrease the concrete's ability to bleed.

The Portland Cement Association (PCA) recommends that the concrete temperature should be held below 80 °F and above 60 °F. The upper limit is established to prevent large thermal stresses during early strength gain. To reduce temperatures, concrete suppliers should shade the aggregates before mixing and replace a portion of the mix water with ice. Water misting is also recommended to reduce the evaporation during hot-weather concreting.

Finishing

Proper finishing can reduce the risk of early shrinkage cracking. The concrete should be thoroughly consolidated and smoothed with a float. Final floating should be delayed until the concrete has finished bleeding. Finishing before the concrete has bled will create a weakened crust on the surface that is susceptible to scaling. If finishing is to be delayed for any reason, mist should be applied to the deck using a fogging nozzle.

Curing

The first few days after concrete placement are critical to its strength, durability, permeability, and volume stability. All of these properties are enhanced with proper curing techniques. Curing immediately after strike off can reduce the probability that plastic shrinkage cracks will form.

Plastic Shrinkage Cracking

Plastic shrinkage cracks occur before the concrete has hardened if environmental conditions are poor, i.e., high temperature, low humidity, and high wind. Plastic shrinkage cracks may be large, but they are seldom structurally significant. They do, however, allow the ingress of moisture, which may corrode the reinforcing steel.

To reduce plastic shrinkage, it is necessary to reduce the evaporation at the exposed concrete surface. This may be done with membrane curing, fogging, or wet matt curing. Polyethylene sheeting is also effective at reducing the loss of bleed water through evaporation, but the sheeting can be cumbersome and impractical.

Continuous Moist Curing

Moist curing consists of water mist, water ponding, or saturated coverings. Any coverings should be pre-wetted so that no moisture is wicked up from the concrete. Moist curing will adequately mitigate evaporation, but it must be applied for a sufficiently long time to allow hydration to proceed to an acceptable level. Plastic sheet materials can also be used to provide proper curing to concrete. One example of this type is polyethylene film, as illustrated in Figure 2.7.

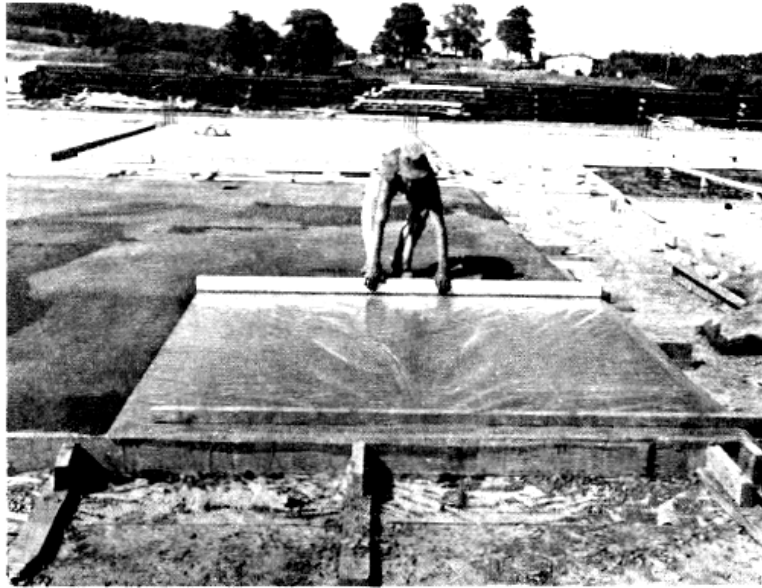


Figure 2.7 Continuous moist curing (polyethylene film) (Kosmatka 1988)

Membrane Curing

Membrane curing consists of spraying a compound onto the surface of the concrete to reduce water losses. Membranes can be applied sooner than wet mats, but they will not cure as well as the mats. The membranes can sufficiently limit the evaporation rates to acceptable limits, but membrane coverage often is not uniform, allowing greater evaporation in areas of poor coverage.

2.5 Methods of Controlling Shrinkage Cracking

Specific methods to properly control shrinkage cracking have been developed and researched. Conventional methods, which include proper material selection, mixture proportioning, and good construction techniques, can be used to a certain extent to control and limit the shrinkage cracking of concrete bridge decks. Unfortunately, because these methods are hard to control, and environmental conditions can vary so much, the shrinkage cracking cannot be entirely prevented. For example, bridge decks in hot, dry, and windy conditions can have much higher rates of water evaporation, thus making them more susceptible to shrinkage cracking. Innovative methods of controlling shrinkage cracking have been found in literature and developed by numerous researchers to help control and eliminate shrinkage cracking. These include using fiber-reinforced concrete, shrinkage-

reducing admixtures, shrinkage-compensating concrete, and extensible concrete. Both categories of methods are summarized in Table 2.3.

Table 2.2 Methods of controlling drying shrinkage

<i>Conventional</i>	<ul style="list-style-type: none"> • Proper Material Selection <ul style="list-style-type: none"> ○ Aggregates ○ Cement Type ○ Admixtures • Mixture Proportioning <ul style="list-style-type: none"> ○ Cement Content • Construction Techniques <ul style="list-style-type: none"> ○ Girders ○ Precast Panels ○ Formwork ○ Curing
<i>Innovative</i>	<ul style="list-style-type: none"> • Fiber Reinforcement <ul style="list-style-type: none"> ○ Polypropylene ○ Steel • Shrinkage-Compensating Concrete • Shrinkage-Reducing Admixtures • Extensible Concrete

2.5.1 Conventional Methods

Shrinkage cracking in concrete is currently being controlled through conventional methods, which consist of the proper selection of materials and concrete mixtures, along with good construction techniques.

Aggregates

The type of aggregate used in concrete mixtures, as well as the aggregate content, can influence the amount of shrinkage in concrete. Krauss and Rogalla (1996) found that

“aggregate type was the most significant [concrete material] factor affecting when concrete cracked” (pg. 24). Specifically, limestone-aggregate concretes proved to be the most resistant to cracking, while Eau Claire river gravel had the shortest time-to-cracking of the aggregates tested. Burrows (1998) also studied the effect of the type of aggregate used on the drying shrinkage of concrete. Again, limestone was found to be one of the aggregates exhibiting the least drying shrinkage while, in this study, sandstone exhibited the highest amount of drying shrinkage, as seen in Table 2.4. The amount of aggregate used in a concrete mixture can also help reduce shrinkage. Research has shown that a higher aggregate content can help reduce shrinkage.

Table 2.3 Aggregate type related to drying shrinkage (Burrows 1998)

Effect of type of aggregate on the drying shrinkage of concrete	
Aggregate	One-year shrinkage (percent)
Sandstone	.097
Basalt	.068
Granite	.063
Limestone	.050
Quartz	.040

Cement Content and Type

The amount of cement proportioned in concrete mixtures has an impact on the amount of shrinkage that concrete will undergo. Specifically, bridge deck cracking has been more prevalent when higher cement contents have been used. Bloom and Bentur (1995) concluded that mixes containing higher cement content cracked much sooner than those with lower cement contents. Krauss and Rogalla (1996), using a ring shrinkage test, also found that cracking occurred sooner as the cement content of the concrete mixes was increased. In the same report, the authors attributed the increased occurrence of bridge deck cracking to AASHTO’s 1973 action of increasing the cement content from 6 to 6.5 sacks per cubic yard.

Directly related to the amount of cement in a concrete mixture proportion is the actual water-cement ratio, which can also influence shrinkage behavior in concrete. Krauss and Rogalla found that “concrete with more water shrinks and creeps more than concrete with less water, but it may not crack sooner because it has higher creep” (pg. 26). Burrows

contends that although concrete mixes with lower water-cement ratios produce stronger concrete, that same concrete can be much more vulnerable to cracking (1998).

The type of cement used also plays an important role in reducing shrinkage cracking. Krauss and Rogalla noted that cements that are ground finer and have higher sulfate contents increase the early strength of concrete while also increasing the early modulus of elasticity and heat of hydration. For example, Type III cement could increase the risk of cracking because of the rapid early strength gains. Burrows also noted that the use of the compound tricalcium silicate (C3S), which has a high rate of hydration, produces higher stresses in the deck during cooling, as a result of thermal contraction.

As mentioned before, HPC has been found to cause a large number of shrinkage cracks in bridge decks. HPC has been defined as concrete with a high strength and a low water-cement ratio of 0.35 (Burrows 1998). This high early strength, and other guidelines for HPC “guarantee severe cracking from self-stresses of thermal contraction, autogenous shrinkage, and drying shrinkage” (pg. 31).

Admixtures

Fly ash, silica fume, set retarders, and accelerators are all admixtures that have been investigated for shrinkage by a number of researchers.

Fly ash has been found to reduce early concrete temperatures and the rate of strength gain, thus reducing deck cracking (Paillere et al. 1989). The process of using fly ash to replace cement is referred to as the creation of “extensible concrete” and is described in detail following this section.

Silica fume, a by-product of silicon metal or ferrosilicon alloys in electric arc furnaces, has been found to increase the cracking of bridge decks (NCHRP Report 410). The silica fume product has an average fineness of about two orders of magnitude finer than portland cement, which causes the bleeding rate of concrete to decrease, and the subsequent water loss resulting from evaporation cannot be replaced. The NCHRP report found silica fume to be a problem with cracking tendency specifically when the concrete is not cured properly. Krauss and Rogalla contend that while some researchers have found bridge deck cracking to be caused by silica fume, the issue is still in question.

Retarders have not been proven either to be the cause of concrete deck cracking or to help reduce the risk of thermal cracking. Plastic cracking could be caused by the addition

of retarders, while retarders have also been found to reduce the risk of thermal cracking by reducing early heat of hydration in concrete.

Construction Techniques

Construction practices and details can play a large role in affecting early transverse cracking. The type of girders and other construction methods used, along with curing and the environmental conditions at the time of bridge deck placement, can all factor into the cracking tendencies of the bridge decks.

Actual bridge design, including the type of girders used, along with other details, can significantly affect shrinkage stresses. The analytical studies performed by Krauss and Rogalla found that decks supported by steel girders usually have higher risks of transverse deck cracking and higher tensile stresses than decks with concrete girder construction. Concrete girders could induce severe localized transverse deck cracking over interior supports. Precast concrete panels, such as those commonly used in Texas, have been known to cause cracking problems near the supports of the panels, where they meet the concrete girders below.

Curing can also cause shrinkage cracking if proper procedures are not followed. Tan and Gjorv (1996) maintain that durable concrete is brought about through proper curing, which includes both the length of time that moist curing is applied and the temperature of curing.

Curing can especially affect bridge decks constructed with high cement content, low water-cement ratios, and HPC. Krauss and Rogalla found that the time-to-cracking of these types of concrete was significantly extended when wet curing was increased to 60 days. The Standard Specification manual, published by TxDOT in 1993, establishes a period of 4 to 10 days for curing all concrete. The curing is accomplished by either form curing (using stay-in-place forms) or water curing. Water curing includes wet matt curing, water spray, ponding, or membrane curing.

In addition to the construction practices and curing methods used, the environmental conditions play a vital role in determining the crack resistance of bridge decks. Concrete exposed to hot, dry, and windy conditions can experience shrinkage cracking from the high rate of evaporation of water from within the concrete. Increases in creep of a concrete can be attributed to higher temperatures; therefore, the temperature effects on shrinkage, creep,

and cracking must be taken into account. As previously mentioned, the ACI Committee 209 Report addresses this issue when calculating shrinkage and creep.

2.5.2 Innovative Methods

Because of the extreme variance of the conventional methods used to control drying shrinkage, innovative methods should be used to help reduce cracking tendencies of concrete. These include fiber-reinforced concrete, shrinkage-reducing admixtures, shrinkage-compensating concrete, and extensible concrete.

Fiber-Reinforced Concrete

Many studies have shown that adding fibers to concrete significantly reduces shrinkage cracking. Various parameters that were investigated include the addition of fibers at low volumes as compared to high volumes, as well as the different types of fibers to be used. Figure 2.8 shows two different types of polypropylene fibers, with the more durable fiber used for bridge deck applications on the left.



Figure 2.8 Polypropylene fibers

Research has shown that when low amounts of either polypropylene or nylon fibers (.1% by volume) are added to concrete, plastic shrinkage cracking in concrete can be prevented (Folliard and Simpson 1999). However, other properties of concrete, including drying shrinkage, are unaffected by the low volume of fibers added to concrete

(Gryzbowski and Shah 1990). Gryzbowski and Shah found that the addition of fibers as low as .25% by volume substantially reduced crack widths resulting from restrained drying shrinkage. Both steel and polypropylene fibers, when added to concrete at higher volumes, have been found to significantly reduce drying shrinkage cracking. The addition of fibers also improves the structural properties of concrete, including flexural strength and toughness, fatigue resistance, and impact resistance.

Shrinkage-Reducing Admixtures

A great deal of research has been performed regarding the development of SRAs used to control shrinkage cracking of concrete. These chemical admixtures, which are added to concrete at dosages of approximately 1–2 gallons per yd³, work by lowering the surface tension of the pore water inside hardened concrete (Folliard and Berke 1997). As previously described in this report, the pore water evaporates from capillary pores in the hardened concrete during drying, and the tension in the liquid is transferred to the capillary walls, resulting in shrinkage. Any stresses generated during drying are proportional to the surface tension of the pore water solution. This surface tension is lowered by SRAs, thus reducing the overall drying shrinkage. Therefore, there are fewer tendencies for shrinkage and resultant stresses to occur in the concrete when the pore water initially evaporates. SRAs affect the nature of the pore water, rather than limiting or reducing the amount of water from concrete during drying. The actual mechanism of shrinkage and stress generation is thereby affected by SRAs.

The same study by Folliard and Berke (1997) investigated the use of SRAs in typical bridge deck concrete. The results showed that SRAs reduced the total amount of shrinkage cracking while increasing the time it took for the concrete to crack. Additionally, Shah et al. (1997) showed that the addition of SRAs considerably reduced free shrinkage of concrete while significantly delaying the cracking of the concrete subjected to restrained shrinkage.

Shrinkage-Compensating Concrete

Shrinkage-compensating concrete is an innovative material that causes expansion of concrete during curing, which in turn reduces the effects of drying shrinkage. If the

expansion is properly restrained, the concrete will be subjected to compression the first few days after concrete placement. Pittman et al. (1999) found that this restraint can substantially reduce net shrinkage by testing a number of different shrinkage-compensating concrete mixtures. Although the shrinkage-compensating concrete will shrink as much as normal concrete once exposed to drying conditions, the net shrinkage will be negligible because the concrete started out with an initial expansion. Folliard et al. (1994) found that the shrinkage-compensating concrete will expand under restraint by about .04–.08% during the moist-curing period. Shrinkage-compensating concrete is typically designed so that residual expansion will continue to be present in the concrete after hydration, reducing shrinkage stresses altogether.

Construction techniques involving shrinkage-compensating concrete are critical for development of proper expansion. Moist curing for a period of at least 7 days has been suggested for the concrete. Pittman et al. (1999) noted that the shrinkage-compensating concrete bar specimens tested exhibited significant early expansion during the first 7 days, as long as moist curing was maintained for this period. Also noted in this study was the comparison of initial expansion from Type K cement, used for shrinkage-compensating concrete, as compared to Type I cement. When proper curing was used, Type K cement expanded up to four times as much as the Type I cement.

The mechanism of expansion in the shrinkage-compensating concrete is a result of the early formation and stability of ettringite. The ettringite crystals need water to expand, and therefore, moist curing must provide this water, or else minimal expansion will result. As mentioned previously, the ACI Committee 223 Report presents guidelines ensuring that the expansion can occur. In addition, the report presents information about the amount and location of reinforcing steel needed to provide proper restraint to the shrinkage-compensating concrete during curing.

Extensible Concrete

Extensible concrete is a term that refers to a combination of factors that are useful for reducing the cracking in concrete (Mehta 1993). Basically, some of the conventional materials and methods mentioned previously can be used in an innovative manner to achieve this type of behavior.

Specific emphasis is on the following properties:

- Low elastic modulus
- Low heat of hydration
- Low strength (low cement content)
- High creep
- High tensile strength and strain capacity
- High volumes of fly ash

A typical extensible concrete would have a high volume of fly ash, low cement content, and a high water-cement ratio. These factors would produce a low heat of hydration, thereby reducing thermal stresses in the concrete while also producing a low elastic modulus and high creep, minimizing shrinkage cracking. Burrows (1998) reinforced this idea by recommending the concrete industry move toward producing concrete with better extensibility, or resistance to cracking, by lowering the fineness, alkali, and C3S of the cement. A possible disadvantage with this method is the slower rate of construction, but delays can be minimized if this process is properly scheduled in the construction scheme. This method, if further researched and implemented, could prove to be economically feasible, possibly lowering the material costs for various jobs, depending on the availability of fly ash.

One property of extensible concrete that was briefly mentioned before is the use of high-volume fly ash (HVFA) in blended cements. Bouzoubaâ et al. (1998) states that in the 1980s, Canada Centre for Mineral and Energy Technology (CANMET) developed HVFA, by which 55% to 60% of the portland cement is replaced. The researchers conducted numerous tests on this concrete, and one of the conclusions was that the drying shrinkage strains were low. This result was attributed to the low unit water content used in the mixtures. The resistance to freezing and thawing cycles was also investigated, and the test prisms were found to perform excellently when subjected to the freezing and thawing cycles. The resistance to chloride-ion penetration was also found to be significantly higher for the fly ash concrete than for the control concrete in the test.

2.6 Conclusions

Restrained shrinkage cracking has been found to be a problem throughout the country. The causes of the cracking include shortcomings in materials, design practices, and construction techniques.

Careful selection of materials and mixture proportions can prevent cracking to some degree. Designers should be careful to specify materials with long-term performance in mind. Mixture proportions should be chosen to allow creep to occur enabling the structure to absorb shrinkage and thermal stresses without cracking. Further research into extensible concrete needs to be conducted. Extensible concrete has been a promising solution in laboratory evaluations, but we must conduct more research to investigate possible construction scheduling difficulties as well as the behavior of the material itself.

Further research also needs to be conducted on the laboratory tests themselves. Currently, there are several tests to determine the shrinkage characteristics of concrete. It is likely that no single test will accurately predict a concrete's shrinkage potential. A standardized battery of tests needs to be identified and put into widespread use; the battery of tests will need to be compared to field observations to improve their accuracy.

With the results of standardized testing, designers will have adequate tools to select materials for durability. Specifications could then be written with knowledge of the impact of cement content, water-cement ratio, admixtures, and strength gain. The concrete properties are the most influential in determining the shrinkage cracking potential. Sensibly choosing the correct material could eliminate some of the cracking problems.

Material properties also need to be considered during the structural detailing process. Some structural details, such as precast panels, are known to induce cracking. Details known to cause cracking need to be reevaluated in light of their impact on the material response. A large survey of the state of current bridges would need to be undertaken to determine problematic details.

Furthermore, full-scale testing should be performed to examine such details so that they may be improved. Such full-scale tests would incorporate the effects of construction practices.

Problems with construction techniques are known to influence cracking. The solutions to improper construction are also well documented. However, proper construction techniques are often sacrificed to expedite a project's completion. The results of a combination of improved materials specification, detailing, and construction techniques would be bridge decks which are less likely to crack, are more durable, and would require less maintenance.

3. Laboratory Evaluations

3.1.1 Introduction

The mechanisms involved in drying shrinkage as well as the various laboratory tests employed throughout the project to evaluate the drying shrinkage tendency of various innovative material based mixtures will be discussed in this chapter. Results for the innovative material laboratory mixtures will be given followed by an evaluation of these results.

3.1.2 Mechanism of Drying Shrinkage

Drying shrinkage of hardened concrete is caused by the loss of water from the capillary pores that are less than 50 nm in size. As the water in the capillary pores begins to evaporate, the force that was held in the surface tension of the water is transferred to the walls of the pore. Once the force has been transferred from the water to the pore wall, the pore will contract slightly. The bulk shrinkage of the concrete is due to the contraction of a large number of pores in the matrix. Typically drying shrinkage can cause a shrinkage strain of 400-1000 $\mu\epsilon$.

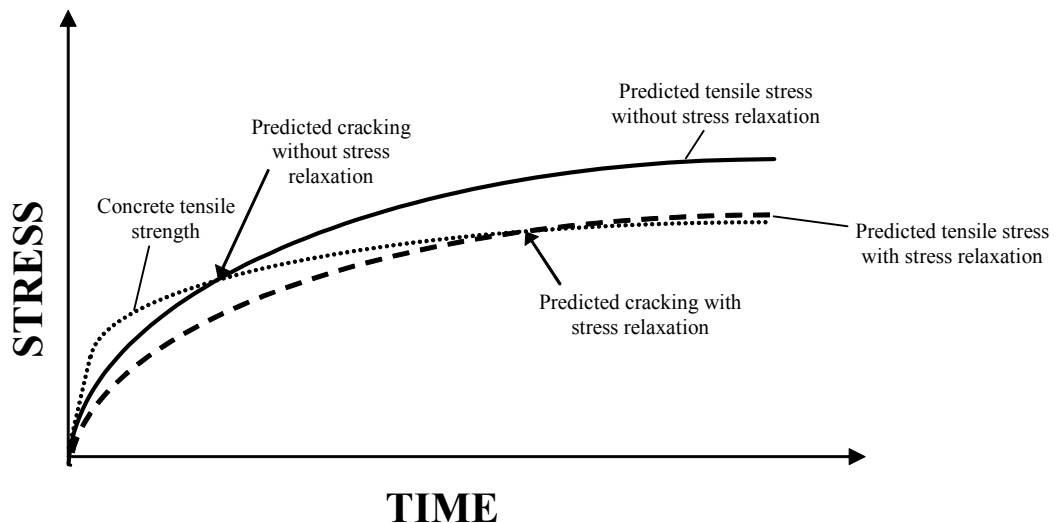


Figure 3.1 Time Dependence of Restrained Shrinkage on Creep (after Mehta and Monteiro 1993)

Drying shrinkage alone will not cause tension or cracking in concrete. The tensile stresses are a result of the restraint. Restraint prevents the concrete from changing volume as the drying shrinkage occurs. The amount of tensile stress developed is a function of restraint, shrinkage strain, and elastic modulus. Hooke's law dictates that stress is equal to the product of strain and elastic modulus ($\sigma = E\epsilon$). Thus, for a unit strain a material with a higher elastic modulus will be subjected to a higher stress than a material with a lower elastic modulus at the same strain level. However, if the stress is maintained, tensile creep can relieve some of that stress, and delay or even prevent cracking. Figure 3.1 illustrates this point graphically above. If a potential concrete mixture has a high creep capacity, shrinkage stress can be greatly reduced. Therefore, to prevent drying shrinkage cracking, a concrete mixture with a low elastic modulus, small shrinkage potential, and a high creep capacity is desired.

3.1.3 Innovative Methods Examined in the Study

For this study, four innovative materials were identified as candidates for testing. Initially, it was believed that each of these materials could serve to prevent or greatly reduce drying shrinkage cracking. Following are the four materials chosen:

- Fiber-Reinforced Concrete (FRC)
- Shrinkage-Compensating Concrete
- Extensible Concrete
- Shrinkage-Reducing Admixture

Each of these materials combats drying shrinkage cracking in a slightly different manner.

Fiber-Reinforced Concrete

To prevent drying shrinkage cracking, high volumes of fibers are needed. Typically, a high volume of fibers is approximately 1.5% of the volume of the concrete or 25 lbs of synthetic fibers per cubic yard of concrete. At such a high dosage, the fibers will enhance the structural properties of the concrete, especially increasing the fracture toughness. Fibers often are used in practice at a much lower dosage than described above. At a low dosage, often 0.1-0.3% by volume of fibers per cubic yard of concrete, only plastic shrinkage can be prevented with no increase in structural properties of the hardened concrete.

For this study, two mixtures using high volumes of different synthetic fibers were used. Both fibers were polypropylene and 2 in. in length. One mixture used a monofilament fiber manufactured from a polymer blend. This fiber has the ability to partially fibrillate upon mixing in order to increase the anchorage of the fiber in the matrix. This fiber will be termed F-I for the purposes of this study. The second type of fibers, F-II, is a sinusoidal-shaped, high-performance fiber. Both fibers were dosed at 15 lbs/yd³.

Shrinkage-Compensating Concrete

Shrinkage-compensating concrete (SCC) is a concrete made with an expansive agent, typically Type K cement. Ettringite crystals form in concrete, soon after the cement is exposed to water. Thereafter, hydration proceeds and the ettringite becomes unstable and decomposes into monosulfate hydrate. However, when Type K cement is used, enough aluminates are present to maintain the stability of the ettringite crystals. Once the crystals are exposed to water they expand causing a volume increase in the concrete. Proper curing is essential to the use of shrinkage compensating cement. To gain the benefit of SCC, it must be restrained against expansion as it is curing. The restrained expansion will place the concrete into compression, similar to that used in prestressed concrete, but much smaller in magnitude. Once the SCC is exposed to drying conditions it will shrink just as a normal concrete mixture. However, the shrinkage will not be enough to overcome the expansion that has already occurred. Therefore, the concrete will have a net compression over its life, thus preventing cracking due to restrained shrinkage.

For this study, the SCC was identical to the control mixture, except that the Type I cement in the control mixture was replaced pound for pound with Type K cement.

Extensible Concrete

The term *extensibility* refers to the combination of factors that will reduce cracking, specifically, low elastic modulus, high creep capacity, and tensile strength (Mehta 1993). Extensible concrete should be able to undergo large deformations without cracking. High volumes of fly ash can produce an extensible concrete. The author considers high volumes of fly ash to be those in which at least 50% of the cement is replaced with ash. As part of this study, an extensible mixture was created using 55% cement replacement with Class F fly ash from a local producer.

Shrinkage-Reducing Admixture

Shrinkage-reducing admixtures (SRA) work by reducing the surface tension of water. As described previously, the water surface tension is one of the driving forces behind drying shrinkage. By reducing the surface tension, drying shrinkage is also reduced. In this study, a commercially available SRA made from a blend of propylene glycol derivatives was used. The admixture was a 100% active liquid with a specific gravity of 0.95 and moderate water solubility. It was dosed at 1.5 gallons per cubic yard as per the manufacturer's recommendation.

3.1.4 Laboratory Testing

Several tests must be performed on the concrete in order to assess its performance in regards to drying shrinkage cracking. First, testing of the typical engineering properties of the mixture must be performed. These properties include compressive strength, tensile strength, and elastic modulus. In addition, tests were conducted to determine the free shrinkage, restrained shrinkage, compressive creep, and chloride ion permeability. Each test is listed below along with the standard under which the test was performed.

Table 3.1 Laboratory Test Methods

Test Number	Description
ASTM C39	Compressive Strength of Concrete
ATM C496	Splitting Tensile Strength of Concrete
ASTM C469	Modulus of Elasticity of Concrete
ASTM C512	Creep of Concrete in Compression
ASTM C1202	Rapid Chloride Permeability
ASTM C157	Drying Shrinkage of Concrete (Free Shrinkage)
ASTM C878	Restrained Expansion of Shrinkage-Compensating Concrete
AASHTO PP34	Restrained Shrinkage Cracking of Concrete

Compressive Strength, Tensile Strength, and Elastic Modulus

The compressive strength was determined by averaging the failure loads of three cylindrical specimens as per ASTM C39. The tensile strength was determined using the splitting cylinder method. In this method, the cylinder is loaded such that a compressive load is applied across a diameter of the cylinder. The diametrically opposed compressive

forces result in a near uniform field of tension in the center of the cylinder. The uniform stress field produces a crack, and results in failure of the cylinder. The elastic modulus was determined in accordance with the specification. However, more data points were taken in order to get a more complete description of the modulus of elasticity. All of the specimens used for the above tests were standard 4 in. x 8 in. cylinders which were moist cured at 73 °F until from the time of final set until testing. Tests were performed at concrete ages of 3, 7, 28, and 91 days to capture the time dependence on all properties.

Drying Shrinkage

Drying shrinkage (sometimes called free shrinkage) tests were performed on concrete prisms measuring 3 in. x 3 in. x 10 in. Two metal studs were cast into the square faces of the prism to serve as reference point throughout the testing. One day after casting, the prisms are demolded, measured, and placed in a lime-saturated water solution at 73 °F for seven days. After the seven-day curing period, the prisms are removed from the limewater bath and placed in the drying shrinkage room. The drying shrinkage room is a large environmental chamber that is maintained at 73 °F and 50% relative humidity as required in ASTM C157.

Once exposed to the lower humidity in the chamber, the prisms begin to shrink. While in the chamber, the prisms are supported by two pieces of plastic pipe. The plastic pipes allow dimensional change without inducing any stresses, producing a true free shrinkage response (Figure 3.2). The shrinkage is measured as the change in the length of the specimen between the two studs that were cast into the prism. The prisms are measured daily for a week, weekly for a month, and monthly thereafter. Three prisms are cast for each mixture.



Figure 3.2 Free Shrinkage Prism (ASTM C157)

Restrained Expansion of Shrinkage-Compensating Concrete

The aforementioned free shrinkage test can not be applied to shrinkage compensating cement because the SCC must be restrained against expansion to obtain the benefit of shrinkage compensation. To achieve the restraint, the SCC is cast around a threaded rod that has a steel plate attached to each end. The threaded rod passes through the prism, and the steel plates on the ends serve as the restraint. The restraining cage is self-reacting and is pictured in Figure 3.3. The curing and measurement regime for the SCC prisms is identical to that of prisms containing traditional concrete mixtures.



Figure 3.3 Mold and Restraining Cage for SCC Prism (ASTM C878)

Creep of Concrete in Compression

Creep tests were performed in order to assess the creep potential of the candidate mixtures. On the day that the creep tests were to begin, stainless steel locating disks were attached to the specimens using a quickset epoxy. These locating disks are used with a Demec mechanical strain gage to determine the length change of the cylinders throughout the test. The ASTM specification requires that the measuring device used in creep testing be accurate to $10 \mu\epsilon$. The Demec gage used for these tests exceeded this requirement. To perform creep tests, one must first determine the compressive strength of the cylinders at the age of creep testing. For this study, the ages of creep testing coincided with the ages of testing for the engineering properties; this was addressed properly.

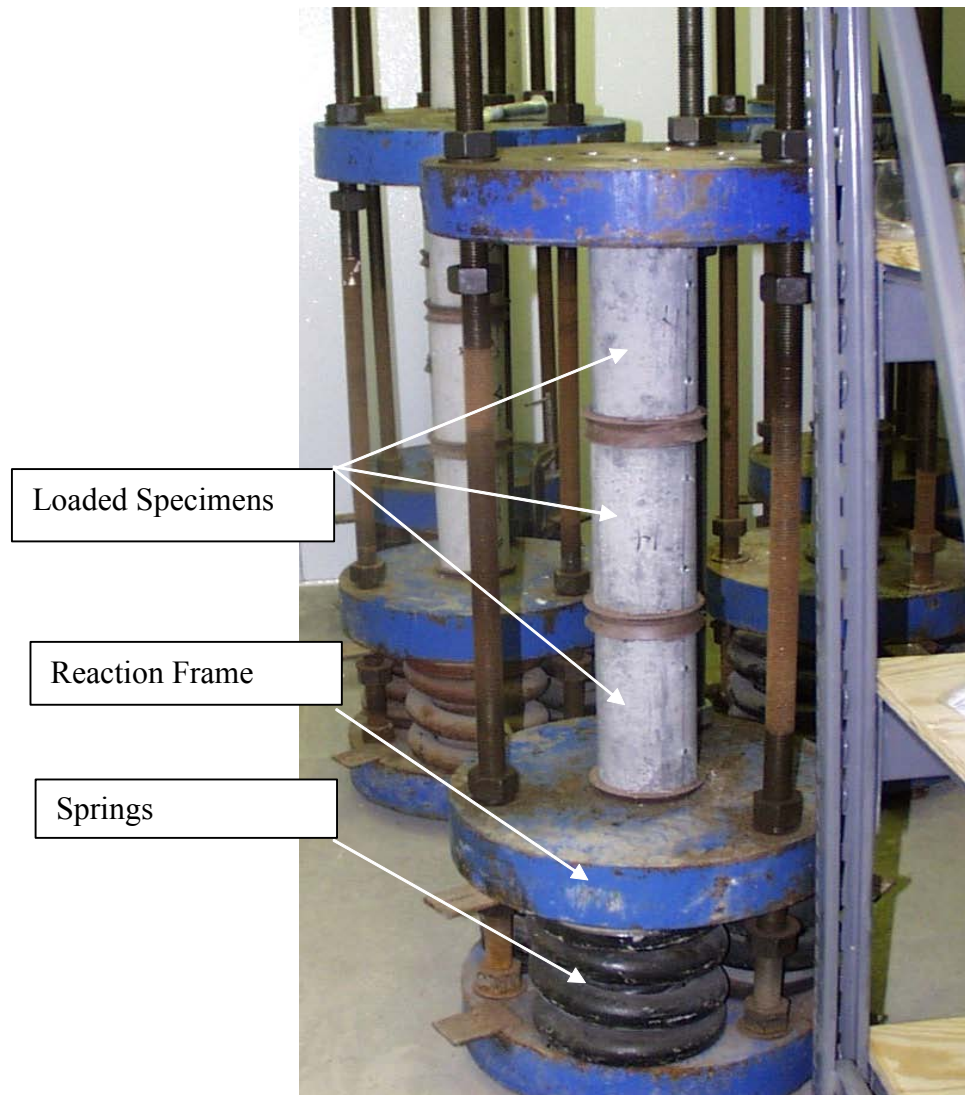


Figure 3.4 Creep Frame and Specimens (ASTM C512)

Once the compressive strength has been determined, cylinders that have had locating disks attached to the surface are placed in a creep frame. A small hydraulic ram is used to compress the creep specimens such that the load is 40% of the compressive failure load. After this load has been achieved, reaction nuts are tightened against a bear plate to maintain the load indefinitely and the ram can be removed. Figure 3.4 depicts a creep frame with three cylinders being tested. Once the load has been transferred from the portable ram to the reaction frame, the springs at the bottom of the frame ensure that a constant load is applied even as the concrete test cylinders deform. The mechanical strain gage is used to measure the distance between the locating disks both before and after the

load is applied. Afterwards, the distance between the disks are measured daily for one week, weekly for one month, and monthly thereafter.

Combined Effects of Drying Shrinkage and Creep

The creep tests are performed in the drying shrinkage room. Due to the humidity conditions within the room, the cylinders are subject to shrinkage as well as creep. To determine the shrinkage that is occurring, two cylinders prepared identically to the cylinders that were loaded are prepared and left in the drying shrinkage room, but remain unloaded. By measuring the change in length of these unloaded cylinders, the drying shrinkage can be measured and subtracted from the creep readings from the loaded cylinders to produce a true creep measurement. The geometry of the loaded and unloaded cylinders is identical, as is the moisture history. Consequently, it is assumed that all cylinders will undergo the same shrinkage.

Permeability

The rapid chloride ion penetration test (ASTM C1202) was also performed on each mixture. This test uses an electric current to drive chloride ions into a concrete sample. The charge passed through the sample during a six-hour period is measured and can be used to infer the permeability of the concrete. For this test, the specimen is a two-inch thick disk that has been cut from a 4 in. x 8 in. cylinder. The experimental set-up can be seen in Figure 3.5.

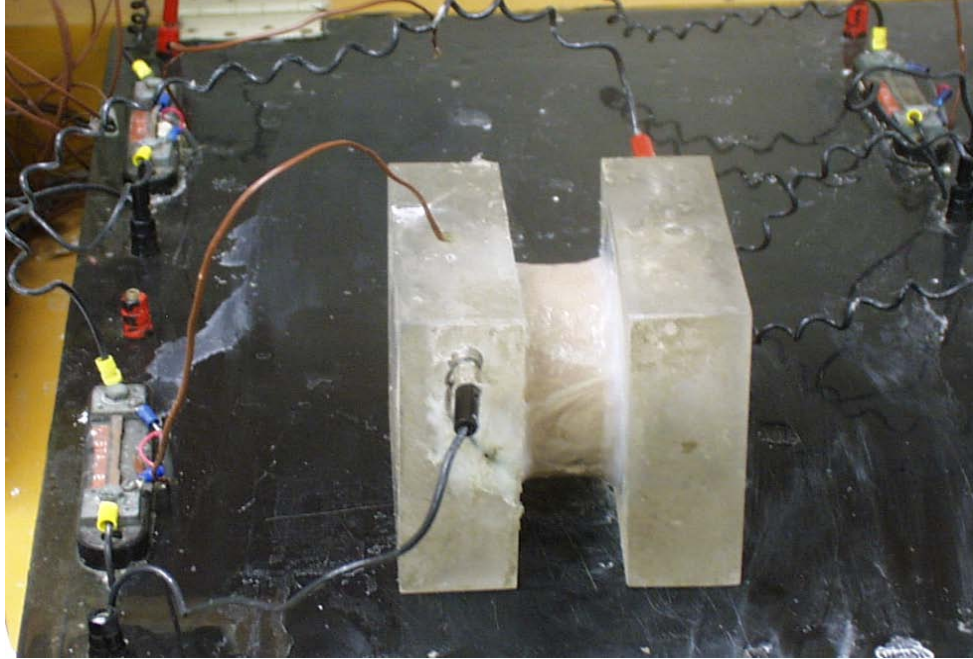


Figure 3.5 Rapid Chloride Ion Penetration Test Setup (ASTM C1202)

Restrained Shrinkage

None of the tests previously discussed truly capture the interrelation between strength development, shrinkage, and creep. In an actual structure, all three mechanisms occur simultaneously and interact in ways that are difficult to predict. To address the inability to test the interaction of all these phenomena, AASHTO has adopted a provisional test to fill the void. The provisional test, AASHTO PP34, was based on work presented in NCHRP Report 380. The test involves casting a concrete ring around the perimeter of a steel ring. A photo of the casting process and a schematic drawing of the specimen can be seen in Figure 3.6. This restrained shrinkage test has been developed by a number of researchers in the past (Weiss et al. 1998; Folliard and Berke 1997) as an accurate method for predicting the length of time until the concrete cracks.

As per the specification, the ring is cured at 73 °F and 100% relative humidity for a period of 24 hours. After the curing period, the top surface of the ring is coated with a waterproof sealant and the ring is placed in the drying shrinkage room (73 °F, 50% relative humidity). The sealant eliminates drying from the top surface, and a wooden base eliminates drying from the bottom surface. As a result, the concrete ring is allowed to dry only from its circumferential face. When the concrete shrinks due to water loss, the ring is

slowly placed into tension as the drying front propagates radially inward toward the center of the ring. Over time the tensile stresses are relaxed due to creep. After some time has elapsed, the tensile strain in the ring will exceed the tensile strain capacity of the concrete producing a crack. The time elapsed from the time of exposure to drying conditions until the time of the first crack is then recorded.

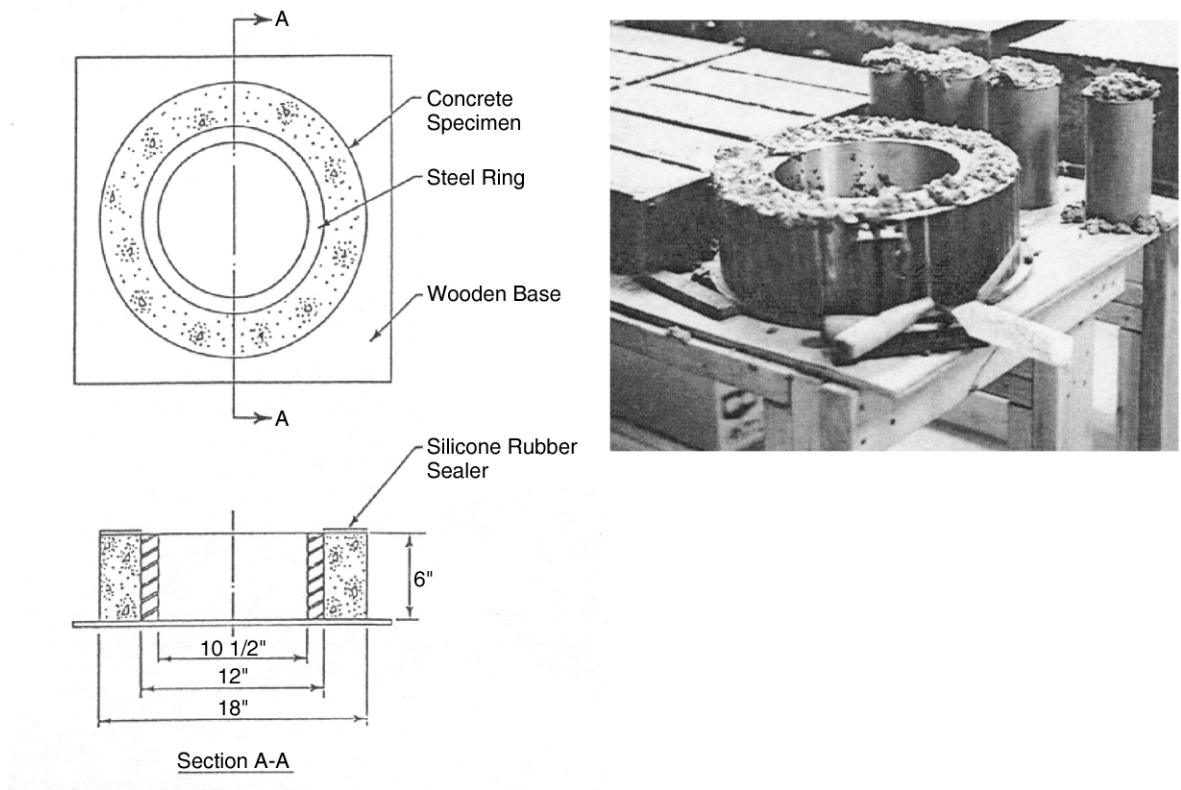


Figure 3.6 Schematic Drawing of AASHTO PP34 Specimen (Shah 1997; Poston 1998)

In order to detect cracks accurately, four strain gages are attached to the inner surface of the steel ring. The gages are at mid-height of the steel ring and spread equally around the circumference. These strain gages are measured automatically every half hour. The specification defines a crack as a decrease of $30 \mu\epsilon$ or more between successive readings on one strain gage. For this study, the researchers visually inspected the rings daily in addition to monitoring the digital strain data.

In this test, a minimal amount of curing and a large amount of restraint are used to provide a worst-case scenario in order to accelerate cracking. It is believed that such harsh

testing is needed to provide meaningful results. If, however, less restraint and more curing were used, the rings would not crack and provide little meaningful data. Also, if a potential concrete mixture performed well under the specified laboratory condition, it likely will perform well under more preferable conditions, which are expected in the field.

3.1.5 Experimental Program

Eight concrete mixtures made up the core of this study. The mixture proportions for the laboratory mixtures are presented below in Table 3.2.

Table 3.2 Mixture Proportions

Mixture Description	Cement lb/yd ³	Class F Fly Ash lb/yd ³	Silica Fume lb/yd ³	Coarse Aggregate lb/yd ³	Fine Aggregate lb/yd ³	Water lb/yd ³	HR WR oz./cwt
Control	611	0	0	1850	1300	275	2
HPC	696	0	56	1850	1193	263	18
Silica Fume	609	0	49	1850	1300	275	10
FRC, F-I	611	0	0	1850	1300	275	9
FRC, F-II	611	0	0	1850	1300	275	7
SRA	611	0	0	1850	1300	269	0
Type K	611	0	0	1850	1300	275	9
HVFA	275	336	0	1850	1300	244	9

Note: HRWR was dosed at fluid ounces of admixture per 100 lb of binder (oz./cwt)

The control, HPC, and silica fume mixtures were chosen because they represent typical bridge deck mixtures used throughout Texas and the nation. The control mixture conforms to TxDOT Class S concrete, which is used for normal deck construction. The HPC mixture was based on the HPC concrete that was used to cast the deck on the Louetta Road Overpass. Recall that the Louetta Road Overpass was inspected as part of the field investigation, and the results are presented in chapter four. The silica fume mixture is typical of deck concrete mixtures used in other states; it is a 7-sack mixture with 7.5% silica fume replacement of the cement.

Each of the other five mixtures was used to determine the effect of an innovative material. Each particular innovative material, as well as the dosage, was outlined earlier in this chapter.

Materials

Because the test results of the laboratory specimens are heavily dependent on the materials used, it is important to discuss the specific materials utilized throughout the project. Each mixture component was chosen at the beginning of the project and kept constant throughout the duration of the laboratory testing. These mixture components include coarse and fine aggregate, two different types of cement (Type I/II and Type K), supplementary cementing materials (SCMs), fibers, and various chemical admixtures.

Aggregate

Table 3.3 Aggregate Properties

Property	Sieve Size	Fine Aggregate (ASTM C33)	Coarse Aggregate (ASTM C33, Size 67)
Cumulative Percent Retained on Sieve Size:	19.0 mm		8
	12.5 mm		46
	9.5 mm		70
	4.75 mm	0	94
	2.36 mm	8	99
	1.18 mm	30	100
	600 μm	54	
	300 μm	83	
	150 μm	97	
	75 μm	100	
Bulk Specific Gravity		2.64	2.62
Fineness Modulus		2.72	7.17
Absorption Capacity (%)		0.8	0.8

Excluding the large-scale bridge deck mixtures and the HPC mixture, the same coarse and fine aggregate content and type were used throughout the project. Deviations in the coarse and fine aggregate quantities were necessary to allow the mixture to function properly. For instance, the HPC mixture fine aggregate was reduced to allow for the higher fines content due to higher cement content. The coarse aggregate used in every mixture for laboratory specimens is natural river gravel and conforms to ASTM C33 (Size 67). Meanwhile, the fine aggregate consisted of river sand and conforms to ASTM C33 (Brown, 2002). Both coarse and fine aggregate properties are listed in Table 3.3. The large-scale

bridge deck mixtures will be discussed separately in chapter five, Large-Scale Bridge Decks.

Cement

Except for the shrinkage compensating concrete (Type K) mixture, all the cement was Type I/II. Furthermore, all the cement was taken from the same batch and producer so that deviations in product quality are minimized (Brown 2002). A table outlining the cement chemistry of the cement used throughout the laboratory program setting can be found in Table 3.4.

Table 3.4 Cement Chemistry (Brown and Sellers 2002)

Chemical Analysis	Type I/II Cement %	Type K Cement %
SiO ₂	19.35	19.5
Al ₂ O ₃	5.29	4.96
Fe ₂ O ₃	2.45	3.10
CaO	64.21	-
MgO	1.15	1.35
SO ₃	3.51	6.80
Na ₂ O	0.085	-
K ₂ O	0.98	-
Loss on Ignition	3.25	1.31
Compound Composition	%	%
C ₃ S	65.32	-
C ₂ S	6.20	-
C ₃ A	10.03	-
C ₄ AF	7.45	-

Supplementary Cementing Materials (SCMs)

Several SCMs, such as Class C fly ash and silica fume were utilized to explore the effectiveness of SCMs to control drying shrinkage cracking. The fly ash is classified as Class F fly ash and conforms to ASTM C618 standards. Its chemical composition is given in Table 3.5. The silica fume, used in the HPC mixture, is of a dry, densified type and is also presented in Table 3.5 (Brown 2002).

High-Range Water Reducer

The superplasticizer (HRWR) used for the necessary mixtures was a commercially available, naphthalene sulfonate formaldehyde-type high-range water reducer, complying with ASTM C494 Type A and F standards. The HRWR was dosed while mixing to achieve a desired slump. The target slump for all mixtures was 5-8 in.

Table 3.5 Fly Ash and Silica Fume Chemistry (Brown and Sellers 2002)

Chemical Analysis	Class F Fly Ash %	Silica Fume %
SiO ₂	54.1	93
Al ₂ O ₃	26.2	
Fe ₂ O ₃	3.0	2.1
CaO	10.8	0.8
MgO	2.4	0.3
SO ₃	0.3	0.2
Na ₂ O	-	0.1
K ₂ O	-	1
Loss on Ignition	0.1	2.4
Compound Composition	%	%
C ₃ S	-	-
C ₂ S	-	-
C ₃ A	-	-
C ₄ AF	-	-

Fibers

The fibers used during the laboratory program involved two different types of fibers, both of which were two-inch-long polypropylene synthetic fibers. One mixture, termed F-I for this report, used a monofilament fiber manufactured from a polymer blend. This fiber has the ability to partially fibrillate upon mixing in order to increase the anchorage of the fiber in the matrix. The second type of fibers, F-II, is a sinusoidal-shaped, high-

performance fiber (Brown 2002). Both of these fibers, F-I and F-II, were dosed at 15 lbs/yd³, a relatively high dosage.

3.1.6 Mix Designs

The eight primary laboratory mixture designs, which were derived from a thorough literature review performed by Greg Sellers and Mike Brown, are all similar in basic proportioning and only deviate from one another when necessary to obtain a desired characteristic. For example, as mentioned in the coarse and fine aggregate paragraph above, the amount of fine aggregate was decreased in the HPC mixture to account for the increased presence of fines found in the cement and silica fume.

Table 3.6 outlines the eight primary mixtures and their respective material proportioning. Several repeat mixtures were performed, denoted by the roman numeral following the mixture name, in order to ensure repeatability and to correlate the results from various mixtures. For instance, each time a repeat mixture was performed, such as HPC II, a corresponding control mixture was made to verify its repeatability.

Table 3.6 Mixture Proportions for Laboratory Specimens

Mixture Description	Cement lb/yd³	Class F Fly Ash lb/yd³	Silica Fume lb/yd³	Coarse Aggregate lb/yd³	Fine Aggregate lb/yd³	Water lb/yd³	HR WR oz./ cwt
Control I, II, III, IV	611	0	0	1850	1300	275	2
HPC I, II	696	0	56	1850	1193	263	18
Silica Fume	609	0	49	1850	1300	275	10
FRC, F-I	611	0	0	1850	1300	275	9
FRC, F-II	611	0	0	1850	1300	275	7
SRA	611	0	0	1850	1300	269	0
Type K	611	0	0	1850	1300	275	9
HVFA I, II, III	275	336	0	1850	1300	244	9

Note: HRWR was dosed at fluid ounces of admixture per 100 lb of binder (oz./cwt)

3.2 Experimental Procedures

In addition to the standard battery of concrete performance tests such as compressive strength, modulus of elasticity, and split-tensile strength, several other tests were performed that focus on the direct measurement of properties of concrete relating to early-age drying shrinkage cracking, such as creep, free shrinkage, and restrained drying shrinkage time-to-cracking. These test methods, discussed in more detail in the results and discussion section, were chosen based on an extensive literature review to identify the ability of the tests to predict the susceptibility of a mixture to drying shrinkage cracking.

The laboratory tests used throughout the project can be categorized into two broad groups based on the plasticity of the concrete: fresh properties, or properties of the concrete while still in a plastic state, and hardened properties, or properties that deal with how concrete behaves after initial set.

Fresh properties used for the purposes of the laboratory program consist of slump, air, unit weight, and temperature. Tight control of these fresh concrete properties was possible due to the controlled conditions during mixing, as well as the relatively small size of the mixture (5.1 ft³). Since the laboratory mixing room was kept constant at 73 °F, it was possible to maintain identical mixture conditions for each mixture as well as make sure that mixture materials, such as the fine and coarse aggregate, were at a known temperature and moisture before mixing began. The opposite is true in the field, where conditions of the concrete are not as easily controlled and large quantities are typically involved. Hardened properties consist of numerous tests and are performed at standard time intervals after the concrete mixture has hardened, in agreement with the appropriate standardized test method being used. Table 3.7 gives a comprehensive list of the test methods used throughout the laboratory program of the project.

Table 3.7 Laboratory Program Test Methods (Brown 2002)

Fresh Concrete Properties
AASHTO T119 – Slump of Concrete
AASHTO T152 – Air Content
ASTM C138 – Unit Weight, Yield, and Air Content
ASTM C1064 – Temperature of Fresh Concrete
Hardened Concrete Properties
AASHTO T22 – Compressive Strength of Concrete
AASHTO T198 – Splitting Tensile Strength of Concrete
ASTM C469 – Modulus of Elasticity of Concrete
ASTM C512 – Creep of Concrete in Compression
AASHTO T160 – Drying Shrinkage of Concrete (free shrinkage)
AASHTO PP34-99 – Restrained Shrinkage Cracking of Concrete (steel ring method)
ASTM C878 – Restrained Expansion of Shrinkage-Compensating Concrete
AASHTO T277 – Rapid Chloride Permeability

3.3 Results and Discussion

Fresh Concrete Properties

Tests were conducted on the plastic concrete to ensure quality control and uniformity among the mixtures. Tests for slump, air content, and unit weight were performed to meet this goal. All the fresh concrete tests were performed to meet the appropriate ASTM specifications. A roller meter was used to determine the air contents. All of the fresh concrete had an initial temperature of 73 °F; the mixing room is carefully controlled to maintain that temperature. All materials were placed inside the mixing room 24 hours before mixing to ensure that all the component materials were at the proper temperature at the time of mixing. The fresh concrete properties for the eight mixtures are presented below in Table 3.8.

The results for the fresh concrete properties demonstrate that there was good uniformity among the mixtures. All eight mixtures had similar unit weight, air content, and slump. For this project, the target slump range was 5-8 in.

Table 3.8 Fresh Concrete Properties

Mixture Description	Slump (in.) ASTM C143	Air Content (%) ASTM C138	Unit Weight (lb/yd ³) ASTM C138
Control	5.25	3.5	145.6
High Performance	6	1.75	146.0
Silica Fume	7.25	2.75	143.3
FRC, F-I	5	2.25	144.6
FRC, F-II	6	2.75	145.3
SRA	5.5	2.75	147.8
Type K	6.25	3.75	145.8
HVFA	7	2.75	148.0

Hardened Concrete Properties

Compressive Strength, Modulus, Split-Tensile Strength

Based on the literature review and familiarity with the various characteristics that affect concrete's compressive strength, modulus of elasticity, and tensile strength, the results observed for the laboratory program mixtures agree with expected behavior.

Compressive Strength (AASHTO T22)

Figure 3.7 is a plot of the compressive strengths of the primary mixtures at various ages. As expected, both HPC I and HPC II mixtures had the highest 3-day through 91-day compressive strengths compared to all the other mixtures. These high compressive strengths are due to the relatively low W/C ratio, which generally causes a decreased porosity and increased compressive strength. Furthermore, the high-volume fly ash (HVFA) gained the most relative compressive strength during the testing period between the 3rd and 91st day ages. This behavior agrees with the typical behavior of Class F fly ash in that it exhibits more strength gain at later ages, typically after the 28th day. In fact, HVFA gained over 135% of its original 3-day strength by the 91st day, whereas all the other mixtures gained around 40% of their original 3-day strengths by the 91st day. On the low end of the relative percent strength gain, both HPC I and HPC II mixtures gained about 28% of their original 3-day compressive strength by the 91st day. Therefore, even though HPC I and HPC II gained the least amount of relative compressive strength between the 3rd and 91st days, they had the highest absolute compressive strengths. This demonstrates

the relatively quick strength development of HPC and the other laboratory mixtures as compared the relatively slow strength gain of HVFA.

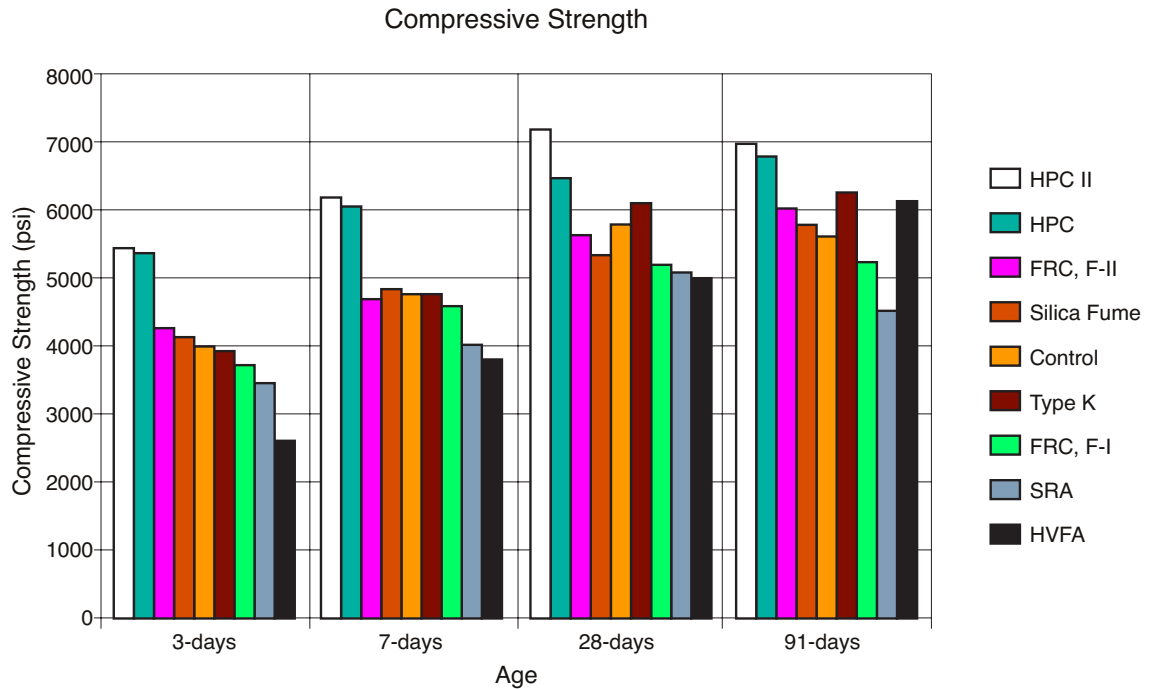


Figure 3.7 Compressive strength for all mixtures at various ages

Modulus of Elasticity (ASTM C469)

The modulus of elasticity provides an important clue into the prediction of the behavior of the concrete during its first few weeks, when the majority of drying shrinkage takes place. Intuitively, a higher modulus of elasticity at an early age means that for a given strain the corresponding stress in the material will be larger. If the concrete is not able to creep adequately and does not have the required tensile strength to resist the stress then a crack will develop to relieve this stress.

Based on Figure 3.8, it is difficult to identify any clear trends, except that both HPC I and HPC II have the highest early age modulus compared to the rest of the mixtures. This agrees with the fact that HPC had the highest early strength of any of the mixtures. This is true, in general, that a higher modulus of elasticity in concrete usually means a higher compressive strength and vice versa. For example, the percent increase in the modulus of elasticity follows a similar trend as that for the percent increase in the compressive strength

since HVFA has the highest relative percent increase in modulus and HPC I and II has the lowest relative percent increase in the modulus.

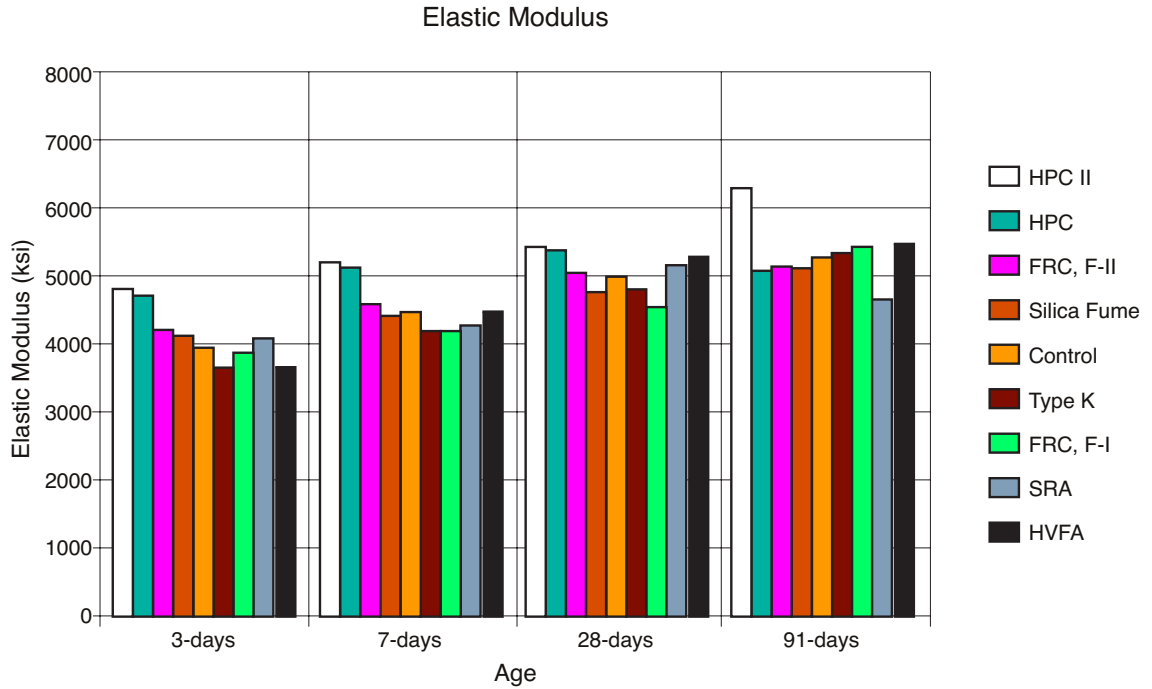


Figure 3.8 Elastic modulus for all mixtures at various ages

Tensile Strength (Split-Tensile Method, AASHTO T 198)

Ultimately, it is the relatively poor tensile strength of concrete that permits the majority of cracks to form, which therefore leads to poor durability. Tensile strength is also one of the most difficult properties to measure directly using experimental methods, and must be done indirectly, such as with the modulus of rupture or split-tensile test. It is impossible to predict, based solely on the tensile strength of concrete, whether a specimen will crack since cracks will typically form around flaws and flaws are difficult, if not impossible, to identify until after failure.

The rate at which a specimen develops tensile strength is just as important as what that tensile strength value is. High early strength gain can be both an advantage and a disadvantage for cracking. The advantage is that the concrete will be able to resist a higher stress before cracking. The disadvantage is that cracking is able to occur much sooner since the concrete is stiffer and can crack. Less stiff concrete will not crack as readily because it is more “flexible” and can handle more deformation before cracking.

A mixture that gains tensile strength quickly, especially during the first few days, means that it can also crack earlier than a mixture that is more flexible and may not form a crack as early. As expected, the HPC mixture had the highest absolute tensile-strength value at an age of 3 days, the earliest reading available for the laboratory program specimens (see Fig. 3.9). However, HVFA eventually eclipses this value by the 91st day and actually has both the largest relative percent increase in tensile strength and the highest absolute tensile strength.

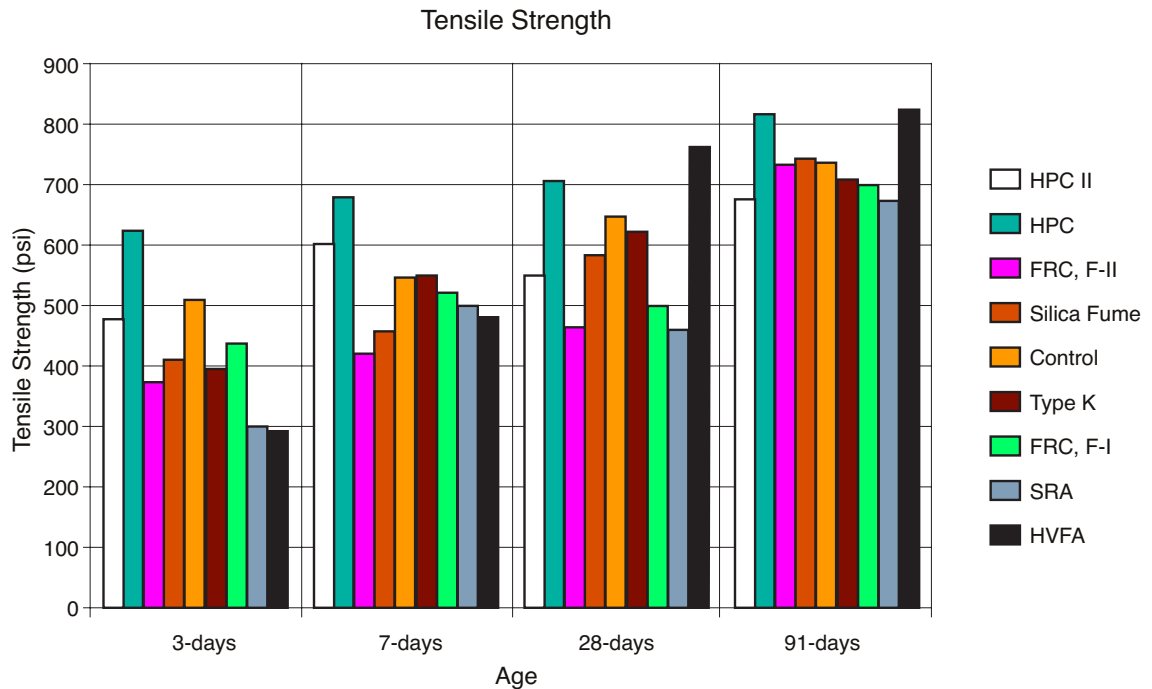


Figure 3.9 Split tensile strength of all mixtures for various ages

Creep of Concrete in Compression Test Results

Due to space limitations, only six of the eight mixtures were tested to determine their creep characteristics. The six mixtures that were creep loaded were: control, FRC F-I, Type K, SRA, HPC, and HVFA. Additional creep frames were unavailable to load the remaining two mixtures (FRC F-II and silica fume).

For each mixture, three cylinders were loaded at ages of three, seven, and twenty eight days. Each mixture occupied three creep frames, one per age of loading, for a total of 18 frames used in the experiment. The following plots depict the specific creep for each loading age as a function of time for each of the six mixtures.

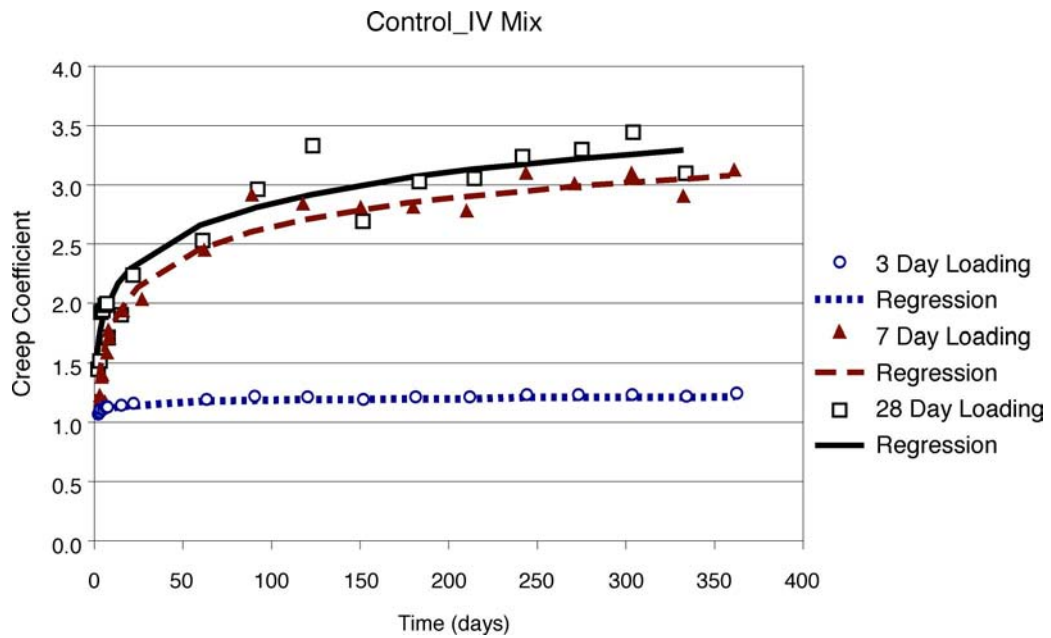


Figure 3.10 Coefficient as a function of time for Control IV mixture

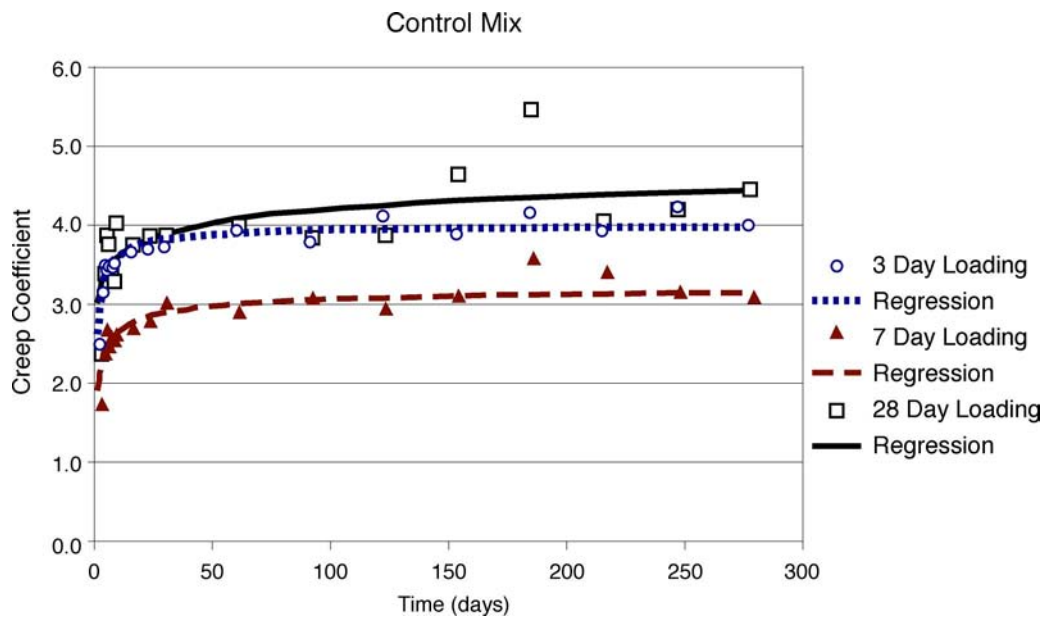


Figure 3.11 Coefficient as a function of time for Control mixture

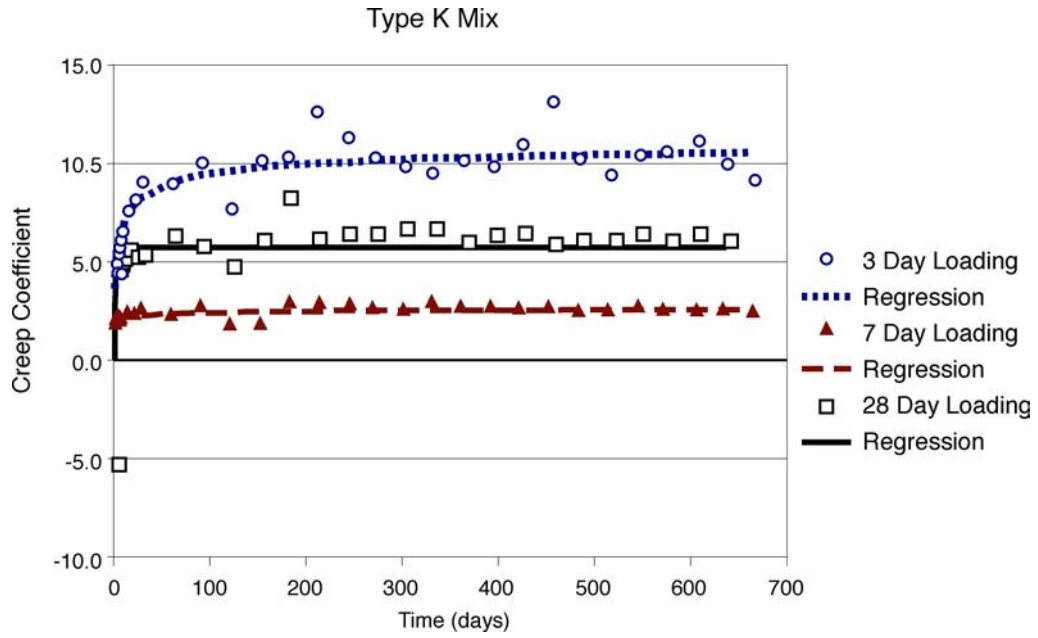


Figure 3.12 Coefficient as a function of time for Type K mixture

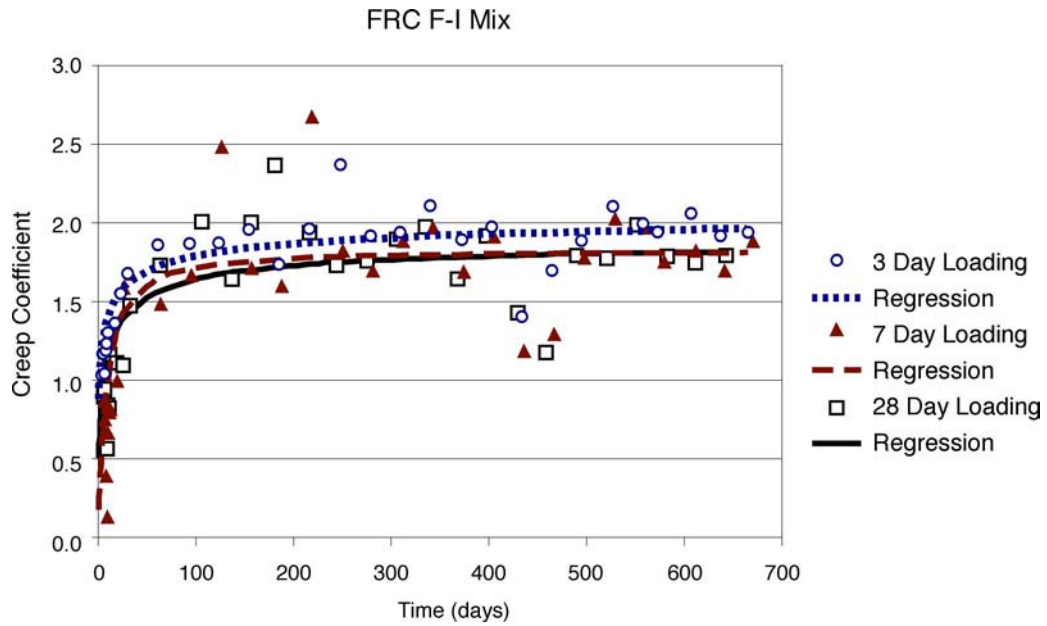


Figure 3.13 Coefficient as a function of time for FRC F-I mixture

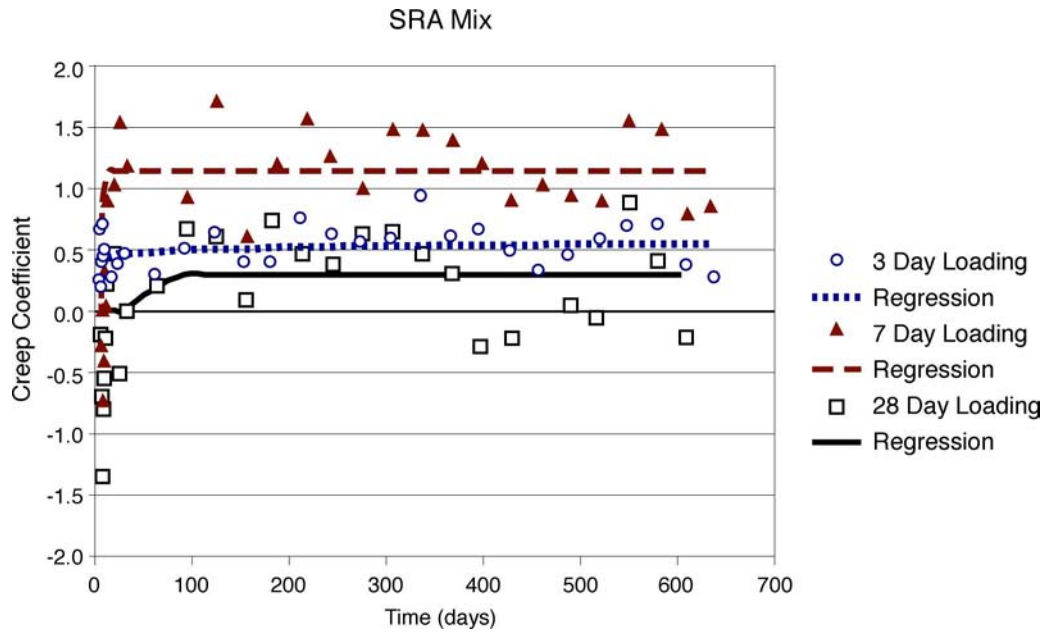


Figure 3.14 Coefficient as a function of time for SRA mixture

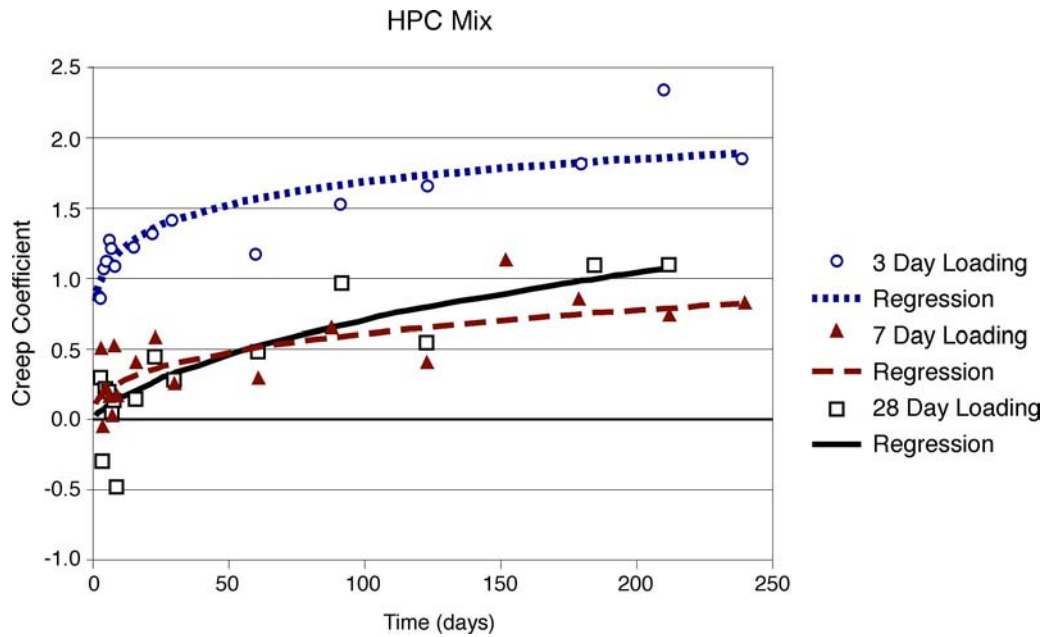


Figure 3.15 Coefficient as a function of time for HPC mixture

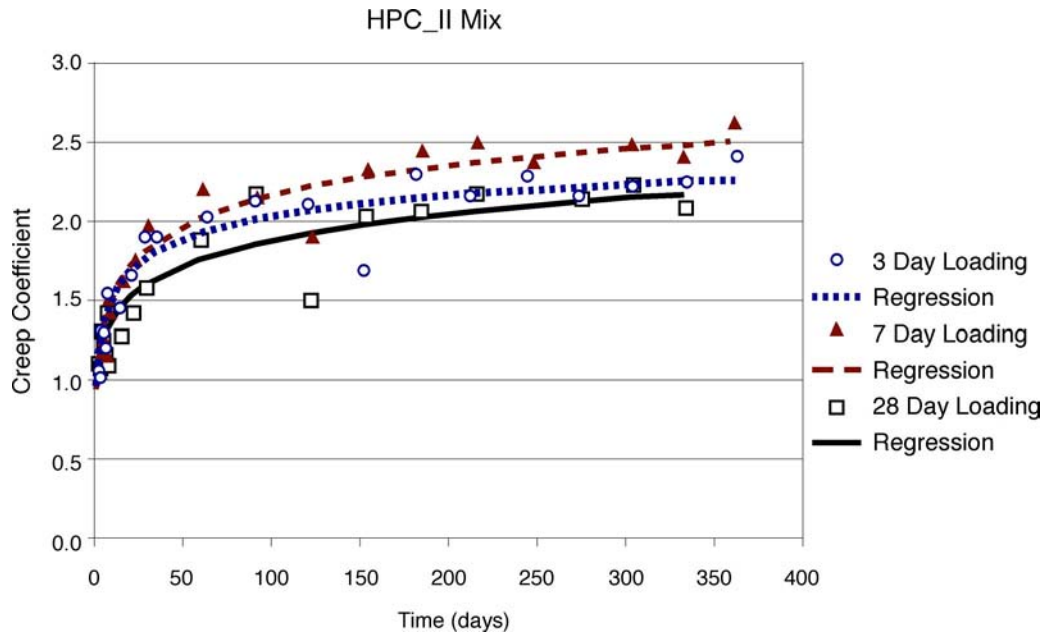


Figure 3.16 Coefficient as a function of time for HPC II mixture

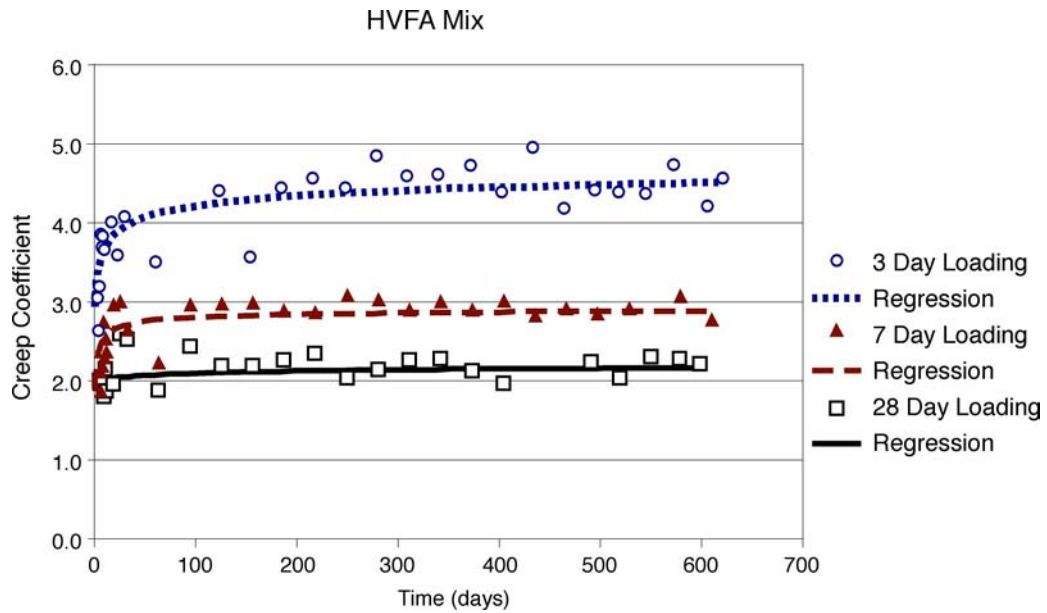


Figure 3.17 Coefficient as a function of time for HVFA mixture

Discussion of Creep Results

It is evident in the plots above that there is significant variability in the results. To reduce this variability, a statistical regression was performed on the data. ACI 209 suggests that a creep response should be of the form:

$$v_t = \frac{t^\psi}{d + t^\psi} v_u$$

where v_u is the ultimate creep coefficient, t is time in days, and d and ψ are constants. A statistical computer program was used to determine d , ψ , and v_u . Note that the above equation predicts creep coefficient, but the plots depict specific creep. Creep coefficient is defined as elastic strain divided by creep strain, and specific creep is defined as creep strain divided by the applied load. The difference between the two creep measurements is only a constant, the modulus of elasticity. It is believed that the predictive equation for specific creep should be of the same form as that of creep coefficient. The results of the statistical fits are shown in Table 3.9. The last column of the table shows the R^2 value for the statistical regression. R^2 is the coefficient of determination, and a value of R^2 equal to unity indicates a perfect fit, or the regression explains 100% of the variability of the data. Note the large range of R^2 values.

Table 3.9 Statistical regression parameters for creep using ACI 209

Mixture - Day	Parameter			
	v_u	d	ψ	R^2
Control 3-day	4.0251	0.5284	0.7001	0.8897
Control 7-day	3.2926	0.7121	0.4963	0.8111
Control 28-day	6.5611	1.1648	0.1589	0.5027
Type K 3-day	11.2796	2.1118	0.5167	0.7939
Type K 7-day	2.7905	0.6025	0.2855	0.4638
Type K 28-day	5.6959	123812.4000	1.8205	0.8215
HVFA 3-day	5.0360	0.7117	0.2795	0.6886
HVFA 7-day	2.9200	0.5562	0.5640	0.6341
HVFA 28-day	2.9730	0.5613	0.0627	0.0926
FRC F-I 3-day	2.1108	1.4147	0.4475	0.7778
FRC F-I 7-day	1.8250	9.4324	1.0727	0.6668
FRC F-I 28-day	1.9077	2.7878	0.6155	0.6917
HPC 3-day	6.0901	6.3825	0.1920	0.7624
HPC 7-day	3.9347	37.2203	0.4146	0.5053
HPC 28-day	3.2748	120.6760	0.7588	0.7690
SRA 3-day	0.9927	1.6849	0.1134	0.0384
SRA 7-day	1.1396	9.1000E+31	38.3602	0.7217
SRA 28-day	0.2889	1.8000E+39	22.2553	0.1184
Control IV 3-day	1.4015	0.3491	0.1345	0.9707
Control IV 7-day	4.3665	3.1350	0.3391	0.9600
Control IV 28-day	7.4532	4.2242	0.2068	0.9143
HPC II 3-day	2.7950	1.9154	0.3542	0.8954
HPC II 7-day	3.6774	2.8996	0.3087	0.9452
HPC II 28-day	5.3084	4.4564	0.1935	0.8418

The control, HVFA, and Type K mixtures each behaved as expected. For each of these mixtures, the 3-day loading produced the most creep, and the 28-day loading produced the least. Early age creep tends to be higher than at later ages. One of the mechanisms of creep is the movement of moisture within the concrete specimen. With older concrete, the pore structure is more refined and discontinuous, thus limiting the ability of water to migrate and limiting creep. However, the relative values of creep were surprising. It was expected that the creep for the Type K and control mixtures would have similar magnitude, and the HVFA much less than either. The results show that the HVFA has similar values of creep to the control mixture, with the Type K having significantly smaller values.

The FRC F-II and silica fume mixtures were excluded from the creep testing because it was believed that the FRC F-II would behave in a similar manner to the FRC F-I mixture, and the silica fume mixture like the HPC mixture. However, the results of some of the creep tests were questionable. As can be seen in Figures 3.10 through 3.17, some of the creep histories produced anomalous results. Both the HPC and silica fume results indicate a negative value of creep, which is physically impossible. The plot of FRC F-I show negative creep early in the time history, but becomes positive after some time; again this is not possible. No meaningful data can be inferred from these results. The plots above are presented only to demonstrate the scale of the errors. Due to the odd results of the creep experiment, the creep tests will need to be repeated in the future.

It is believed that some of the error in the creep tests may have been due to the loading frames. ASTM C512 requires that the loading frames be able to maintain the applied load within 2% of the initial value. The creep frames used in this study may not have been able to meet this criterion. The creep frames were spring type, rather than the more accurate and reliable hydraulic type. It is possible that the springs in the frame, and the frame itself, relaxed over time gradually reducing the load on the concrete specimens. Another possible source of error is the frequency of measurements. Since the specimens were measured only once per month, any anomaly on the day of measurement could not be checked against previous or successive readings. Both problems are to be solved in the repetition of the creep tests.

Free Shrinkage

Free shrinkage experiments were performed on each mixture as described above. The plots of free shrinkage versus time are presented in Figures 3.18 through 3.25.

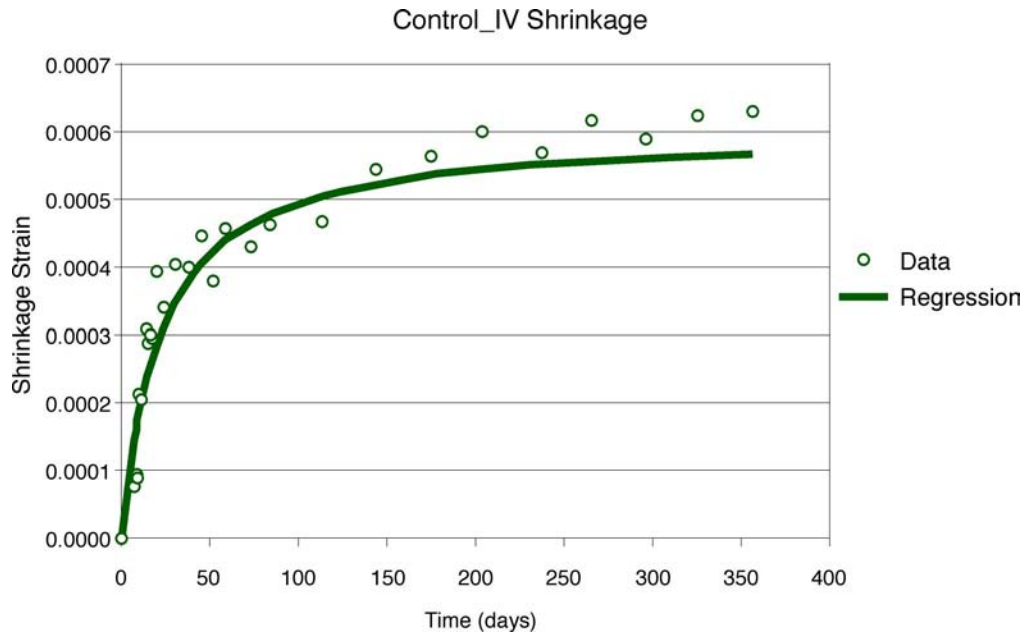


Figure 3.18 Shrinkage Strain as a function of time for Control IV mixture

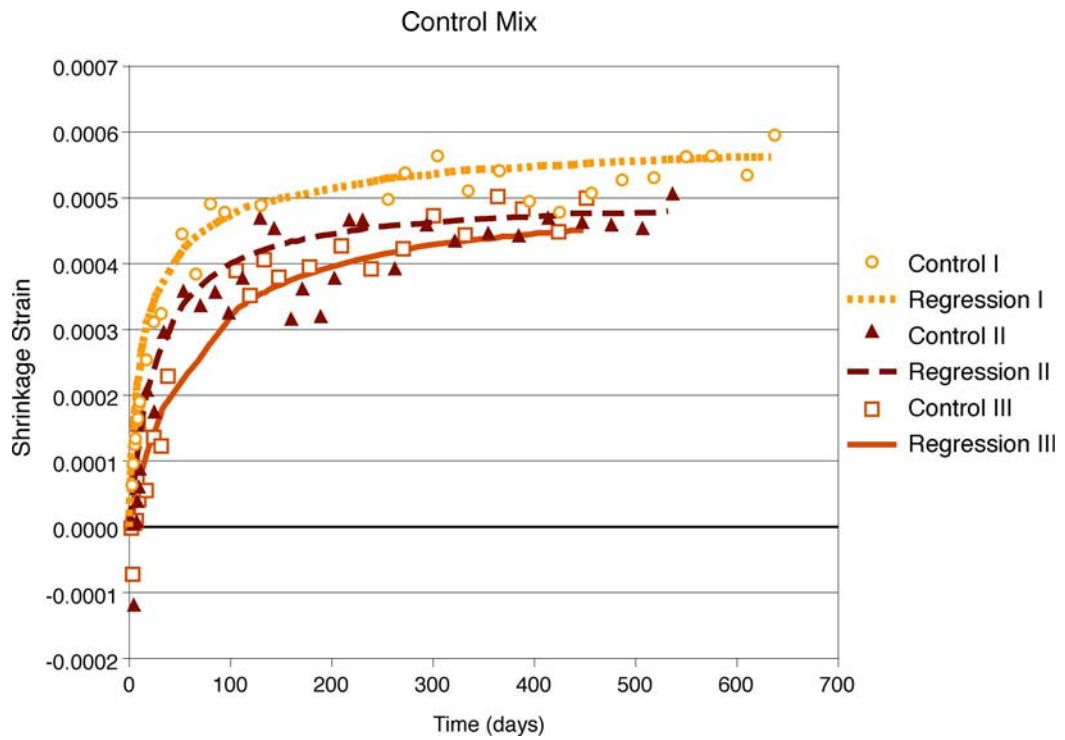


Figure 3.19 Shrinkage Strain as a function of time for Control mixture

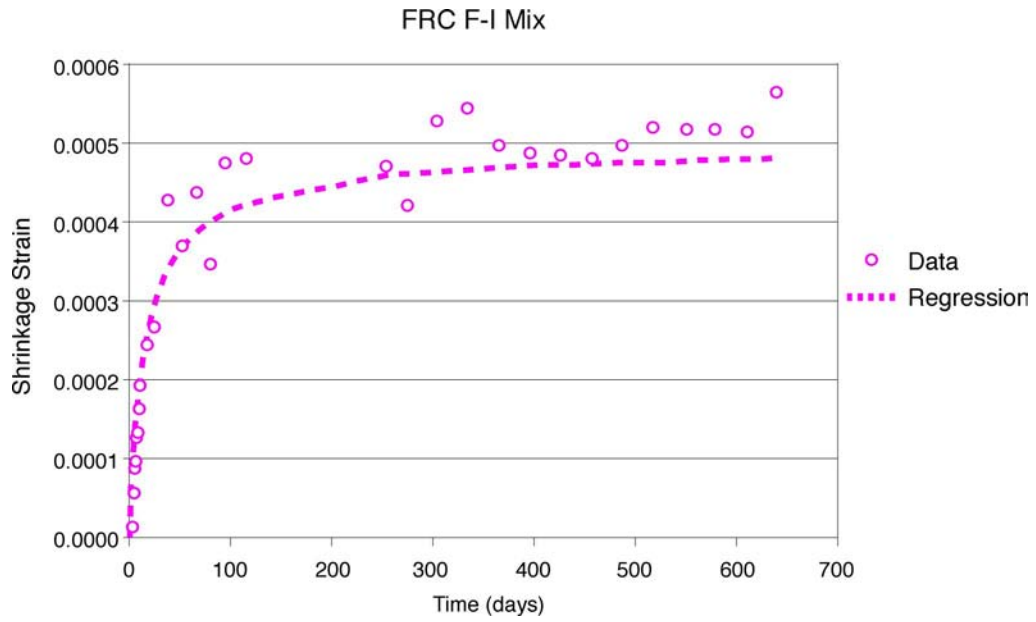


Figure 3.20 Shrinkage Strain as a function of time for FRC F-I mixture

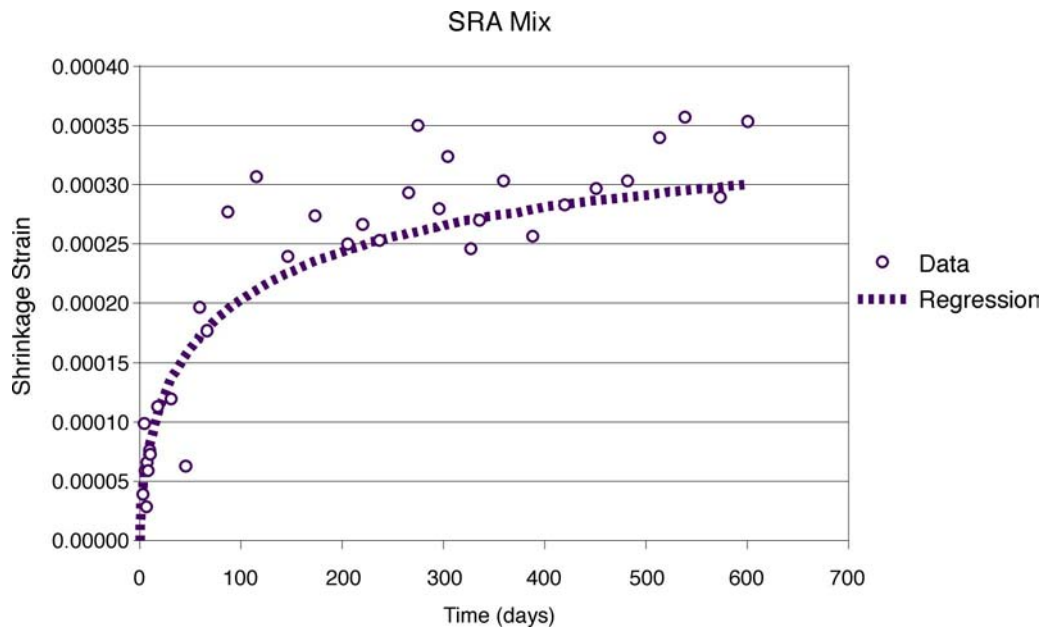


Figure 3.21 Shrinkage Strain as a function of time for SRA mixture

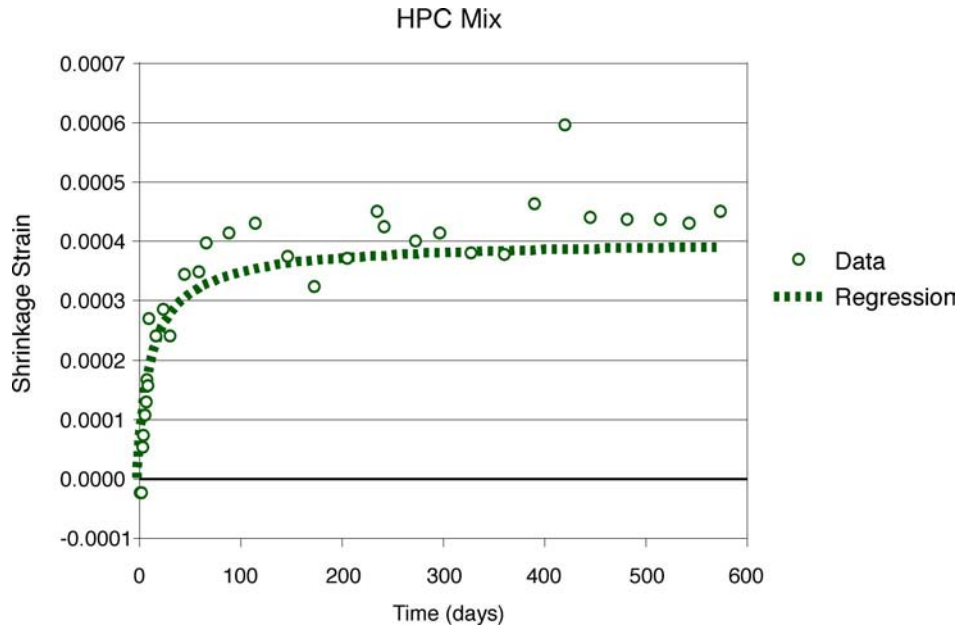


Figure 3.22 Shrinkage Strain as a function of time for HPC mixture

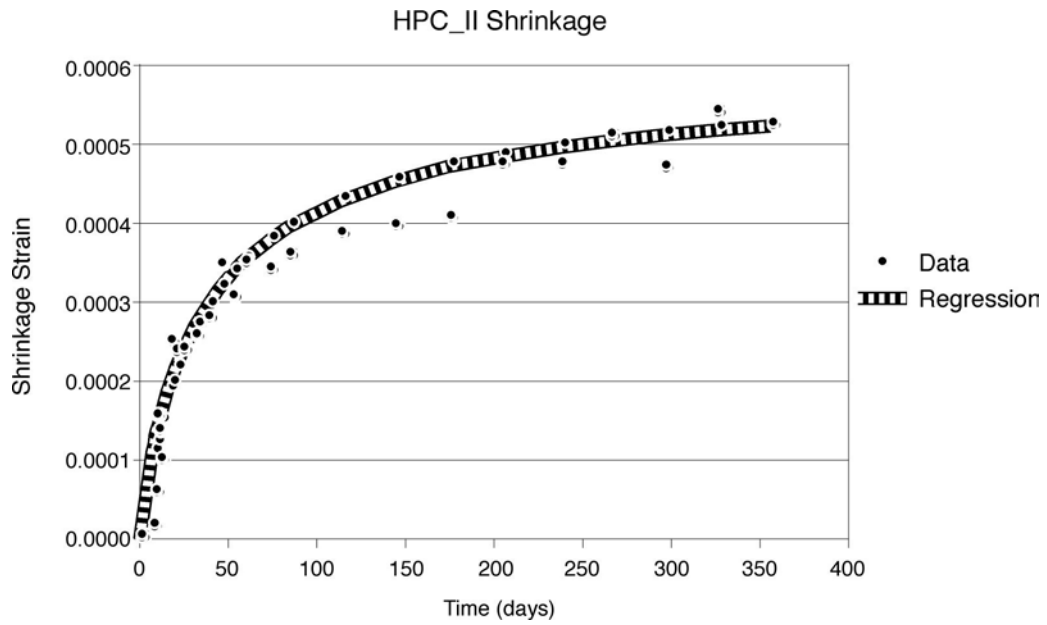


Figure 3.23 Shrinkage Strain as a function of time for HPC II mixture

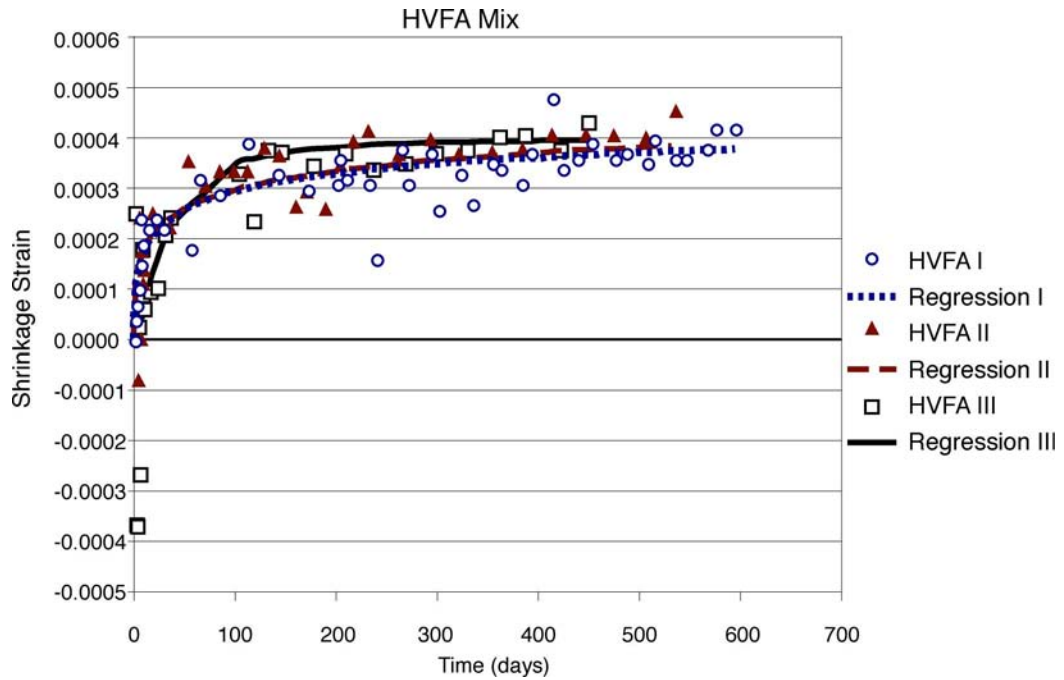


Figure 3.24 Shrinkage Strain as a function of time for HVFA mixture

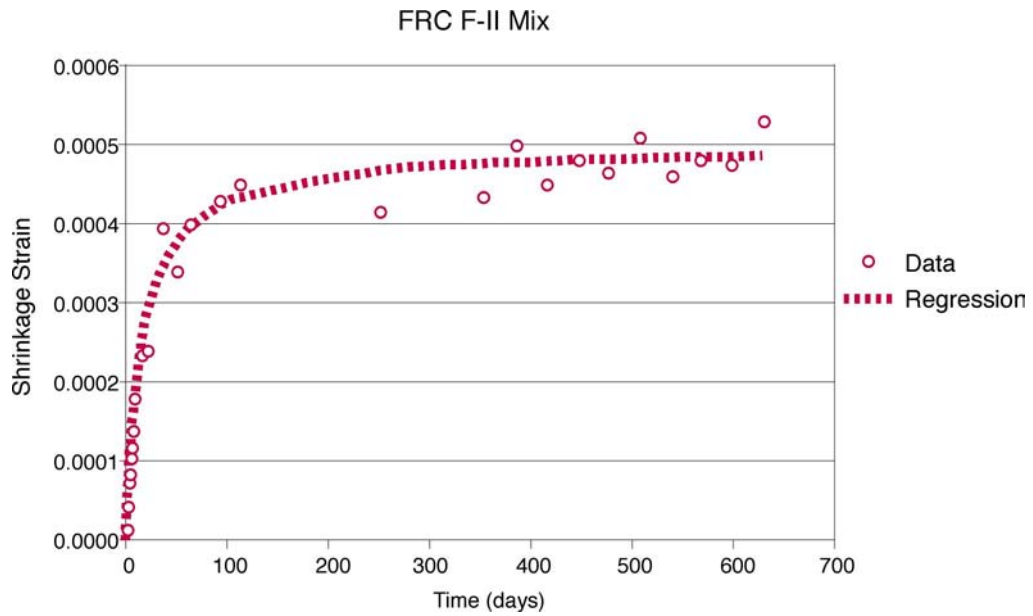


Figure 3.25 Shrinkage Strain as a function of time for FRC F-II mixture

Discussion of Free Shrinkage Results

As with the creep data, the free shrinkage data was fitted to an equation presented in ACI 209. The equation is of the same form as that presented above for creep.

$$\epsilon_{sh,t} = \frac{t^\psi}{f + t^\psi} \epsilon_{shu}$$

In this equation, ϵ_{shu} is the ultimate shrinkage strain, t is time in days, and ψ and f are constants to be determined for the specific data. The same statistical regression program was used to determine the constants for shrinkage results as was used to determine the creep results above. The regression constants as well as the R^2 values are presented in Table 3.10 below.

Table 3.10 Statistical regression parameters for shrinkage using ACI 209

Mixture - Day	Parameter			
	ϵ_{shu}	f	ψ	R^2
Control	0.00061	8.06	0.694	0.967
Type K	N/A	N/A	N/A	N/A
HVFA	0.000359	5.21	0.706	0.853
SRA	0.00040	29.06	0.461	0.823
FRC F-I	0.00050	11.38	0.902	0.961
FRC F-II	0.00045	13.80	1.100	0.974
HPC	0.00040	7.74	0.984	0.826
Silica Fume	0.00045	18.90	0.909	0.898
Control IV	0.0006	23.52	1.019	0.934
HPC II	0.0006	24.44	0.867	0.939

From the plots, it is apparent that there are pairs of mixtures that are performing similarly. Both FRC mixtures have similar shrinkage versus time plots, as well as similar statistical values for the ACI 209 equation. It was expected that both fiber mixtures would behave the same; the mixtures were identical and both types of fibers had similar characteristics. The FRC mixtures show slightly less shrinkage than the control mixture. The HPC and silica fume mixtures also performed similarly. The HPC mixture has a higher shrinkage rate at early ages. The higher early shrinkage rate is likely due to the increased binder content and lower water-cement ratio. Both lower water-cement ratio and higher

binder content should result in larger shrinkage strains based on the available literature. However, both HPC and silica fume appear to be asymptotically approaching a shrinkage strain of approximately 0.0004. The last pair of similarly performing mixtures are the HVFA and SRA mixtures. Both of these mixtures show much less shrinkage than any of the other six mixtures. The HVFA mixture should have less shrinkage due to the pore size distribution of the matrix. Large amounts of fly ash reduce the number of pores that are responsible for drying shrinkage, and therefore reduce the overall shrinkage of the mixture. As described above, the SRA works by reducing the surface tension of the water in the pores. Since shrinkage is a direct consequence of the surface tensions, less surface tension results in less shrinkage. The plots confirm this belief when compared to the control or other mixtures.

There were two interesting (and unexpected) sets of results. First, the HPC and silica fume mixtures exhibited less shrinkage than the control. Based on the literature, the HPC and silica fume mixtures should have had significantly more shrinkage than the control mixture. A possible reason for these strange results is the shift in pore size due to the addition of silica fume. As with high volumes of fly ash, silica fume should produce concrete with finer pores that are less likely to cause drying shrinkage. In the literature, the increased shrinkage in concrete when silica fume is used has been attributed to autogenous shrinkage. ASTM C157 dictates that free shrinkage prisms be cured for seven days in a limewater solution. Storage in limewater is an excellent curing environment, and could have offset the autogenous shrinkage, which is most active at early ages. Because drying shrinkage measurements were not taken until after the seven-day cure, a significant portion of the shrinkage of the HPC and silica fume mixtures may have been overlooked.

The Type K mixture showed strange results as well. Typically, shrinkage compensating concrete will shrink as much as a similar mixture using a Type I/II cement. It is only the early age expansion that differentiates SCC from a traditional portland cement concrete. The early ages expansion should be of such magnitude that all the subsequent shrinkage is not enough to overcome it. In this study, the Type K mixture demonstrated much more shrinkage than the control mixture. A possible source for this error is the method of measuring the Type K specimens. In Figure 3.3, a restraining cage for SCC shrinkage prisms is shown. The acorn nuts on the outside of the cage serve as the

measurement points. These nuts were made of a soft metal that was gouged by the anvil of the measurement device as each measurement was taken, progressively shortening the nut. These gauges artificially reduced the length of the specimen and could account for some of the seemingly large shrinkage. The shrinkage curves as determined from the regressions are plotted in Figure 3.26 below. From this plot the relative values of shrinkage for the mixtures can be seen. Because of the early age expansion of the SCC, its shrinkage response can not be modeled by the ACI 209 equation; therefore it does not appear in the figure.

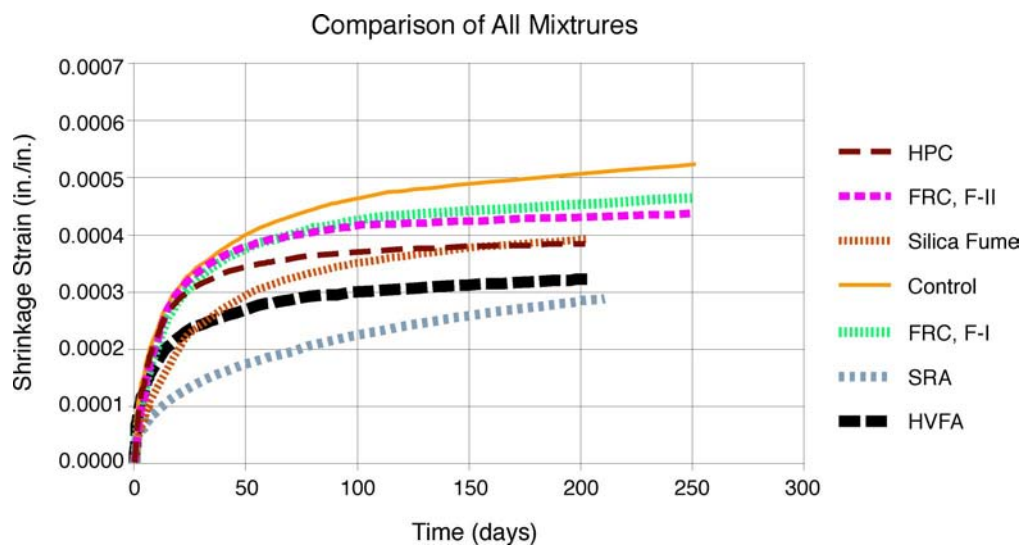


Figure 3.26 Shrinkage responses for all mixtures

Restrained Shrinkage

The restrained shrinkage test is intended to be a synthesis of all the tests previously described. The strain histories of the restrained shrinkage rings are plotted below for each mixture (see Figures 3.27 through 3.37). Each curve on the plots represents the average or four strain gages on a ring.

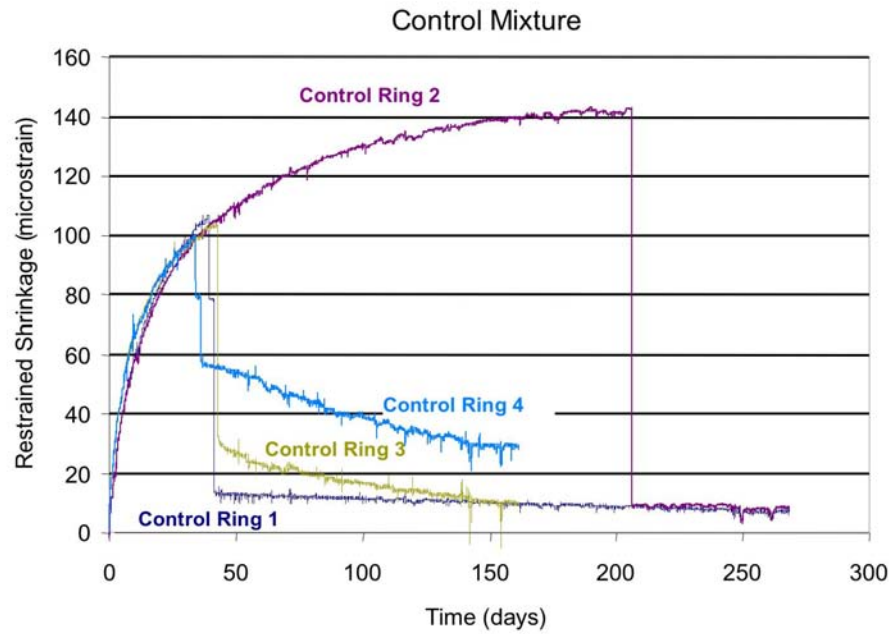


Figure 3.27 Restrained shrinkage results for Control mixture

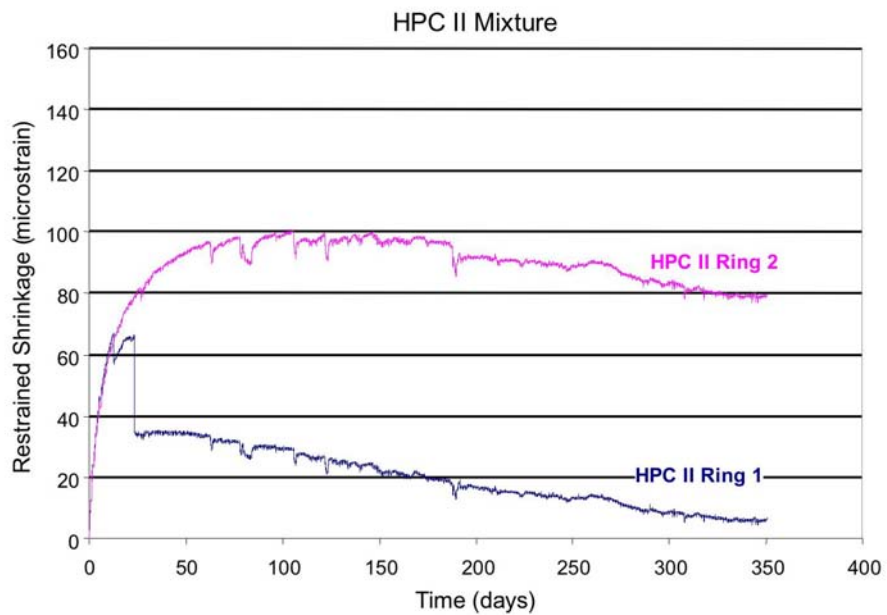


Figure 3.28 Restrained shrinkage results for HPC II mixture

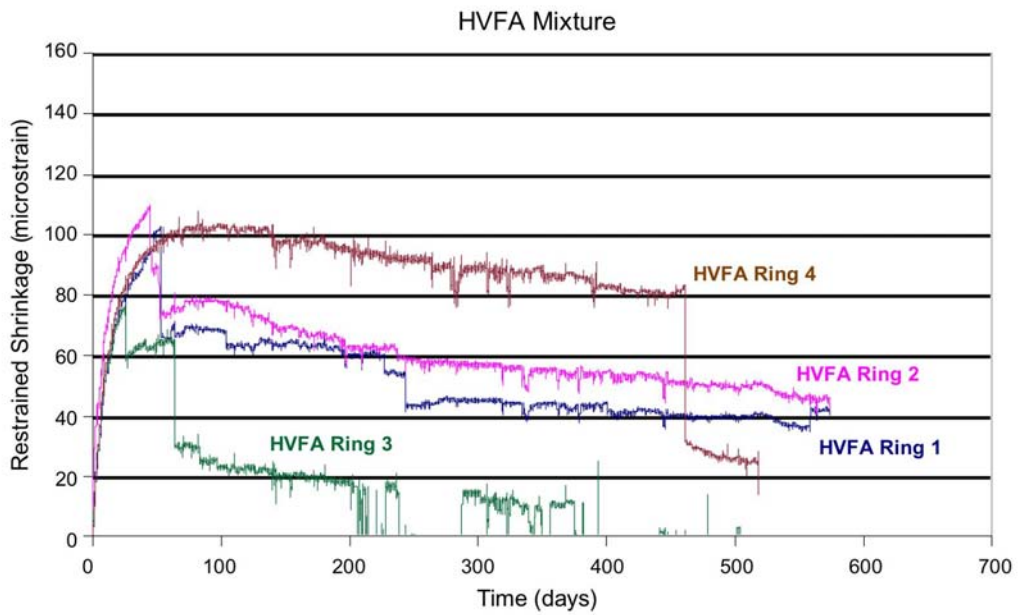


Figure 3.29 Restrained shrinkage results for HVFA mixture

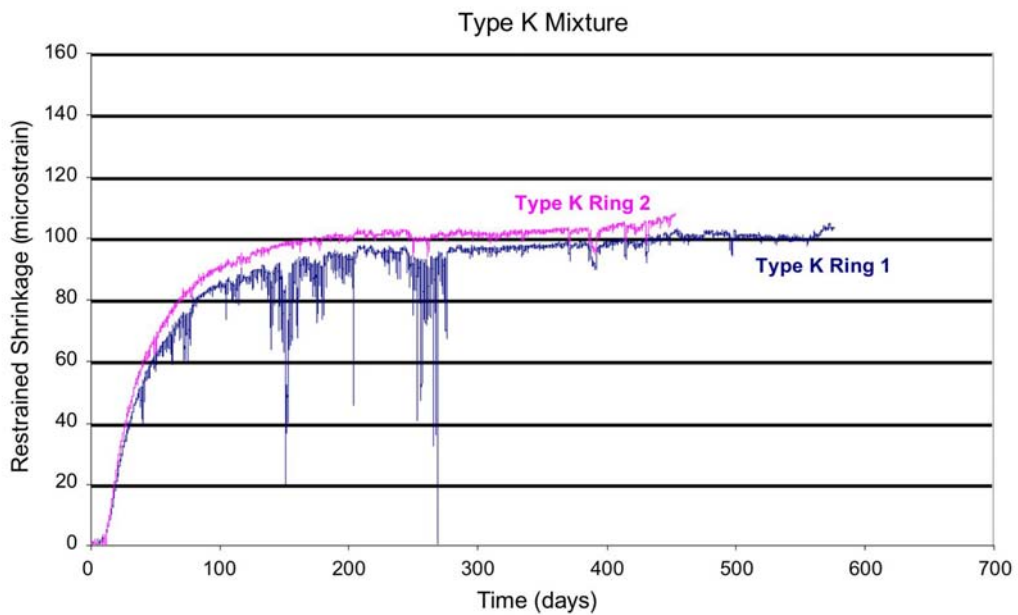


Figure 3.30 Restrained shrinkage results for Type K mixture

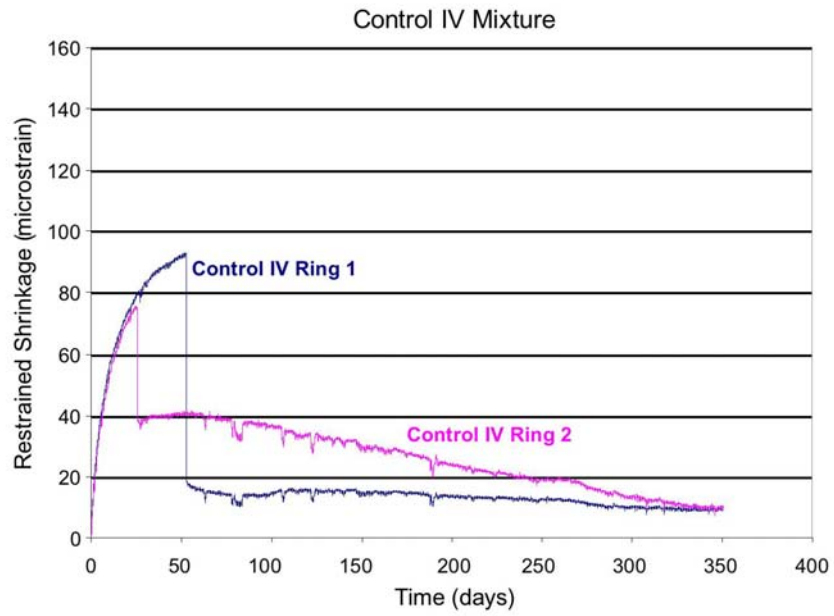


Figure 3.31 Restrained shrinkage results for Control IV mixture

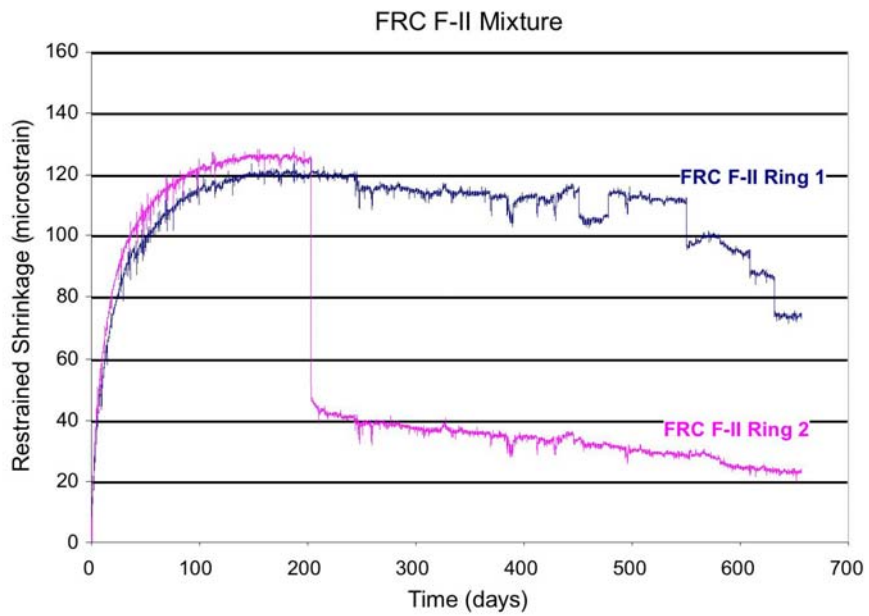


Figure 3.32 Restrained shrinkage results for FRC F-II mixture

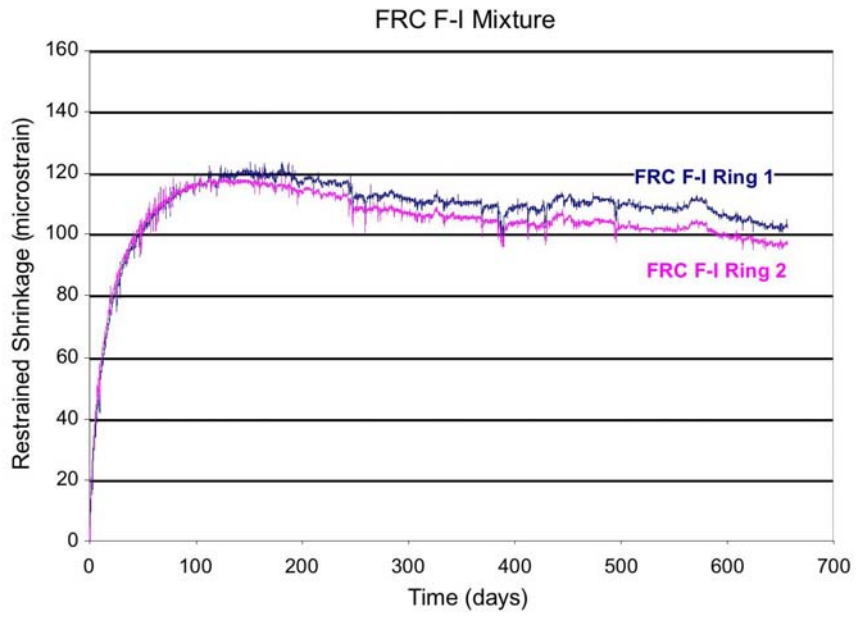


Figure 3.33 Restrained shrinkage results for FRC F-I mixture

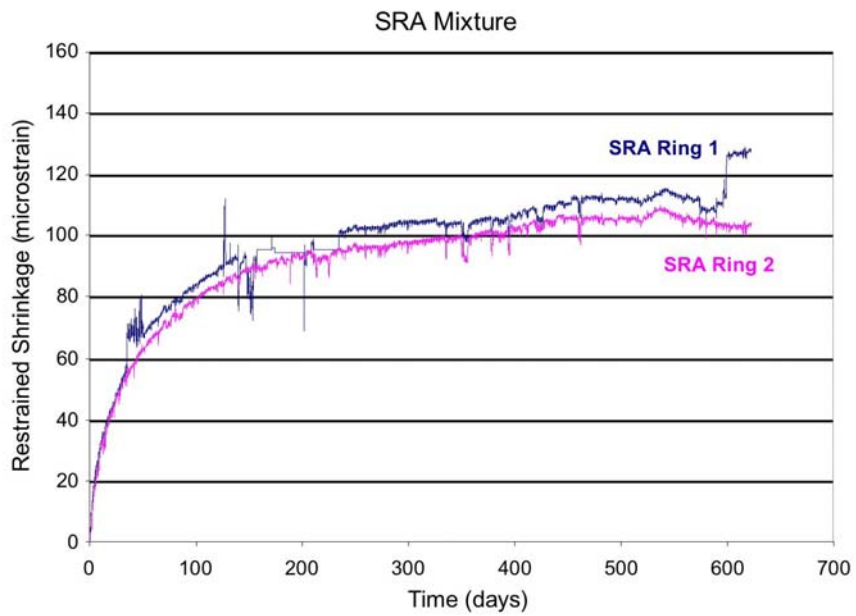


Figure 3.34 Restrained shrinkage results for SRA mixture

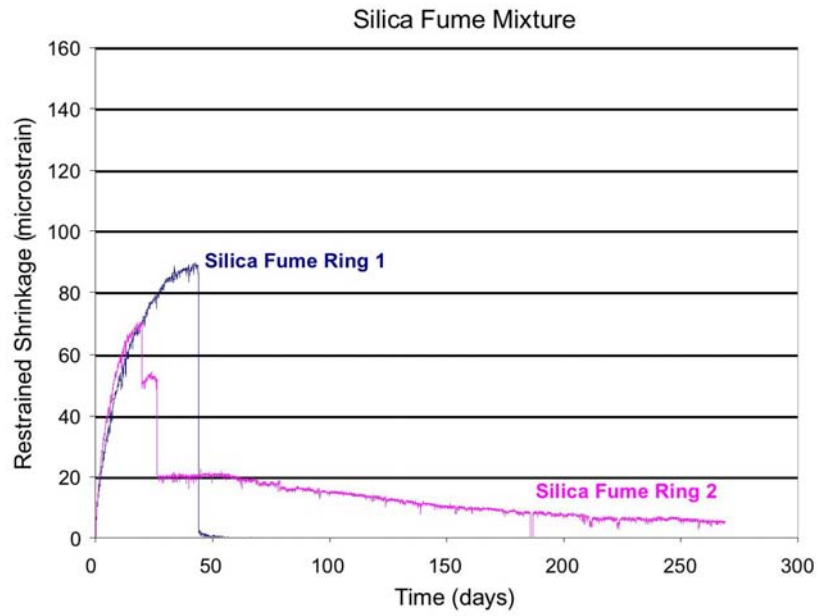


Figure 3.35 Restrainted shrinkage results for Silica Fume mixture

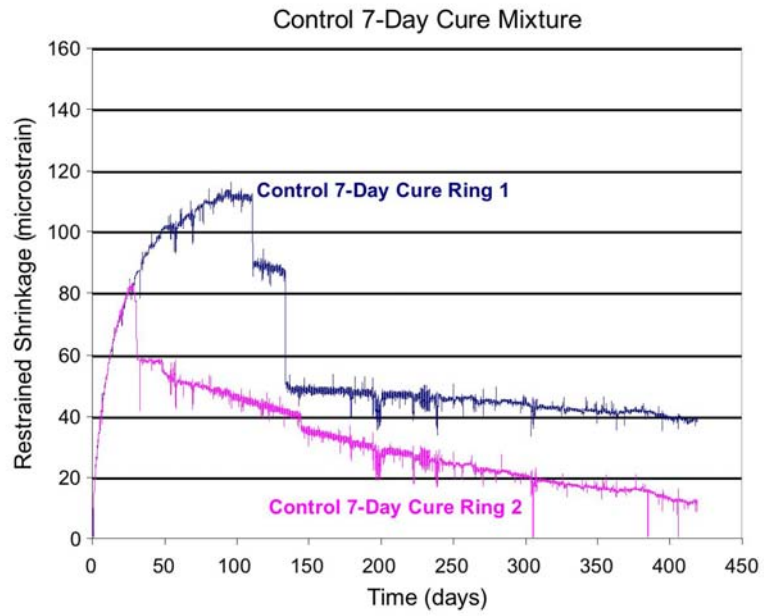


Figure 3.36 Restrainted shrinkage results for Control 7-day Cure mixture

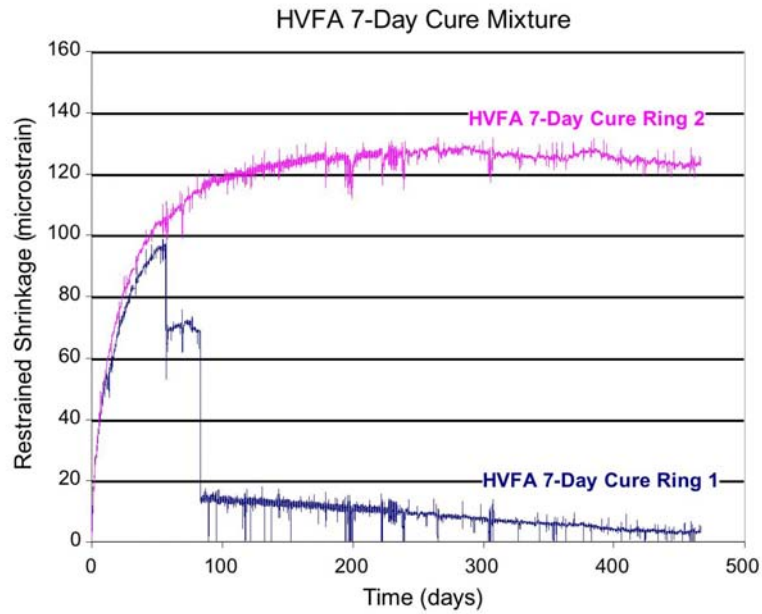


Figure 3.37 Restrained shrinkage results for HVFA 7-day Cure mixture

On several of the graphs, a large vertical drop in the strain histories can be seen. The vertical drop indicates a crack. Generally, the magnitude of the drop will correlate with the size of the crack on the ring. It can be seen in the graphs that the largest drop in strain occurs on the control mixture rings one and two. Indeed, these are the largest cracks visible on any of the ring specimens. The crack on control ring one is pictured below in Figure 3.38. When a drastic change in the strain history was observed, a visual inspection of the ring was performed in order to verify the computerized strain data.



Figure 3.38 Large Crack in Restrained Shrinkage Ring Specimen

Apart from the width of the crack in the figure above, it is typical of all observed cracks. There is usually one continuous crack that appears vertically on the outer face of the concrete ring.

On several of the rings, a secondary crack appeared. The secondary crack was diametrically opposed to the first crack, and usually smaller in width. In Figure 3.27, the plots show the strain history for the formation on the secondary crack in the curves for rings three and four. In the plots there is a large drop in strain followed by a small plateau, which is followed by another large drop. The plateau and second large drop in strain indicate the formation of a secondary crack.

Results of Restrained Shrinkage Test

The result of the ring test is the time elapsed from the exposure of the specimen to drying conditions until the first crack is detected. Table 3.11 lists the average time to cracking for the rings of each mixture. For mixtures where no number is listed for time to cracking, no cracking has occurred at present.

In summary, the silica fume and HPC rings cracked first as expected based on arguments presented in the literature, i.e., high elastic modulus, fast strength gain, and low

creep capacity. The HVFA mixture cracked later than the control mixture. The delayed cracking of the HVFA mixture was expected based on the same principles (modulus, strength gain, and creep capacity) working in opposite directions. However, it was expected that the HVFA cracking would be delayed much more than was observed. The Type K, SRA and FRC F-I did not crack, which, again, was expected. One of the FRC F-II cracked unexpectedly late for unknown reasons. After the crack had occurred in the FRC F-II mixture, the crack width was visibly smaller than other mixtures, probably due to the fibers' ability to carry tension across a crack.

Table 3.11 Restrained Ring Test Results (Brown 2002)

Mixture	Average Time to Cracking (Days)
Control	39
Type K	No Cracks at 620+ Days
HVFA	41
SRA	No Cracks at 590+ Days
HPC	35 (35, None)
Silica Fume	31 (43, 18)
FRC F-I	None
FRC F-II	202 (202, None)
Control 7-Day Cure	71 (30, 112)
HVFA 7-Day Cure	57 (57, None)
Control IV	40 (53, 26)
HPC II	13 (13, None)

The results are not as clear as the table above indicates. There were some problems with the repeatability of this test. This is the reason for the extra rings that were cast for the control and HVFA mixtures (note the extra curves in Figures 3.27 and 3.29). For these two mixtures, all of the laboratory testing was repeated. The repeated mixtures were identical to the original ones. The same mixture proportions, aggregate and temperature control, were used for the repeated mixtures. The results presented above for the control and HVFA mixtures are those values obtained from the repeated mixtures with the exception of creep. Due to the long-term nature of creep testing, it was impractical to repeat the creep tests; therefore, the creep results presented above reflect the first control and HVFA mixtures. The researchers recommend that in the future, three rings for each mixture should be cast. With only two rings, results are difficult to interpret if only one of the two rings cracks.

The control and HVFA mixtures were later repeated again. This time the repeated mixtures were used to determine the effects of curing on time to cracking. The AASHTO specification recommends only 24 hours of moist curing for the ring test. With such minimal curing, the pozzolanic reaction does not have the necessary time to occur with the fly ash. If the pozzolanic reaction does not proceed toward completion, the high volumes of ash in the mixture provide little benefit to the mixture. The researchers believed that the performance of the HVFA mixture would improve with increased curing.

Increased curing did in fact delay the cracking of the HVFA rings. Unfortunately, only one of the two rings that were cured for 7 days has cracked for the HVFA and control mixtures. Curing the HVFA for 7 days rather than one delayed cracking by 16 days, conversely curing the control ring for 7 days accelerated cracking by 8 days. Only one or the two rings for each of the mixtures cured for 7 days cracked. Owing to the repeatability concerns, the data on extended curing is not conclusive, but does offer some evidence to the benefit of extended curing.

Trends in Experimental Data

A large amount of effort was put forth in an attempt to find a trend within the results of the testing. To date, no significant trend has been found.

The first attempt involved searching for a pattern in the ratio of free shrinkage strain to restrained shrinkage strain. No discernable pattern could be found. Creep plays an important role in the restrained shrinkage response, and affects the ratio of free to restrained shrinkage.

In the second attempt, a ratio of free shrinkage minus creep to restrained shrinkage was evaluated for all mixtures. Again, no pattern emerged from the data. It was believed that the restrained shrinkage response should be similar to the response of free shrinkage minus creep. However, the creep, as determined by laboratory investigation, is due to a compressive force. In the restrained shrinkage ring, creep is caused by a tensile force. The behavior of tensile creep is not the same as that for compressive creep. If tensile creep data were obtained, the ratio of free shrinkage minus tensile creep to restrained shrinkage may yield a more conclusive trend.

A third effort to find a trend involved comparing shrinkage and time-to-cracking. However, there was no clear trend in this comparison either. The silica fume and HPC

rings were the first to crack, but had less free shrinkage than either the control or Type K. The Type K mixture has the highest amount of free shrinkage, but has yet to crack in the restrained shrinkage test.

The final attempt to find a trend yielded some results. In recent papers by Altoubat and Lange (1995), it is suggested that the rate of early age shrinkage is of primary concern for restrained shrinkage cracking. In Figure 3.39, the restrained shrinkage history for all mixtures is plotted for the first three days of drying.

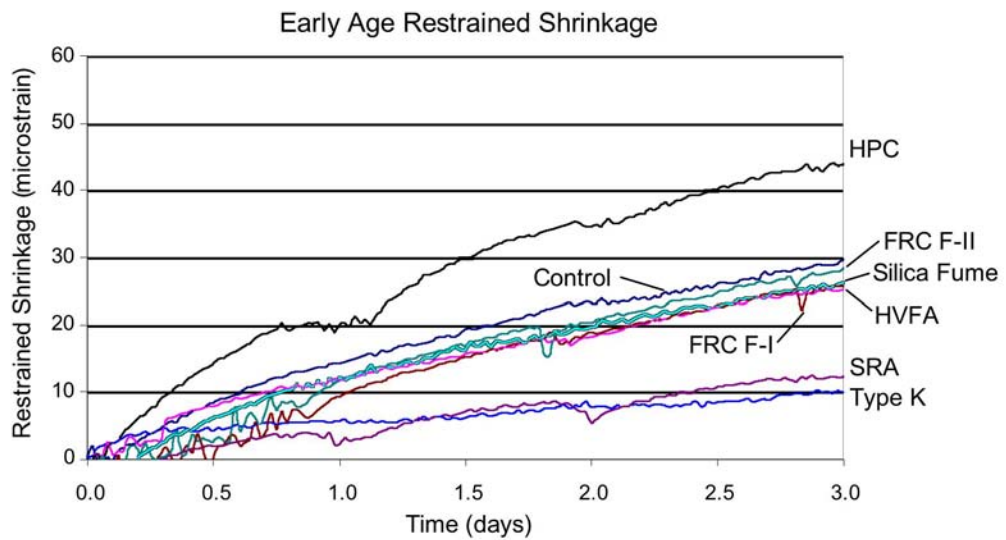


Figure 3.39 Restrained Shrinkage at early age

In the figure, the slope of a given curve can be interpreted as the rate of early age restrained shrinkage. For example, the yellow curve for the HPC mixture has the highest slope. Based on the work by Altoubat and Lange (1995), the steep slope of the restrained shrinkage of the HPC mixture would indicate a large potential for cracking. In fact, the HPC was the second mixture to crack. Also in the figure, it is clear that the Type K and SRA mixtures have the smallest slope, indicating a low restrained shrinkage cracking potential. The data from the ring tests verify this since the Type K and SRA mixtures have

not yet cracked. Unfortunately, the other five mixtures have nearly identical slopes, making it impossible to gather any meaningful conclusions about the cracking potential.

3.3.1 Summary of Experimental Results

Control Mixture

The control mixture was based on the TxDOT specification for Class S concrete, which is generally used for bridge decks. Class S concrete has a maximum water-cement ratio of 0.45, and a minimum cement content of 6.5 sacks per cubic yard. The control mixture was used as the basis for comparison. The control mixture had the greatest amount of free shrinkage and a high amount of specific creep.

HPC Mixture

The HPC mixture was designed to mimic the deck concrete used for the Louetta Road Overpass in Houston, Texas. This HPC mixture was optimized for both strength and durability. As expected, the HPC had the highest early-age strength, and a relatively short time to cracking of only 34 days. In this mixture, the cement content increased and the water-cement ratio decreased relative to the control mixture. The literature suggested that these two changes should decrease the time to cracking of a restrained shrinkage ring. The HPC ring cracked 4 days sooner than the control mixture. Free shrinkage for the HPC mixture was less than that of the control mixture, possibly due to the decreased permeability. The creep data for this mixture was questionable and the creep testing will be repeated in the future.

Silica Fume Mixture

The silica fume mixture is based on bridge deck mixtures that are common throughout the nation. For this mixture, 7.5% of the cement was replaced with dry densified silica fume. This mixture had second highest early-age strength behind the HPC mixture, and had the shortest time to cracking of any of the mixtures tested. The silica fume rings cracked at an average of 30.9 days. The silica fume mixture, like HPC, had less shrinkage than the control mixture, yet cracked sooner—most likely a consequence of the high early age strength and elastic modulus.

Type K Mixture

For the Type K mixture, the same mixture proportions were used as in the control mixture, the only difference being Type K cement rather than the standard Type I/II cement. The Type K was the first of the innovative materials investigated in this study. By creating early age expansion, the Type K induces a small amount of prestress into the structure, which can overcome the subsequent shrinkage. The data for creep of the Type K mixture showed less specific creep than that shown in the control mixture. While the Type K mixture exhibited the largest amount of shrinkage, the free shrinkage of an SCC mixture can not be directly compared to traditional PCC mixtures. The amount of shrinkage of an ASTM C878 prism is calibrated to a specified size of threaded rod creating restraint within the prism. The strength of the Type K mixture was similar to the control mixture at all ages. The Type K restrained shrinkage ring has not cracked as of the submission of this report, despite the relatively high shrinkage and low creep. The early age expansion is apparently overcoming these obstacles.

Fiber-Reinforced Concrete

The FRC contained structural polypropylene fibers dosed at 15 lb/yd³. The FRC mixtures performed quite similarly to each other and to the control mixture. The FRC mixtures exhibited slightly less shrinkage than the control mixture. It was not expected that the introduction of fibers to a mixture would change the free, drying shrinkage response. However, the fibers did change the restrained, drying shrinkage response. Only one of the four FRC rings cracked, and the ring that cracked did so at 202 days.

Shrinkage-Reducing Admixture

The SRA attacked the source of drying shrinkage, the surface tension in the pore water. Reducing the surface tension necessarily reduced the magnitude of drying shrinkage cracking. The SRA mixture showed similar strength and modulus characteristics to the control. While the creep data for the SRA mixture is inconclusive, the free shrinkage data shows a dramatic decrease in shrinkage. The restrained shrinkage ring also demonstrated the effects of the SRA. The SRA ring had not cracked at the time of submission of this report.

High Volume Fly Ash

For the HVFA mixture, 55% of the portland cement was replaced with Class F fly ash, with the intent of creating an extensible mixture as defined by Mehta (1993). An extensible mixture is one that can tolerate a large strain without cracking due to its large creep capacity and low modulus of elasticity. The mixture used in this study did exhibit a low elastic modulus and strength, but had a surprisingly low time to cracking. The HVFA ring cracked only 4 days after the control ring. It was expected that the ring containing the HVFA mixture should crack extremely late, if ever.

By adjusting the curing of the HVFA ring, it was hoped that the time to cracking could be improved. While the time to cracking was extended, the improvement was not as large as expected. In fact, the time to cracking of the control ring that was cured longer dropped compared the ring cured only 1 day. The behavior of both sets of rings cured for 7 days is curious.

3.4 Conclusions

1. The strain gages mounted in the rings provided excellent data, and were instrumental in detecting cracks. However, visual inspection was also necessary to detect slow forming cracks that the strain gages did not detect.
2. The ring test was able to demonstrate the synthesis of creep and shrinkage. Such a synthesis can not be explained by the individual creep and shrinkage results at this time.
3. The repeatability of the ring test is in question. With only two rings cast per mixture, it can be difficult to identify outlying data.
4. The conclusions reached in the literature appear to be sound. The data in the literature allowed the researchers to predict the response of each mixture to the laboratory testing. While the predictions were not perfect, they were accurate enough to validate the conclusions in the literature.

4. Field Evaluations of Selected Bridge Decks in Texas

4.1 Introduction

In order to better understand the concrete deck issues presented in NCHRP Report 380, a small field investigation was performed. This investigation was performed to assess the state of restrained shrinkage cracking in the state of Texas. To this end, two bridges were inspected in detail by the researchers. The first bridge was the Louetta Road Overpass in Houston, and the second was the Dow Barge Canal Bridge in Freeport, Texas.

Due to the vast number of bridges in the state of Texas, it was prohibitively difficult to inspect a statistically significant number of them. Therefore, the two bridges mentioned above were chosen because it was known that they exhibited deck cracking, although the cause of the cracking was unknown at the time.

In Texas, the preferred method of constructing a bridge deck uses prestressed, precast panels. Figure 4.1 below illustrates the precast panel detail. Both the Louetta Road Overpass, and the Dow Barge Canal Bridge use this type of construction.

4.2 Inspection Procedure

The same inspection procedure was used for the two bridges. To inspect the bridge decks, it was necessary for TxDOT to close a portion of each bridge to traffic. In each inspection, TxDOT closed the lane adjacent to the shoulder. The

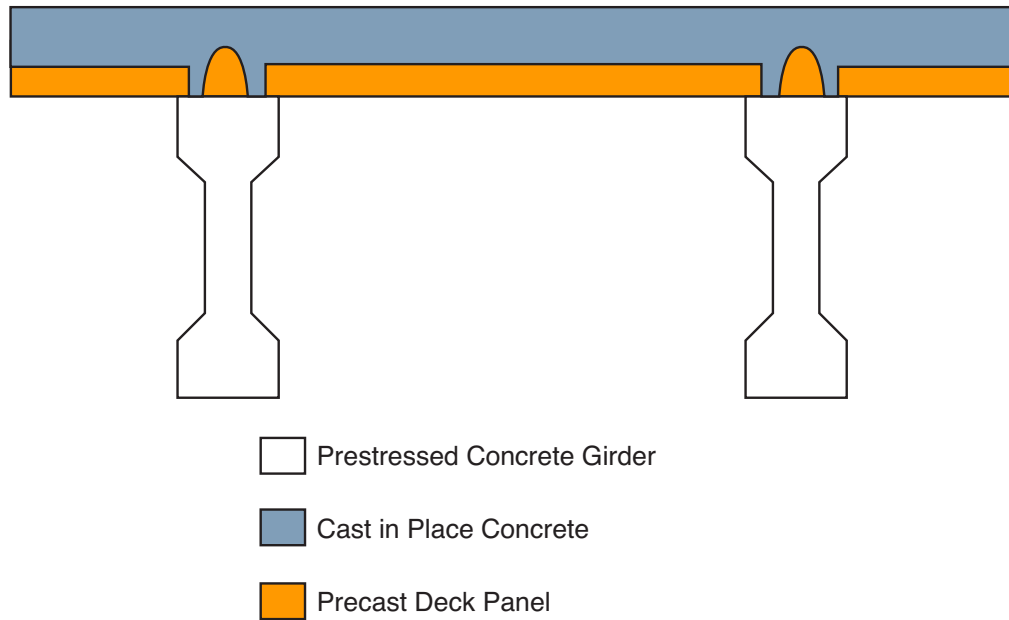


Figure 4.1 Typical Precast, Prestressed Panel Details

researchers were then allowed access to the shoulder and the closed lane. In this way, the majority of the deck could be inspected.

The goal of the inspection was to map the cracking on the bridge decks with the hope that the cracking could be linked to specific design details. To perform this inspection, the researchers broke into teams of two. One member of the team performed the inspection of the bridge deck, and used a construction marker to mark any cracking on the deck. The second member of the team followed behind, and mapped the cracks onto paper. While this technique does not exactly record the crack length or location, the accuracy is sufficient to obtain meaningful data.

4.3 Louetta Road Overpass Inspection

4.3.1 Description of Louetta Bridge

The Louetta Road Overpass was part of a previous research project in which the use of high performance concrete (HPC) was investigated. As part of that project, the materials were optimized for strength and durability. To compare the performance of different mixture proportions, two geometrically identical bridges were constructed. One of the bridges featured HPC in the deck whereas the other did not. The structure carrying the

northbound traffic had a design compressive strength of the deck concrete of 4,000 psi, while the southbound structure had a design compressive strength of 8,000 psi. The details of the mixture proportions can be seen in Table 4.1.

The situation at Louetta was ideal for examining some of the assertions that Krauss and Rogalla (1996) had made about material properties in a side-by-side comparison. Specifically, Krauss and Rogalla claim that higher strength, higher elastic modulus, higher cement content, and a smaller aggregate should increase the cracking potential of a concrete mixture. Note that the southbound deck exhibits all of the above-mentioned material properties. Based solely on the mixture proportions, it was expected that the southbound lanes would exhibit much more cracking than the northbound lanes.

Table 4.1 Mixture Proportions for Louetta Deck Concretes

	Louetta Northbound Deck	Louetta Southbound HPC Deck
Mixture Proportions		
Coarse Aggregate, Type	Crushed Limestone 1 ½ in max	Crushed Limestone 1 in max
Quantity	1856 lb/yd ³	1811 lb/yd ³
Fine Aggregate	1243 lb/yd ³	1303 lb/yd ³
Water	229 lb/yd ³	244 lb/yd ³
Cement (Type I)	383 lb/yd ³	474 lb/yd ³
Fly Ash (ASTM Class C) Percent Replacement	148 lb/yd ³ 28%	221 lb/yd ³ 32%
Retarder (ASTM Type D)	8.5 oz/cwt	3.2 oz/cwt
Water-Cementitious Ratio	0.43	0.35
HRWR (ASTM Type F)	None	17.8 oz/cwt
Air Entrainment (ASTM C260)	0.4 oz/cwt	None
Design Strength	4,000 psi	8,000 psi

Note: oz/cwt denotes fluid ounces of chemical admixture per hundred pounds of binder per cubic yard of concrete

4.3.2 Inspection Results

Northbound Lanes

In general, the northbound lanes were not heavily cracked. There was little transverse cracking that is usually associated with restrained shrinkage cracking. Of the transverse

cracks that were seen, none were more than 4 ft in length, and there were few cracks of this size. There was more pronounced cracking in the longitudinal direction. These longitudinal cracks appeared in pairs that were roughly 8 to 10 in. apart, and there was roughly 6 ft between the pairs of cracks. These paired cracks tended to be long and straight, some in excess of 25 ft in length.

Additionally, there were intersecting crack patterns near the expansion joints. The bridge has a 33° skew. Near the skewed expansion joints there was a stair-step pattern in the cracking. The sketch of this pattern can be seen in Figure 4.2. This pattern was evident at both sides of all the expansion joints, as well as both ends of the span. Also, note from the figure that the pairs of cracks described above also interact with the stair-step pattern.

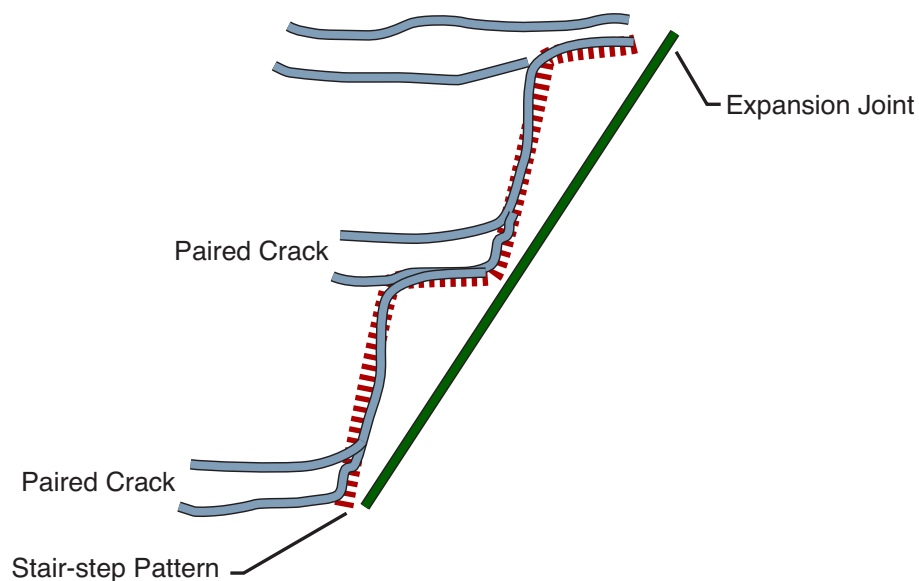


Figure 4.2 Typical Stair Step Cracking

Southbound Lanes

As mentioned above, the southbound deck was an HPC mixture, and according to the available literature should have exhibited much more cracking than its northbound counterpart. The field inspection confirmed this assumption.

The southbound deck was much more heavily cracked than the northbound. However, the same cracking patterns were apparent. The long pairs of cracks were apparent in the southbound lanes as well, but they tended to be much longer than what was seen on the non-HPC deck. On the HPC deck, these pairs of crack tended, on occasion, to

turn toward the transverse direction. However, once the crack had turned toward the transverse direction, they did not propagate far, usually less than 5 ft. These turned cracks did not interact with other paired cracks to form a recognizable pattern, except at the expansion joint. At the expansion joints, the same stair-step cracking patterns were evident. In addition to the stair-step cracks, there were cracks that started in the stair-step pattern but would continue parallel to the expansion joint. These cracks, which were parallel to the expansion joint, did not seem to affect the stair-step pattern. It appeared that the parallel cracks were superimposed upon the stair-step cracks without any interaction.

In summary, the HPC deck exhibited the same type of cracks as the non-HPC deck. While the decks had the same cracking patterns, the HPC deck had much longer cracks. It is believed that the stair-step cracking pattern is related to the construction technique used for the bridge. This belief will be examined in greater detail near the end of this chapter.

4.4 Dow Barge Canal Bridge Inspection

4.4.1 Description of Dow Bridge

The Dow Barge Canal Bridge is a typical TxDOT bridge. The bridge crosses over a private canal on the Dow Manufacturing site in Freeport, Texas. The data for the exact mixture used in the bridge is unavailable, but it was cast using TxDOT Class S concrete. Class S concrete is the standard material that TxDOT uses for bridge decks. It has a maximum water-cement ratio of 0.45, minimum cement content of 611 lb/yd³, and minimum 28-day strength of 4,000 psi.

The bridge is on a heavy skew, over 45°. The plans for this bridge, like the mixture designs, were unavailable to the researchers. This large skew was used to accommodate the canal underneath the bridge. It is the span over the canal that was of the most concern as it was the most heavily cracked. The spans over the water were approximately 120 ft. However, the deck was continuous over three spans with expansion joints only at the ends. There was approximately 360 ft of continuous deck supported by three 120-ft simply supported spans.

4.4.2 Inspection Results

For this bridge, TxDOT was able to close the shoulder and two of the five lanes on the bridge. Therefore it was possible to inspect much more of the bridge than we had been

able to do at the Louetta Bridge. Unfortunately, it began to rain shortly after the inspection began, and it was not possible to get as detailed an inspection as possible, but some meaningful data was obtained.

There were definite trends in the cracking on this bridge. The trends were similar to those seen at the Louetta Bridge. Pairs of cracks that ran in the longitudinal direction were found. These cracks were similar to those found at the Louetta Bridge. Unlike the Louetta Bridge, these paired cracks were much longer; some of them extended the entire length of the span. Again, the same type of stair-step cracking near the expansion joints that was apparent at the Louetta site on both the HPC deck and the non-HPC deck.

In addition to the cracks described above for the Louetta Bridge, there were some transverse cracks of interest. These transverse cracks crossed from one pair of longitudinal cracks to the adjacent pair. Additionally, they were spaced regularly, at 8 ft. This pattern is illustrated in Figure 4.3 and 4.4, and shown in a photograph from the Dow Bridge in Figure 4.3. Note that the cracks are outlined in yellow for visibility purposes.



Figure 4.3 Stair-step Cracking on the Dow Bridge near Expansion Joint

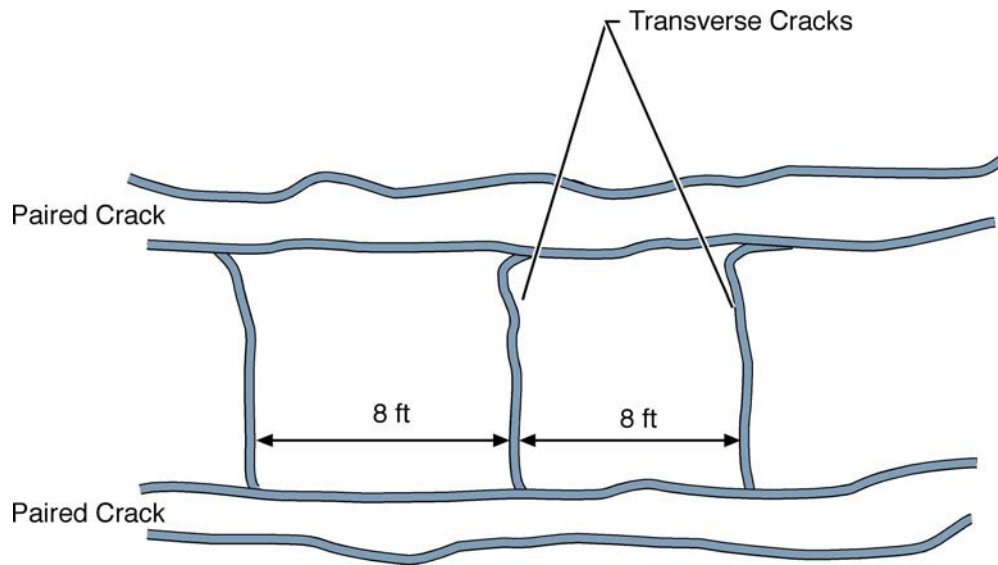


Figure 4.4 Typical Transverse Cracking

4.5 Conclusions

Based on the data presented above, the stair-step cracking patterns, and the regularly spaced transverse cracks, it is believed that the precast-prestressed deck panels are a source of the cracking in both bridges. Figure 4.1 is an illustration of the typical TxDOT details for using the precast-prestressed deck panels. The deck panels are placed on the girders; typically, the panels are placed on fiberboard shims to ensure that the panels are level. After the panels are placed, the cast in place (CIP) concrete is poured. The cast in place concrete envelops the panels as well as the shear reinforcement that extends beyond the top of the girder. In this type of construction the precast panels initially serve as formwork for the CIP concrete. After the CIP concrete has hardened, the panels then become a composite structural component of the deck.

The precast panel will necessarily be older than the CIP deck concrete. Consequently, the precast panel will not exhibit as much shrinkage as the CIP concrete. This differential in shrinkage will cause the panel to serve as a large restraint in both the longitudinal and transverse directions. An illustration of the suspected restrained cracking can be seen in Figure 4.5. The mechanism pictured below is a feasible cause for the longitudinal pairs of cracks seen in both the Louetta and Dow Bridges.

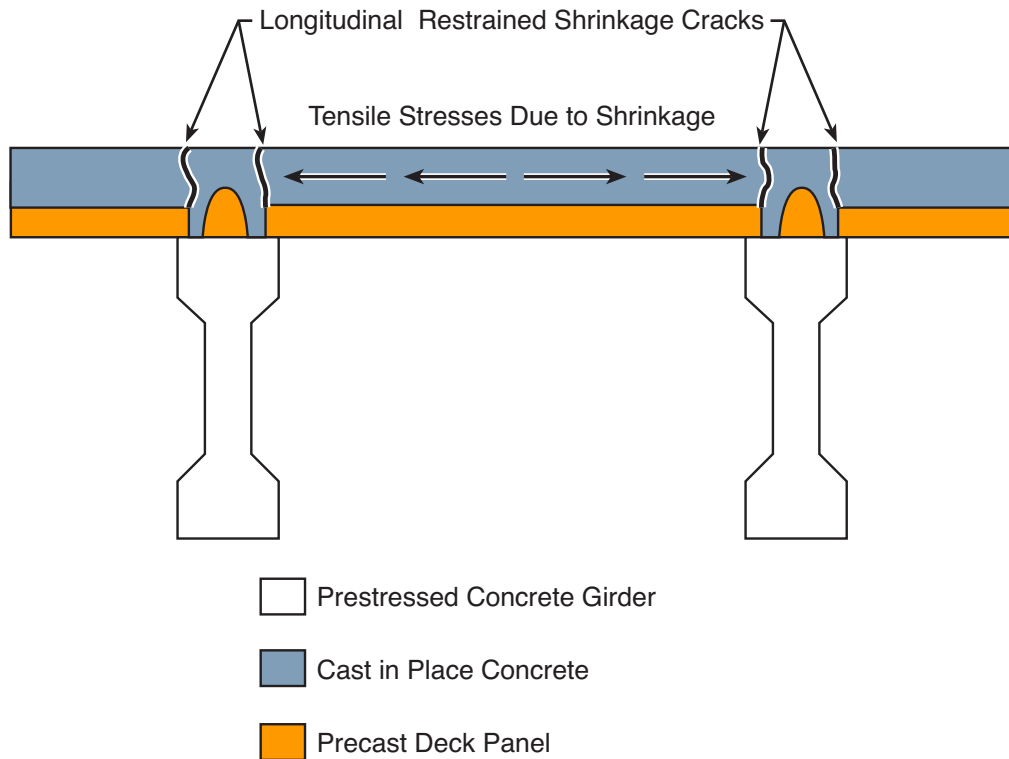
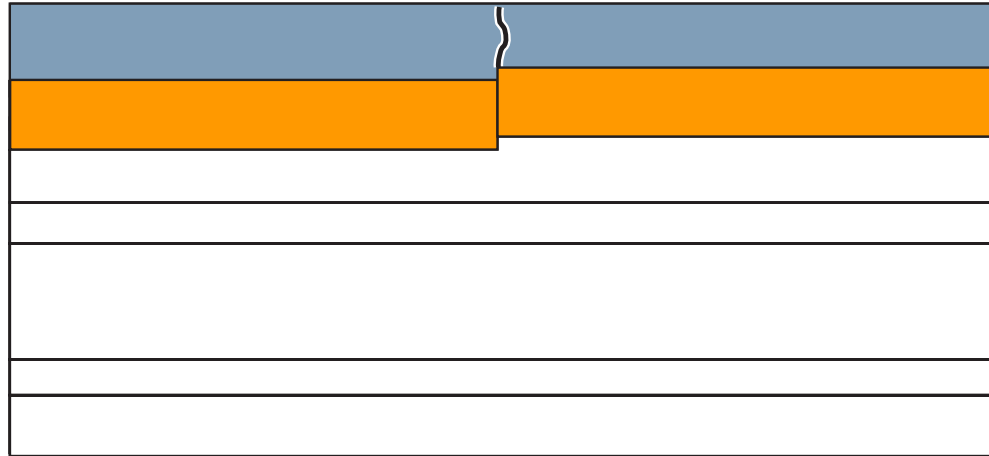


Figure 4.5 Suspected Crack Locations

The precast panels are sized to span between on top of the girders, as shown in the figure above. However, in the direction out of the plane of the drawing, the panels are typically 6 to 8 ft long. At the joints where one panel butts up against the adjacent panel, there is no connection between the two panels. CIP concrete is cast over the panel butt joint; the CIP concrete is continuous while the panels are not. This discontinuity causes a weakened plane within the deck itself and a likely point for restrained shrinkage cracking. Additionally, the precast panels may not be placed in the same plane (Figure 4.6). The top of one panel may be at a significantly different elevation than the top of the adjacent panel. Often, the mismatch in panel elevation is due to the camber of the prestressed beam. The panels are leveled but, due to the camber, one panel will be shimmed more than the adjacent panel.





-  Cast in Place Concrete
-  Precast Deck Panel

Figure 4.6 Section Through Panel to Panel Butt Joint

Note that on the Dow Bridge, transverse cracks were seen to extend from one pair of longitudinal crack to the adjacent pair at regular intervals of 8 ft. The discontinuity at the panel-to-panel butt joint is a likely location and cause of the regular cracking pattern observed at the Dow Bridge.

5. Large-Scale Bridge Decks

5.1 Introduction

In order to bridge the gap between experimental laboratory tests and real world conditions, several large-scale concrete bridge decks (LSBDs) were constructed that blend the defining characteristics of a typical TxDOT bridge deck (i.e., span-to-width ratio, high degree of translational restraint, use of precast concrete panels) with the repeatability and quality control of a laboratory experiment (nearly identical setup, similar time-temperature histories, careful measurement of concrete properties). Furthermore, the large-scale bridge deck represents an experimental midpoint between the laboratory program discussed in chapter two and an actual bridge. The large-scale bridge decks are the culmination of this project and serve as more realistic testing conditions for how various innovative materials, chosen from laboratory testing and literature reviews, will perform when subjected to actual environmental exposure conditions.

The LSBD test setup and the final LSBD results will be discussed in three sections, namely the design and modeling of the LSBD, the construction and performance of the Phase I LSBDs, and the construction and performance of the Phase II LSBDs.

5.2 Design and Modeling of LSBD

The rationale for the design of the LSBD is to observe and verify the drying shrinkage crack resistance of various innovative materials. Prior to their use in a LSBD, these innovative materials were included in the literature review and laboratory test methods phases completed earlier in the project. In order to accomplish this while meeting cost, space, and time requirements, it was necessary to come up with a test setup that emulates a typical TxDOT bridge deck, yet is smaller in size and complexity than a real bridge deck. One of the most important capabilities, besides mimicking a typical TxDOT bridge deck, is the ability to run several tests simultaneously to minimize variability in environmental conditions between each bridge deck. Thus, the LSBD must be small enough in size so that six to eight tests can be run simultaneously.

After several brainstorming sessions and rough calculations, a preliminary design was conceived that balanced the constraints of the project while emulating a standard bridge

deck. It was decided that a rectangular deck section measuring approximately 10 ft x 20 ft and heavily restrained at both ends would be ideal for the constraints set by the project initially. Conceptually, this design resembles a dog-bone specimen, which is often used as the laboratory specimen shape to force a behavior to occur in a specific region. However, instead of necking or decreasing the cross-sectional area of the specimen, the LSB setup will effectively neck or decrease the restraint provided in the center region. Heavy restraint at either end and little restraint in the middle will encourage any drying shrinkage cracking to occur in the middle section of the deck.

An initial width-to-span ratio of 1:2 was selected to obtain a typical proportioning of a TxDOT bridge. The fact that the longitudinal direction is twice as long as the transverse direction means that there is twice as much concrete that wants to shrink in the longitudinal direction than in the transverse direction. Consequently, a transverse crack is expected to develop in order to relieve a larger tensile stress in the longitudinal direction.

A review of standard TxDOT bridge deck specifications revealed that an 8 in. total deck thickness would be appropriate. Since the majority of TxDOT bridge decks are built using precast concrete panels (PCP), it was decided to emulate this design and use 4 in. thick 8 ft x 8 ft precast concrete panels from a precast plant that supplies the majority of TxDOT's PCPs throughout the state. Figure 5.1 provides a picture of a typical PCP used. Each PCP has one roughened surface to ensure there is interlock between the cast-in-place layer and the PCP. In this case, the top layer is roughened and every other surface is smooth, since the top surface is where the cast-in-place concrete will eventually be placed.

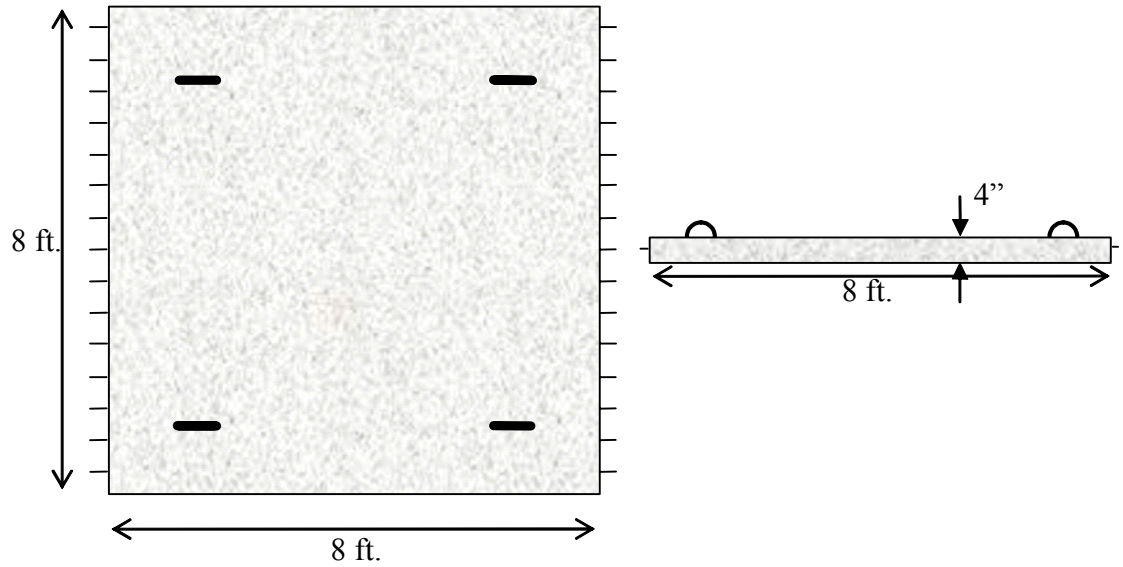


Figure 5.1 View of a typical precast concrete panel used as stay-in-place forms on the LSBDs

The final 8 in. thick concrete bridge deck would consist of 5 in. of PCP (each 4 in. thick PCP is raised an inch) and about 3 in. of cast-in-place concrete above that. However, the last 1.5 ft longitudinally on each end of the test setup, where the majority of the restraint would be provided, would consist of 8 in. of cast-in-place concrete. Figure 5.2 provides a cross-sectional view of the bridge. The details of how the restraint is provided as well as the structure supporting the deck girders will be given in the following section.

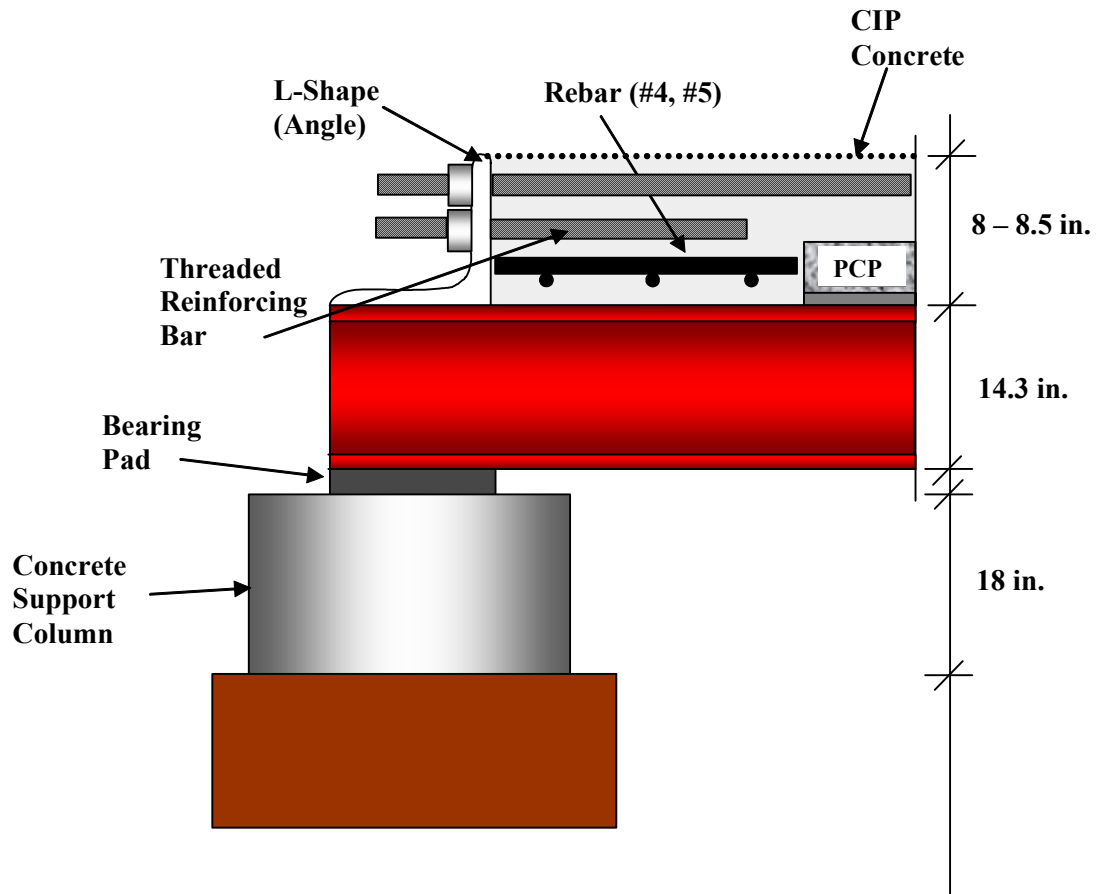


Figure 5.2 Detail of restrained end of LSB using threaded reinforcing bar

Two portions of the LSB structure required a careful design; mainly, the end restraint and the deck support structure. These two portions were particular to the experiment and did not have existing specifications or plans on how to produce them.

The main purpose of the girders, which run the length of the deck structure, is to transfer the load of the deck into the columns. However, from the literature review it is known that the type of girder material used affects the amount of restraint imparted to the deck, and affects the propensity for drying shrinkage cracking. Most bridge girders are either steel or concrete, so the final choice of girder type was based on the potential for reusability and customization. Thus, a steel girder was chosen because steel girders would be reusable as well as their relative ease of drilling and attaching, via bolting or welding components to the girder. In addition, the placement of shear studs can be controlled, allowing adaptation of the number and position of shear studs along the flange.

The purpose of the end restraint is to provide almost infinite restraint at the ends so that when the concrete deck shrinks it will tend to pull apart from the center, where there is less restraint, and therefore cracking should occur near the center region (see Figure 5.3). How this full restraint is accomplished is another matter.

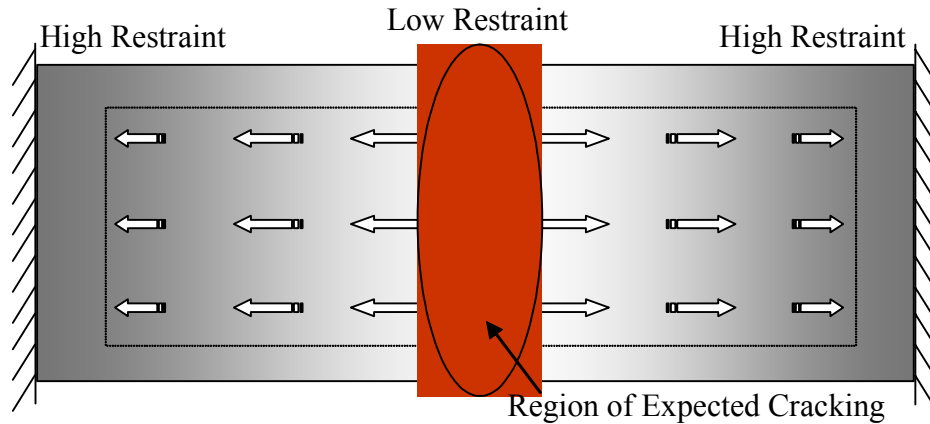


Figure 5.3 A conceptual representation of “dog-bone” restraint setup so that cracking will most likely occur in the middle region of the bridge deck. Relative magnitude of shrinkage is represented by the arrows.

After review of several preliminary designs, a design involving the use of threaded reinforcing bar anchored to an 8 in. x 8 in. steel angle, which, in turn, is bolted to the ends of the steel girders (see Figure 5.4). The effectiveness of the restraint relies on the concrete-threaded reinforcing bar bond. Thus it is difficult, if not impossible, to accurately predict the degree of restraint that the concrete experiences because restraint depends on how much the concrete shrinks and creeps.

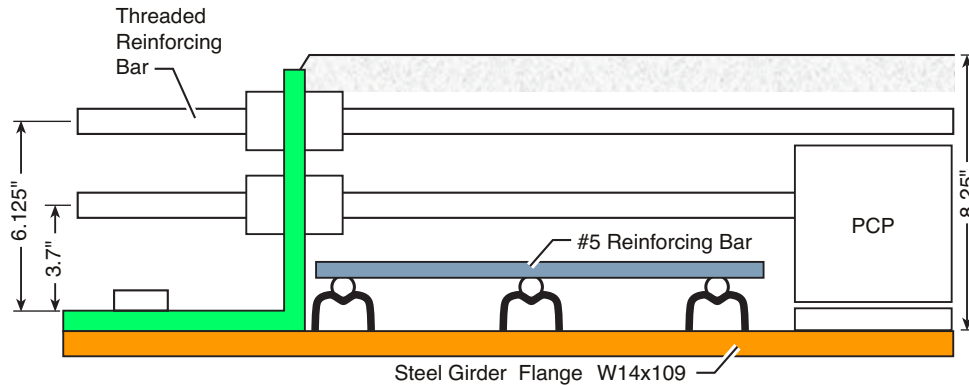


Figure 5.4 Side view of end restraint. The end region beyond the PCP is heavily reinforced to encourage drying shrinkage to occur in the central portion of the deck.

Initially an elastic analysis of the preliminary setup was performed using hand calculations to arrive at adequate steel member sizes. Excessive deflections and yielding of the girder's web, flange, and the potential for lateral-torsional buckling were considered. The *AISC 3rd Ed. Manual of Steel Design* was used to check these different failure modes in steel. A steel W14 x 109 provided the necessary strength as well as the required flange width.

In order to arrive at specific member sizes for the girders as well as the presence of stress concentrations, a preliminary finite element model was created in SAP2000. A preliminary finite element of the proposed LSB D was created before the actual LSB D apparatus was built in order to verify the potential of the LSB D's functionality. Once the finite element model was verified itself with simple, elastic hand calculations, the finite element model was used exclusively for further analysis.

The goals of the finite element model of the LSB D are the following:

- 1) Center-line deflection
- 2) Yielding/Buckling in steel (Local flange, local web, lateral-torsional)
- 3) Simulate shrinkage in decks
- 4) Determine the stress concentrations due to shrinkage

All of the goals for the finite element program were met, with the exception of the ability to simulate the shrinkage in concrete bridge decks. This is due to the fact that the finite element model was used primarily as a design tool instead of an analysis tool so that several aspects of the LSB D were simplified and assumed to behave in a certain manner, even when this was not experimentally proven. This is true of all models, since structural

models are simplifications of an actual structure and certain simplifying assumptions must be made. For example, no reinforcing bar was taken into account as a source of restraint within the deck, nor was friction present in the interfacial layer between the concrete and steel. In fact, the only true restraint accounted for in the finite element model is in the assumption that both concrete deck ends are fixed with respect to translation. In reality, there is significant friction between the precast concrete panels and the cast-in-place concrete as well as friction between the steel girder flange and the cast-in-place concrete edges.

The model in no way purports to predict or even analyze the drying shrinkage of concrete in the LSBD in the field. Several unknowns that cannot be incorporated into the finite element model include modeling creep, temperature variations within the material due to daily temperature cycles, the time dependent strength gain of concrete, frictional restraint between the cast-in-place deck and the PCP and steel girders, moisture conditions, and the changing modulus of concrete with time.

The following screenshot in Figure 5.5 is from the SAP2000 finite element model and is provided to illustrate the finite element modeling performed during the design phase.

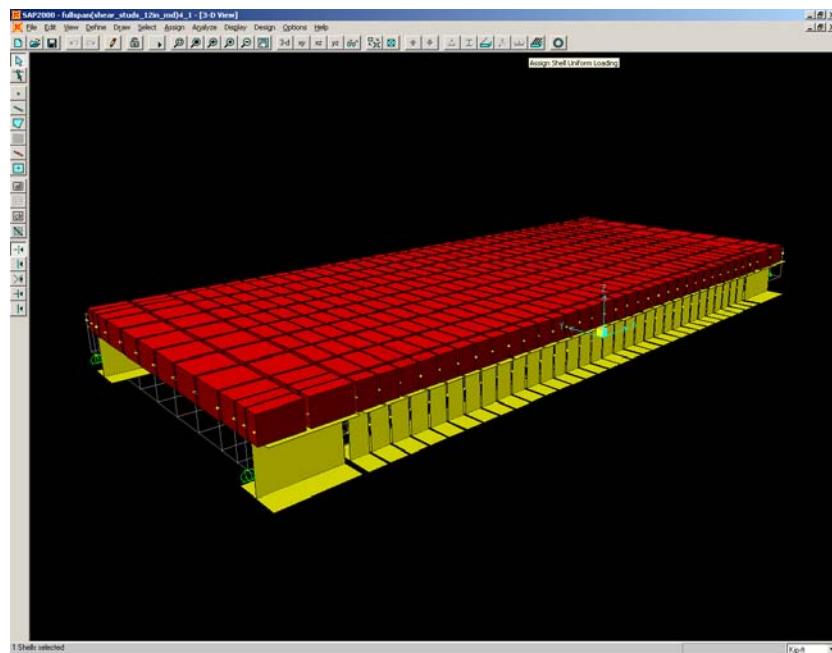


Figure 5.5 Meshing of LSBD for design purposes. Stresses in the girders and deck were determined to validate the preliminary design

Because of the high degree of uncertainty in the prediction of cracking, it was decided to divide the development of the LSBD into two phases, called Phase I and Phase II. Phase I is simply a preliminary phase in which two complete LSBDs will be built that utilize two mixtures with low and high propensities for drying shrinkage cracking. Phase II will serve as the heart of the LSBD portion of the project and will compare the innovative material-based mixtures selected from the literature review and laboratory program results. Phase II will incorporate improvements and design modifications learned from the Phase I LSBDs.

5.3 Phase I

There are two main objectives of Phase I of the LSBD. The first objective is to verify that drying shrinkage cracking is indeed discernable when tested in the LSBD format. The second objective is to verify that the laboratory test methods are producing acceptable and expected values based on the existing laboratory program test results already gathered. An advantage of breaking the testing into two phases is the ability to look for ways to improve upon the LSBDs from Phase I so that the construction and instrumentation are straightforward and understood before the initiation of Phase II, the final deck construction phase.

5.3.1 Design and Construction

The design and construction of the Phase I LSBDs depended heavily on preliminary design and analysis, as discussed earlier. Shaped heavily by the initial constraints of the project in terms of space, time, and cost, the Phase I LSBDs represent large-scale test specimens which are able to provide a way to evaluate a concrete mixture's propensity for drying shrinkage cracking.

The Phase I LSBD consisted of several discrete components including the columns, formwork, PCP and pads, and various sources of restraint against shrinkage. Each of these components will be discussed in terms of its purpose as it relates to the testing of the drying shrinkage cracking resistance of various innovative material concrete mixtures.

5.3.2 Columns

The columns are present to provide a more realistic bridge deck exposure condition in which the deck itself is exposed on the top, both sides, and the bottom. The columns are built so that all the bridge decks are level with each other, even if the ground was not. Typically, this meant an exposed column height of about 1.5 ft to 2 ft above ground level. Furthermore, the columns were designed to resist the dead-load of the LSBDs and prevent settlement of any of the supported corners of the bridge deck. Although the girders are simply supported on the columns, any significant settlement of any one column would induce stresses in the bridge deck. To assure that the potential for settlement was minimized, the column shaft was continued down until a stable layer of limestone was reached during the excavation phase. The columns also provide a flat and even surface on which to place the steel girders to ensure a flat grade on the bridge deck surface so that the cast-in-place portion of the bridge deck has a uniform thickness. Figure 5.6 provides a photograph of the columns.



Figure 5.6 Photograph of poured columns used to prevent differential settlement of the LSBDs

5.3.3 Formwork

Formwork, although not critical to the results of the LSB, is important because its failure can lead to a failed pour and jeopardize the experimental advantage of pouring the decks within a short time frame to achieve similar time-temperature histories. Problems in the formwork such as breakage or leaking, can affect the integrity and quality of the cast-in-place portion. To ensure that safe and appropriate formwork can be installed and easily removed at the appropriate time, the *ACI SP-4 Formwork for Concrete Design* guidelines are used.

5.3.4 Precast Concrete Panels (PCP)

PCPs are utilized to both cut down on the amount of removable formwork required and mimic a typical TxDOT bridge deck. As mentioned earlier, the majority of TxDOT bridge decks are currently built using PCP as stay-in-place forms. The PCP measure 8 ft x 8 ft with a thickness of 4 in. (see Figure 5.7). This size is common and was obtainable, making it an ideal dimension to use.



Figure 5.7 Photograph of actual PCP used in the construction of the LSBs

5.3.5 Sources of Restraint

The shear studs, heavily reinforced end regions, and presence of the PCP serve as the main sources of external and internal restraint for the LSB cast-in-place concrete. The

shear studs, though not typical shear studs used in practice, consist of 6 in. long, $\frac{3}{4}$ in. diameter, fully threaded hex-head high-strength steel bolts attached to the steel girder through drilled holes via heavy hexagonal steel nuts. The purpose for securing the shear studs in this fashion is the ability to remove them from the steel girder and reuse the steel girders for future tests. It also permits the ability to vary both the number and heights of the shear studs if the need arises.



Figure 5.8 Photograph of shear studs a day before the cast-in-place concrete was poured

The shear studs, as seen in Figure 5.8, were placed in pairs at intervals of 6 in., center-to-center, to provide both longitudinal restraint and composite action. In this particular application, the shear studs are present mainly to provide longitudinal restraint to the full 8 in. depth cast-in-place concrete on either side of the PCP. In reality, the shear studs are present to provide composite action, but since this bridge deck is not being loaded beyond its dead load this is not a concern.

The heavily reinforced end regions consist of both deformed reinforcing bar and threaded reinforcing bar. These end regions, two per LSB, are approximately 1.5 ft x 9 ft and consist of a full depth (8 in.) cast-in-place concrete section with three layers of reinforcing bar, as seen in Figure 5.9.



Figure 5.9 Photograph of the end region showing two layers of threaded reinforcing bar as well as a bottom layer of deformed reinforcing bar

Unlike the deformed reinforcing bar, the proprietary threaded reinforcing bar is attached to an 8 in. x 8 in. steel angle using proprietary threaded locking nuts, which effectively lock the threaded reinforcing bar to the steel angle (see Figure 5.10). The steel angle is attached to the steel girders using two heavy hex bolts attached at either end of the angle. The connection relies on the friction between the steel angle and the steel girder.



Figure 5.10 Photograph of 8 in. x 8 in. steel angle. The steel angle is bolted to the steel girder to provide a source of high restraint.

The deformed reinforcing bar is present to provide tensile reinforcement for the transverse span between the girders since there is no stay-in-place formwork below the end region and the concrete must support itself in this region.

One important difference between a typical TxDOT bridge deck and the LSBs used throughout this project is that the LSBs lack the top mat of reinforcing steel, typically consisting of #4 and #5 deformed reinforcing bar. Generally the top mat of reinforcing steel is present mainly to control shrinkage and thermal fluctuations in the bridge deck. It provides little, if any, added benefit in terms of resisting moments generated from deck loading, since most bridge decks do not experience significant negative moments. The top mat of reinforcement was removed in order to enhance the crack width of any drying shrinkage cracks that may appear. The concern was that, with the top mat in place, any cracks that may appear would not be large enough to see initially or that the cracks would distribute themselves so that more cracks would appear, but each crack would be smaller and harder to identify. Without the top mat of reinforcement, the same cracking will still occur, but the cracks should be fewer in number and larger in size, making it easier to keep track of.

5.3.6 Concrete Mixtures

The concrete mixtures for the Phase I LSBP were selected to verify that the Phase I bridge decks were functioning as expected. In other words, two mixtures were chosen so that one mixture had a high probability of experiencing drying shrinkage cracking while the other should not crack at all. The crack-prone mixture is an HPC (high performance concrete) with a low water-to-cement ratio of 0.27 dosed with a superplasticizer to facilitate placement and enhance workability. A table with the mixture design for both mixtures appears below (Table 5.1). The mixture that should not crack at all is an SRA (shrinkage reducing admixture) based concrete mixture. The SRA mixture relies on the ability of the shrinkage-reducing admixture to lower the surface tension of the water trapped in capillary pores so that the eventual loss of water from capillary pores smaller than 50 nm will not cause large tensile stresses to be transferred to the capillary walls, the main mechanism of drying shrinkage.

Both mixtures were procured on the same day from a local concrete supplier and delivered on-site.

Table 5.1 Phase I Mixture Proportions

<u>Material</u>	<u>Mixture (per yd³)</u>	
	<u>SRA</u>	<u>HPC</u>
3/4 Rock (lbs)	1227	1863
Sand (lbs)	1204	1161
1 1/2 Rock (lbs)	661	0
Cement 1 (lbs)	443	677
Fly ash (lbs)	140	169
Water (lbs)	247	230
AEA (lbs)	4.6	0
WRA (Type A) (oz)	17.5	0
MRWR (oz)	0	16.9
HRWR (oz)	0	135.4
Water Added (lbs)	33	66
SRA (lbs)	63	0

5.4 Results and Discussion

Similar to the results and discussion section in the second chapter on the laboratory program, the fresh properties of the Phase I mixtures will be discussed first, followed by

the hardened properties associated with the laboratory program test methods (i.e., restrained shrinkage rings, free shrinkage, compression, split-tensile, and modulus of elasticity).

5.4.1 Fresh Properties

The fresh properties of the concrete mixtures for the Phase I LSBDs consist of the slump and temperature values provided in Table 5.2.

Table 5.2 Fresh Properties of Phase I Mixtures

Property	Mixture	
	HPC	SRA
Initial Slump (in)	8	5
Initial Temperature (°F)	94	90

The high slump value for the HPC mixture is a consequence of the necessary use of a superplasticizer to enable adequate workability with such a low water-to-cement ratio mixture as HPC. This high slump made the HPC mix easy to place.

5.4.2 Hardened Properties

The hardened properties measured for the Phase I LSBD mixtures were not as comprehensive as those hardened properties measured during the laboratory program. For example, creep was not measured on either the Phase I or Phase II specimens because of a lack of adequate measurement equipment. Had an adequate number of creep frames been available, specimens from both phases would have been included in creep testing. The laboratory testing performed on the Phase I LSBD, however, includes free shrinkage (both under real conditions and controlled laboratory conditions), restrained shrinkage rings, compression, tensile strength, and the modulus of elasticity.

Compression, Modulus, Tensile Strength (AASHTO T22, ASTM C469, AASHTO T198)

Measurements of the compressive (Figure 5.11) and tensile (Figure 5.12) strength as well as the elastic modulus (Figure 5.13) were taken at 3, 7, and 28 days. It is ideal to take as many measurements as possible, but the focus of this project is on the early-age drying shrinkage cracking and therefore measurements beyond 28 days were not performed.

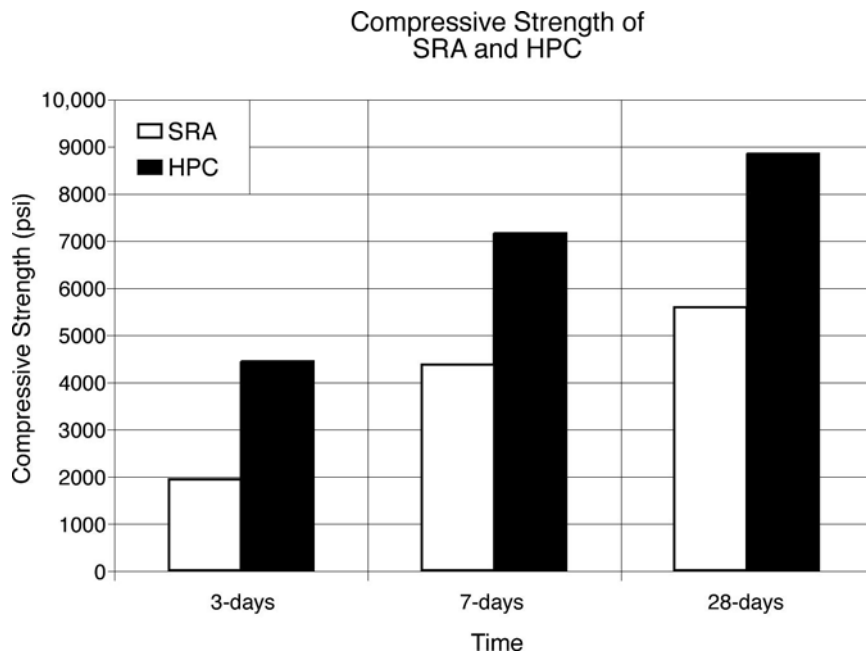


Figure 5.11 Compressive Strength of Phase I LSBDs: SRA and HPC

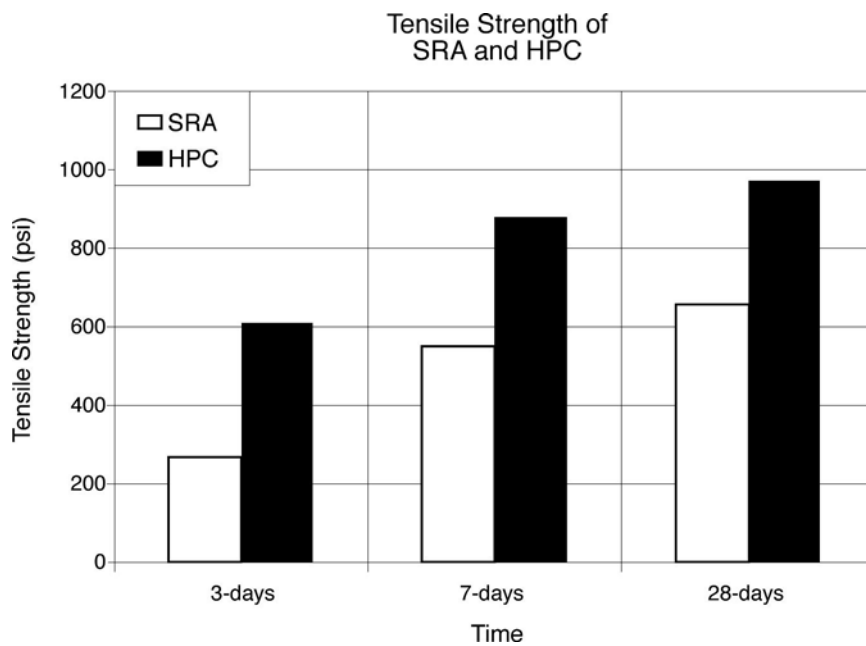


Figure 5.12 Tensile Strength of Phase I LSBDs: SRA and HPC

The fact that HPC has a high 3-day compressive strength and a high 3-day tensile strength demonstrates that HPC gains strength much faster than the SRA mixture does. According to the findings of the literature review, a high early strength indicates a much

higher probability for susceptibility to drying shrinkage cracking than a mixture where the strength gain is relatively slow. Cracking is more likely to occur in a low water-to-cement ratio mixture like 0.27 in HPC because of higher drying shrinkage and thermal stresses, as well as a higher elastic modulus and lower creep.

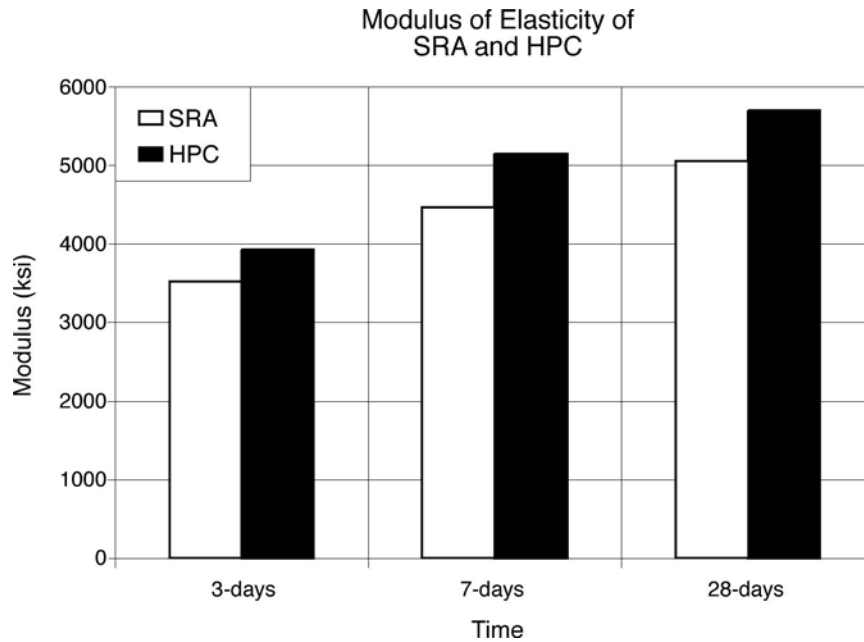


Figure 5.13 Modulus of Elasticity for Phase I LSBDs: SRA and HPC

The modulus values do not exhibit a clear trend like the compressive and tensile measurements do. In fact, the 28-day modulus values for SRA and HPC only differ in magnitude by about 13%. However, more important is the early-age modulus value; in this case the earliest values recorded are 3-day modulus values. A high early-age modulus means that for a certain strain a larger equivalent stress will result than compared to a low early-age modulus. Nonetheless, in this case it is difficult to argue that HPC should have a significantly higher probability for cracking due to drying shrinkage cracking because both 3-day modulus values for both mixtures are within 12% of each other.

Free Shrinkage (AASHTO T160)

Although the Phase I free shrinkage tests were performed in an identical fashion to the free shrinkage tests completed during the laboratory program, more specimens than needed were created to examine the effect of moisture and temperature on free shrinkage.

These additional specimens served as outdoor specimens that are subjected to the same environmental conditions as the LSBDs are. This permitted comparison between the drying shrinkage characteristics of environmentally controlled specimens found in the shrinkage room with the drying shrinkage characteristics of specimens subjected to actual exposure conditions. To accomplish this, the outdoor specimens were brought into the environmentally controlled chamber, maintained at 73°F and 50% relative humidity, and allowed to assume the temperature of the specimens already situated in the environmentally controlled chamber to minimize the variation in length due to temperature. Typically, this translates into a delay in the extensometer measurements of approximately 1.5 hours to allow for thermal equilibrium to take place. The free shrinkage values are plotted in Figure 5.14.

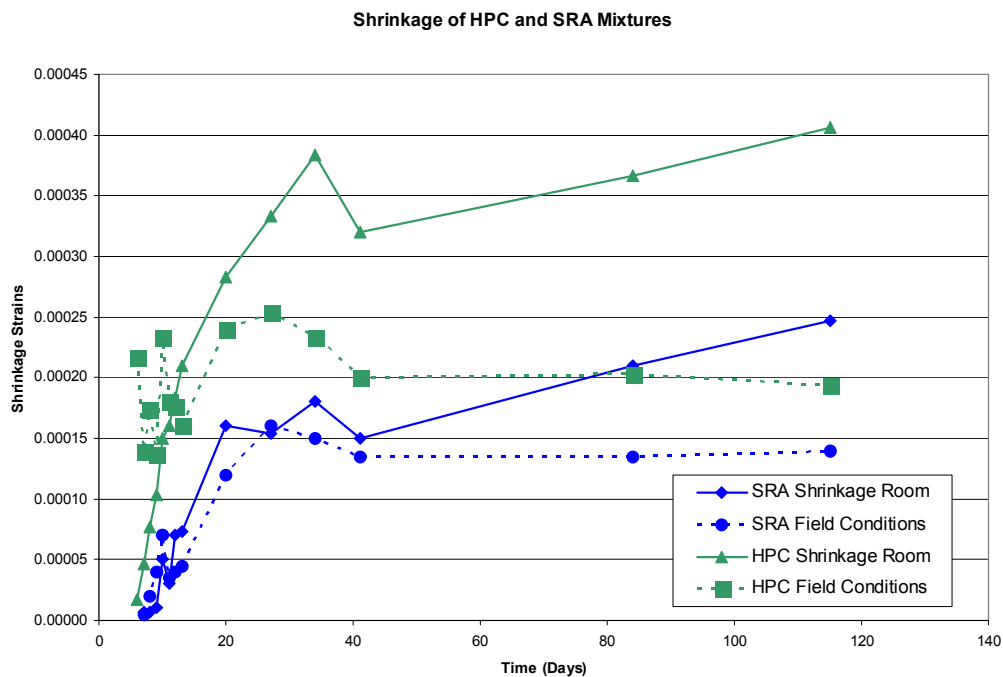


Figure 5.14 Free shrinkage strain of HPC and SRA mixtures, both in the shrinkage room (solid line) and the field conditions (dashed line)

The free shrinkage results illustrate the effect that environmental conditions have on the shrinkage characteristics of the two Phase I concrete mixtures. The free shrinkage is initially higher for the prisms exposed to the field conditions (i.e., outside), and then drops off after about 3 days of exposure. After the first three days of exposure the shrinkage of

the field condition specimens for either mixture are less than the prisms kept in the environmentally controlled shrinkage room. As expected, the HPC shrinks more than the SRA mixture such that HPC has a shrinkage room free shrinkage strain value of approximately -0.00033 in/in at 27 days whereas the SRA mixture has a shrinkage strain value of -0.00015 in/in. This behavior is true in both the field and environmentally controlled exposure conditions. This demonstrates, at least for the HPC and SRA mixtures, that the material itself affects the free shrinkage of a specimen, even in a variable exposure conditions, such as the field conditions.

However, it must be emphasized that the relative difference in shrinkage strain between the shrinkage room specimens and the outdoor specimens for a given mixture is dependent on the outdoor conditions. Obviously, if the outdoor environment has a higher relative humidity than the shrinkage room (50%), then the results may be reversed so that the outdoor specimens shrink less.

Restrained Shrinkage Rings (AASHTO PP34-99)

Restrained shrinkage rings help to enable comparison between the relative time-to-cracking for different concrete mixtures. The repeatability of the restrained shrinkage rings depends heavily on the ability to cast the rings evenly so that the thickness of the ring is constant throughout.

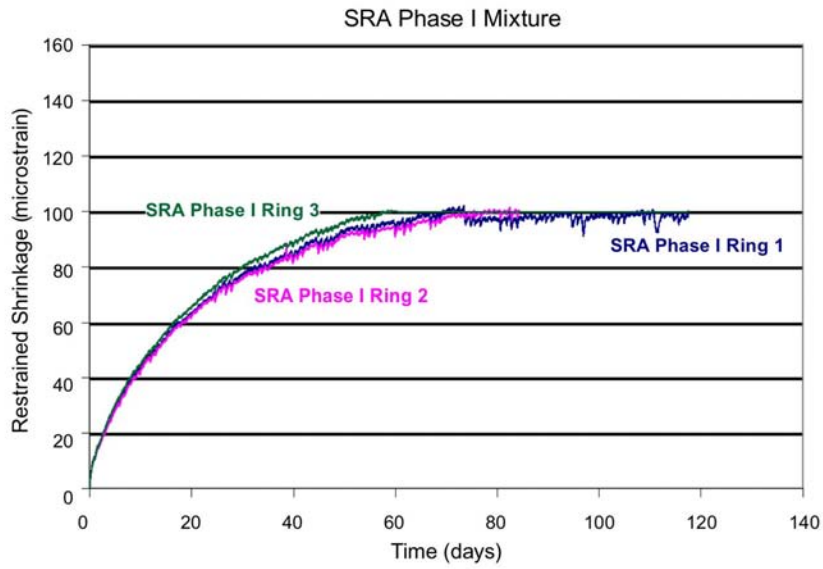


Figure 5.15 Restrained shrinkage strain gage output for SRA

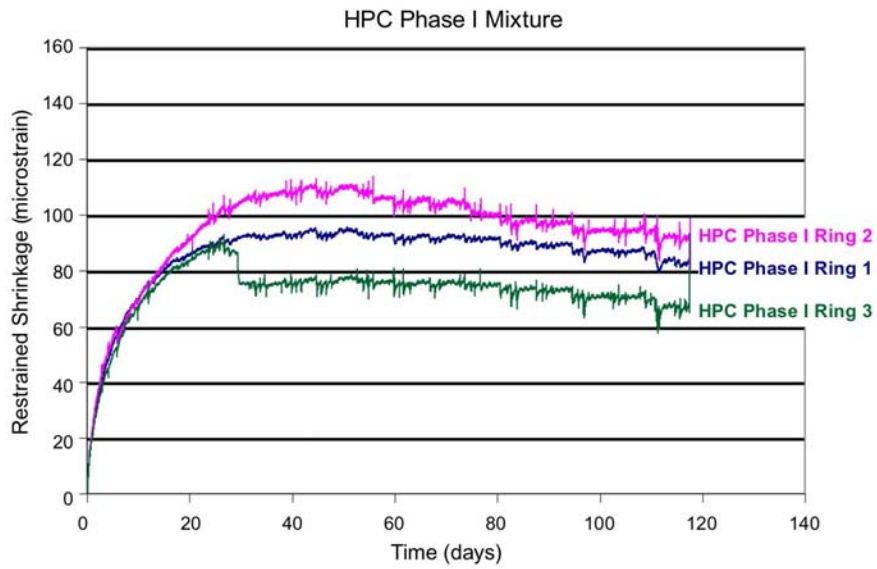


Figure 5.16 Restrained shrinkage strain gage output for HPC

The results of the restrained shrinkage rings for the Phase I LSBDs, plotted in Figure 5.15 (SRA) and Figure 5.16 (HPC), are not consistent enough to accurately predict a time-to-cracking value. However, the fact that one of the HPC rings cracked while none of the SRA rings cracked signals that HPC should have a higher probability of cracking. It is incorrect to assume that since an HPC ring cracked at an age of approximately 30 days that the concrete deck will crack at that same age. The only pertinent information that can be drawn from the restrained shrinkage rings in this case is the relative propensity for drying shrinkage cracking. The higher number of restrained shrinkage rings that crack for a specific mixture translates into a higher probability for susceptibility to drying shrinkage cracking. Furthermore, the higher number of restrained shrinkage rings that crack at about the same time indicate the relative time to cracking.

5.4.3 Instrumentation

The only internal instrumentation in the Phase I LSBD are permanent temperature probes placed at six different locations in the deck.

These temperature probes were used to determine the internal temperature of the concrete at various time intervals. Most important were the initial heat of hydration readings taken during the first 24 hours after the pour. These early temperature readings provided a maximum heat of hydration temperature for each LSBD as well as the ability to determine the temperature of the bridge decks at any time.

A plot of the initial temperature readings during the first 24 hours after pouring for each bridge deck is presented in Figure 5.17. In order to facilitate comparison with the ambient conditions, the internal concrete temperatures for each deck as well as the ambient temperature are plotted on the same figure.

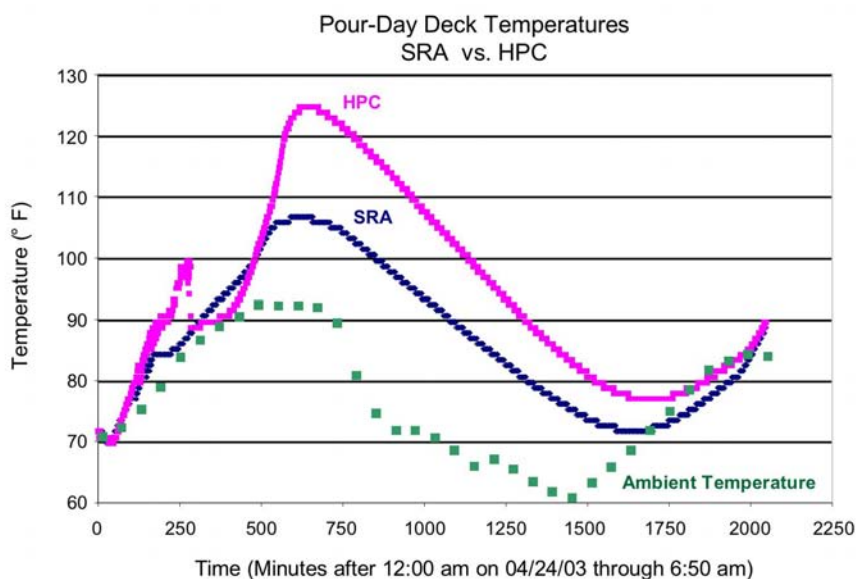


Figure 5.17 Initial internal temperature for HPC and SRA compared to the ambient temperature

As expected, HPC had a higher heat of hydration due to the much higher cement content as compared to the shrinkage reducing admixture. However, the HPC mixture was also poured later in the morning and therefore its peak heat of hydration corresponds with the maximum ambient temperature during the day of the pour.

Further external instrumentation of the bridge decks included the use of extensometer readings in the central region of the bridge deck. Although readings were taken almost every day, the use of this data was abandoned due to the complex nature of the variables affecting these readings. For example, each extensometer reading was taken at a certain time, but the temperature of the deck was not constant. Therefore, in order to obtain results that represent the shrinkage of the deck, it would be necessary to back out the effect due to temperature, which was deemed too difficult for the impact of the data.

5.4.4 Cracking

As expected, the Phase I HPC deck mixture cracked in the middle region while the SRA mixture has not cracked at all. In fact, the HPC mixture exhibited drying shrinkage cracking within 5 days of pouring the bridge deck. The initial crack did not span the entire transverse length however, but instead started in the middle and propagated outward

toward the edges. Within 8 days the crack had propagated the entire transverse width of the deck and had cracked almost full depth on the outside visible edges (see Figures 5.18 and 5.19).

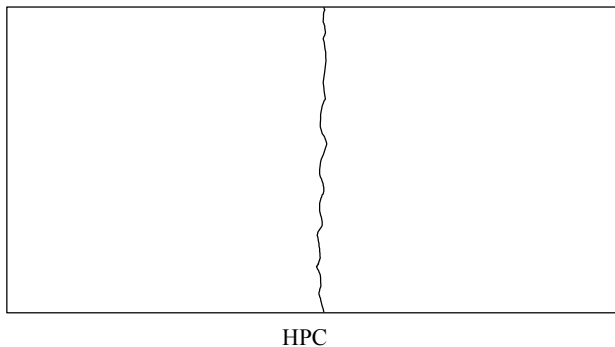


Figure 5.18 Observed cracking on the HPC Phase I LSBD. Cracking initiated after five days and completely spread to either edge after eight days.

From this point on, no further cracking appeared, but the crack width of the deck increased from a hairline crack measuring about 0.001 inches to 0.005 inches in approximately 18 days. These cracks widths are difficult to interpret though, because the thermal expansion and contraction of the deck due to the ambient temperature variations affects the crack width value. Therefore, the general trend in the HPC deck after initial crack formation was that the crack propagated and grew from the center toward the edges.



Figure 5.19 Photograph of drying shrinkage cracking on HPC Phase I LSBDD after eight days. Crack is outlined in black for visual reference

5.4.5 Conclusions

The Phase I LSBDDs were deemed a success because the observed cracking behavior of the decks agreed with the initial hypothesis that the HPC mixture would crack in a manner characteristic of drying shrinkage (transverse crack near the center of the bridge deck) and that the SRA would not crack at all. Therefore, the first objective was satisfied, since it was possible to discern the difference in the resistance to cracking between the mixtures based on the results of the Phase I LSBDDs. The results of the laboratory program tests for hardened concrete properties from the Phase I mixtures and the laboratory program results from the laboratory-based mixtures agree in magnitude. For instance, the shrinkage strains after 28 days for the Phase I LSBDDs specimens and the laboratory program HPC mix are both approximately 0.0003 in/in. Likewise, a similar agreement between SRA in the Phase I LSBDDs and the laboratory program is present since both 28-day shrinkage strains are approximately 0.0001 in/in. Comparison of other hardened properties such as compressive strength and tensile strength demonstrates that there exists a general agreement in magnitude between the Phase I hardened concrete properties and the laboratory program hardened concrete properties.

Improvements to Phase I LSBDDs

However, even though the Phase I bridge decks were deemed successful, several improvements were made to the Phase I design in order to improve the performance of the final LSBDD that will be used in Phase II. Although the HPC deck mixture did in fact crack,

its crack width was almost too small to measure initially. A handheld crack microscope had to be used in order to accurately gauge the crack width. To help increase the crack width two improvements were proposed. The first involved removing the shear studs from the center portion of the girders so that the concrete on the flanges of the steel girders is no longer restrained as much as when the shear studs were present. Second, the amount of restraint in the end regions was increased through the use of more threaded reinforcing bar. This was done to increase the amount of restraint near the ends to make sure that any shrinkage would manifest itself in the less restrained middle region.

5.5 Phase II

The design for the Phase II LSBDs was based on the Phase I LSBDs design with the incorporation of the two improvements mentioned previously; specifically, the decreased number of shear studs in the middle region and increased restraint in the end regions (see Figure 5.20). These improvements are meant to enhance the manifestation of drying shrinkage cracking in the various mixtures to make the cracking more pronounced. Six mixtures from the original eight mixtures considered during the laboratory investigative program were selected as candidates for determining drying shrinkage cracking resistance based on the literature review and laboratory program results. To this end, the Phase II LSBDs consisted of six newly constructed LSBD, with each LSBD containing a different concrete mixture. Besides the different mixtures tested in each bridge deck, all six LSBDs were identical. Accordingly, the mixture design for each LSBD will be described in detail in the following section.

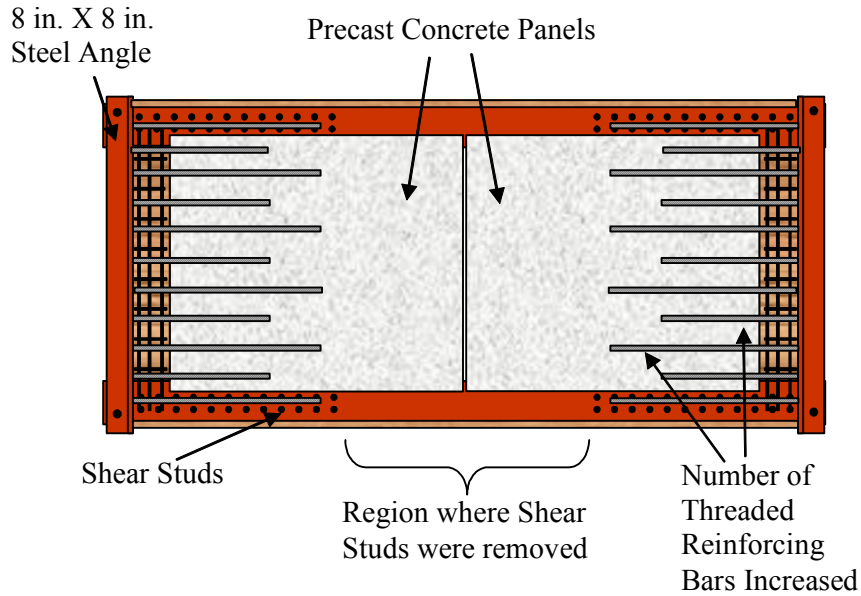


Figure 5.20 Top view of Phase II LSB D before cast-in-place concrete (shows formwork)

5.5.2 Mixture Designs

The final mixture designs were selected based on the laboratory program results discussed in chapter two according to the ability to resist or prevent early-age drying shrinkage cracking. These mixtures are presented in Table 5.3 below. The six mixtures include a control (TxDOT class S), high-volume fly ash (HVFA), high-performance concrete (HPC), calcium-sulfoaluminate admixture (CSA), shrinkage-reducing admixture (SRA), and a mixture with fibers. Each mixture contains the same amount of cementitious material, except for HPC, which has a higher cementitious content. This was done to further improve the comparability between the six mixtures.

Table 5.3 Mixture Proportions for Phase II LSBDs

Mixture Description	Cement lb/yd ³	Class F Fly Ash lb/yd ³	Coarse Aggregate (3/4 in) lb/yd ³	Fine Aggregate lb/yd ³	Water Lb/yd ³	Water Added (lbs)	100 XR
Control	611	0	1809	1315	275	58	9.2
HVFA	275	336	1806	1312	275	33	9.2
HPC ¹	677	169	1863	1161	230	0	12.7
CSA ²	550	0	1809	1315	275	75	9.2
SRA ³	611	0	1809	1315	262	75	9.2
Fibers ⁴	611	0	1759	1365	275	0	9.2

Notes

¹ HPC was dosed with 16.0 oz. of superplasticizer

² CSA had 61 lbs of Calcium-sulfoaluminate admixture per cubic yard (10% replacement by weight)

³ SRA was dosed with 1.5 gallons of shrinkage reducing admixture per cubic yard

⁴ Fibers was dosed with 4 lbs of fibers per cubic yard

Control

The control was chosen because it provides a useful reference or baseline throughout the duration of the project and provides verification of behavior so that previous results both from the laboratory program and the field tests can be compared to each other.

HPC

HPC was used again with the exact same mixture proportions as it had been in the Phase I testing, in order to provide another source of verification between the results of the Phase I and Phase II LSBDs. In other words, HPC's behavior serves as a gauge as to the ability of the new Phase II LSBDs to perform as expected.

HVFA

The HVFA mixture contains 55% Class F fly ash and serves as an example of an extensible concrete mixture. Extensible concrete is concrete that is made from conventional materials, such as cement, fly ash, and/or slag, but is proportioned in an unconventional way (Mehta 1993). Some of these unconventional proportions include a high pozzolanic content; in this case 55% Class F fly ash, as well as low cement content and a relatively high water-to-cement ratio. The motivation for these unconventional proportions is the desire to obtain concrete with the following properties:

- Low elastic modulus

- Low strength (particularly at early ages)
- High creep
- Low early heat of hydration
- High tensile strain capacity

Of these characteristics, the low early strength, low elastic modulus, and high creep, were emphasized during the design of this mixture. However, due to the close relationship that many of these extensible properties have with each other, the remaining properties tend to consequently manifest themselves. For example, the low early heat of hydration, while not directly pursued through the use of Type IV cement (low early heat of hydration), was a consequence of the low early strength gain imparted to the mixture through the use of a high percentage of Class F fly ash.

CSA

The CSA mixture actually consisted of a 10% replacement, by weight, of the normal Type I/II cement used throughout the project with a calcium-sulfoaluminate admixture. This admixture was selected because Type K cements are not available in large quantities in the Austin area. The CSA mixture was consequently used as a surrogate for a similar Type K mixture.

In the presence of adequate reinforcement and sufficient curing, the CSA will function as a chemical prestressing agent in which the concrete expands during the first few days, thus putting the concrete into compression. The CSA mixture will still shrink like a normal concrete mixture, however, but because of this built-in compression the concrete is never subjected to tensile stresses that exceed the tensile capacity of the concrete.

The use of adequate reinforcement and curing is important since the successful application of these determines the success of the CSA mixture. If, for example, inadequate curing is provided, the CSA mixture will not expand enough to impart a compressive stress into the concrete. Adequate curing depends on the dosage rate of the CSA admixture, but at typical doses of 10% by weight a curing period of at least 7 days is required, since during this 7-day period is when the majority of the expansion takes place. Furthermore, adequate reinforcement must be present according to ACI 223. ACI 223 specifies a reinforcement ratio based on the expected maximum member expansion and the maximum restrained concrete prism expansion measured according to ASTM C878. The

reinforcement is required to ensure that enough internal restraint is created so that the concrete puts itself into compression evenly along the length of the slab or deck.

CSA Trial Mixtures

Due to the lack of experience with the particular CSA admixture used, it was necessary to perform trial tests in order to determine the percent expansion associated with a 10% dosage rate of CSA. When the CSA admixture is added to the cement at a 10% replacement by weight, the measured percent expansion was 0.069% after 4 days and 0.074% after 12 days. It is obvious that the CSA mixture will complete almost 95% of its expansion in the first 4 days. This underscores the importance of adequate curing during the first 7 days for the CSA mixture.

The trial tests were also performed to get an idea of slump loss as a function of the time delay of when the CSA admixture is added during the mixing process. From the trial mixtures it was determined that simply delaying the addition of the CSA admixture at a 10% replacement rate by about 9 minutes after the water is added to the cement will cause an absolute 0.026% drop in the expansion. This is a fairly large drop considering the normal percent expansion range for expansive hydraulic cement, according to ASTM C845, varies from 0.04% as a minimum and 0.1% as a maximum. Therefore, it was decided that the CSA should be added at the batch plant instead of at the job site to ensure adequate expansion.

SRA

The SRA mixture made use of a shrinkage reducing admixture dosed at 1.5 gallons per cubic yard of concrete. The shrinkage reducing admixture essentially attacks the shrinkage problem at its source: the loss of water from capillary pores less than 50nm in diameter and subsequent imparting of tensile stresses onto the hardened concrete capillary walls. SRA accomplishes this by lowering the surface tension of the trapped water so that when the water inevitably escapes from the smaller capillary pores (< 50 nm) it will not impart as large a tensile stress onto the capillary walls, and will prevent large shrinkage strains. However, the shrinkage-reducing admixture does not lower the amount of water lost, but rather lowers the ability of water to impart tensile stresses onto the concrete.

Fibers

The mixture with fibers consisted of 4 lbs synthetic structural fibers per cubic yard of concrete. The structural fibers do not prevent drying shrinkage from occurring, but rather limit the crack width by improving post-crack toughness and ductility. Although this dosage rate puts it near the “low-volume” classification of fiber reinforced concretes (1-1.5 lbs per cubic yard), the dosage rate is high enough so that crack widths will be smaller on average. This is as opposed to non-fiber concrete in which fewer cracks will form but each crack will have a larger average crack width. Smaller cracks are preferable because they are less likely to permit ingress of corrosive and harmful substances into the concrete.

5.5.3 Construction

The construction of the Phase II LSBDs was almost identical with that of the Phase I decks. The only differences were the use of fewer shear studs in the middle region and the increase in the number of threaded reinforcing bar at the end regions. Both of these changes, as mentioned previously, are meant to increase the crack width of any cracks that may form so that the cracks manifest themselves near the middle region of the LSBD.

5.5.4 Results and Discussion

Both the fresh and hardened properties of the six concrete mixtures tested during the Phase II portion of the project will be given below. The fresh properties consist solely of the slump and temperature while the hardened properties include the compressive strength, tensile strength, modulus of elasticity, free shrinkage, and restrained shrinkage (ring method).

Fresh Properties

The fresh concrete mixture properties for the Phase II LSBDs consist of the slump and temperature and appear below in Table 5.4 for each mixture.

Table 5.4 Fresh Properties for Phase II mixtures

Property	Mixture					
	Control	HVFA	HPC	CSA	SRA	STRUX
Initial Slump (in)	4	5	10	6	6	6
Initial Temperature (°F)	90	91	93	84	85	85

The initial slump values were all within an inch of each other, except for the HPC at 10 in. This relatively high HPC slump value is a consequence of the high dosage of superplasticizer required to ensure adequate workability and to account for slump loss between the pour site and the batch plant.

Concrete temperatures were consistent and were dependent on the daily temperature. The pours were intentionally scheduled for the morning hours to avoid high delivery temperatures and prevent faster set times.

Hardened Properties

The determination of the Phase II hardened properties is identical to those tests used to determine the hardened properties of the Phase I LSBDS.

Compression, Modulus, Tensile Strength (AASHTO T22, ASTM C469, AASHTO T198)

Measurements of the compressive (Figure 5.21) and tensile (Figure 5.22) strength were taken at 1, 7, and 28 days, while the modulus of elasticity (Figure 5.23) was taken at 1 and 28 days. It is ideal to take as many measurements as possible, but the focus of this project is on early-age drying shrinkage cracking and measurements beyond 28 days were not done. Unlike the Phase I measurement of the compression, modulus, and tensile strength, it was decided that one-day measurements would be more useful than three-day measurements and therefore, one-day measurements replaced the three-day measurements.

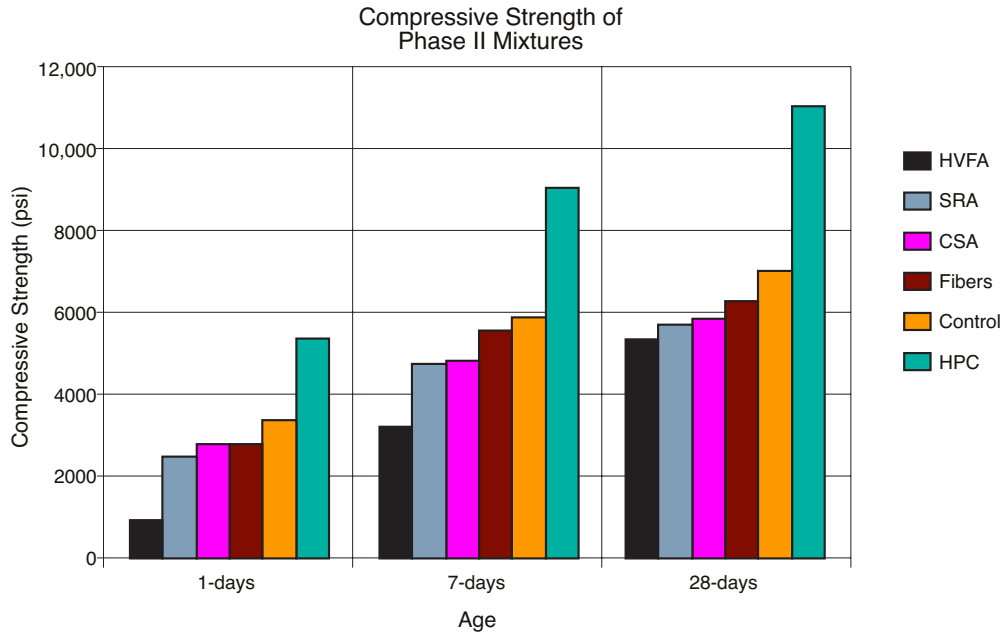


Figure 5.21 Compressive strength of the Phase II mixtures

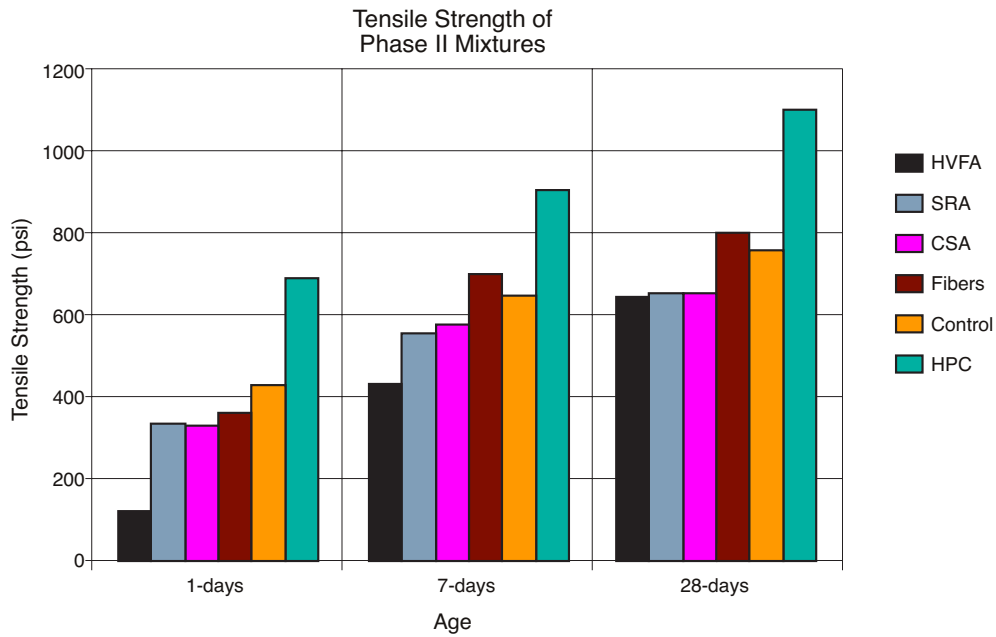


Figure 5.22 Tensile strength of Phase II mixtures

The compressive strengths of the various mixtures agree with initial expectations. For instance, HPC has a high-early compressive strength compared to the other mixtures due to its extremely low water-to-cement ratio. In fact, it reached over 11,000 psi by the

28th day, a relatively large compressive strength compared to the other mixtures. However, most important is the fact that the HPC mixture already had a compressive strength of approximately 5,300 psi after only one day. The second highest mixture in terms of compressive strength after one day of curing is the control mixture with a compressive strength of approximately 3,300 psi. This relatively high early strength, and the subsequent high early tensile strength, is one of the primary reasons that these two mixtures eventually cracked in a manner indicative of drying shrinkage cracking. The remaining mixtures had average one-day strengths in the neighborhood of 2,600 psi. An exception to this was the HVFA mixture with a one-day compressive strength of 921 psi. The low early strength of the HVFA is indicative of one of the many beneficial properties associated with an extensible concrete, mainly a low early strength and low modulus of elasticity. The low early strength and the low modulus of elasticity are due to the 55% replacement by weight of cement with Class F fly ash.

Of particular interest are the rates at which these various mixtures gain strength, both compressive and tensile, as well as the corresponding modulus of elasticity as a function of time. Even though HVFA started out low with the lowest one-day compressive strength, lowest one-day tensile strength, and lowest one-day modulus, it actually gained the most relative compressive strength compared to any of the other mixtures between the 1st and 28th days. In fact, HVFA gained over 480% of its original one-day compressive strength by the 28th day. It also gained about 440% of its original one-day tensile strength by the 28th day. However, HPC had one of the lowest relative compressive and tensile strength increases between the 1st and 28th days with relative gains of 105% compressive and 60% tensile strength. This demonstrates the effect that strength gain has on the susceptibility to drying shrinkage cracking. The strength of a mixture should not be treated as a time-independent quantity when considering drying shrinkage cracking.

It is not just the value of the strength, but when the strength develops, that is important, since strength gain has a large role in the resistance to drying shrinkage cracking. Thus, even though HVFA may have a relatively high strength gain between the 1st and 28th day, it is the fact that the initial relative strength gain of the HVFA was low during the first few days compared to the HPC, which had to go from zero to 5,300 psi in only one day, a 5,300% increase. The same is true for the HPC tensile strength, which

went from 0 to 690 psi in only one day. The fact that both the control and the HPC had the highest one-day tensile strengths and that both these mixtures ended up cracking while in the LSBs in a manner indicative of drying shrinkage cracking is not coincidental. Furthermore, the modulus of elasticity for both the HPC and control mixtures was the highest of any of the Phase II mixtures. Their modulus values were about 4,800 ksi and 4,000 ksi, respectively. Extensible concretes are ideal for drying shrinkage crack resistance because the majority of the strength and modulus gain take place later in the concrete's life, not during its initial few days when the tendency to shrink is at its highest.

Delayed strength and modulus gain is ideal for resisting drying shrinkage cracking because the majority of the drying shrinkage or water loss takes place during first few weeks of the concrete's life. Consequently, a high initial modulus means that any shrinkage will manifest itself into a higher tensile strain. As the concrete loses moisture during its first few days, it will attempt to shrink and since the concrete is already relatively "stiff" it will be more likely to form fewer but larger cracks in one location than for a concrete that has a lower "stiffness." This is because the stress concentrations at preexisting flaws in the concrete will be larger and crack propagation is more likely to occur when a concrete has a high modulus (i.e., is relatively stiff). The lower stiffness concrete will still have preexisting flaws or cracks in it, just like all concrete, but the cracking will be distributed more evenly and the stress concentrations will not be as high at a flaw and the severity of cracking will not be as large.

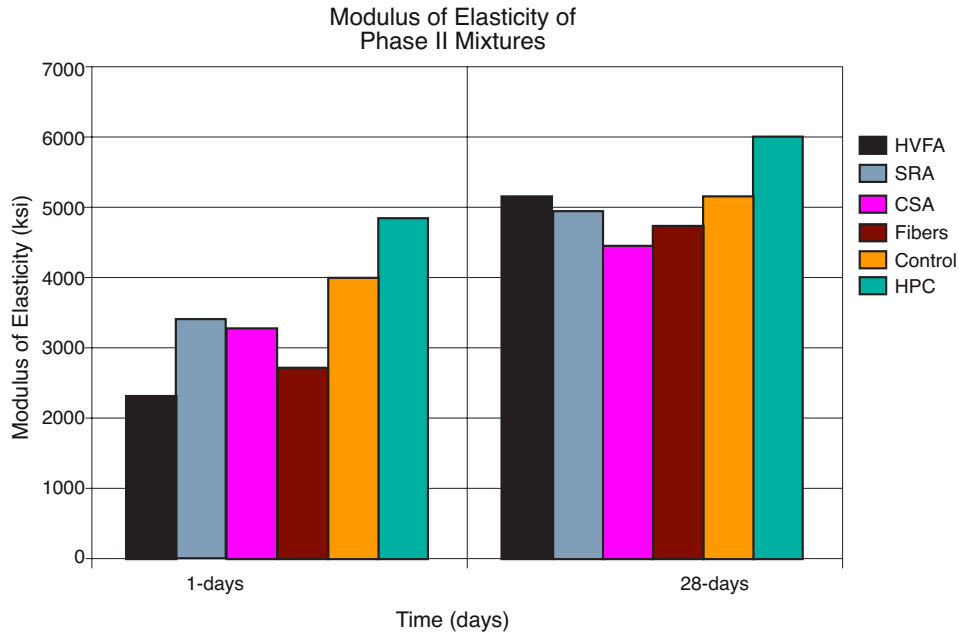


Figure 5.23 Modulus of Elasticity for Phase II mixtures

An interesting behavior is that from the mixture with synthetic fibers. If one were to only use the tensile strength as an indication of the propensity for cracking then it appears that by the 7th day the fibers mix has a higher tensile strength than the control mix and therefore, should be expected to crack based on the cracking behavior of the control and HPC mixtures, which also have high early tensile strengths. However, looking at the modulus of elasticity graph, the fibers mix has the second lowest modulus value. Even though the fibers mixture may have an apparently high tensile strength and therefore should have a relatively high modulus value, but does not, is because of the fibers themselves. Based on literature, synthetic fibers generally have a negligible effect on strength and elastic modulus, especially at the low dosage rate used for this mixture, until the concrete cracks in the surrounding region. The fibers act as bridges across onto which stresses may be placed only after the concrete has cracked. The fibers also act as a secondary defense against the manifestation of drying shrinkage cracking by distributing the stresses that build up around an existing crack or flaw in the concrete. The fibers behave as a second line of defense to limit crack propagation because they help to distribute the stresses in the concrete around existing cracks so that the cracks stay relatively small.

Free Shrinkage (AASHTO T160)

The free shrinkage of the Phase II innovative material specimens represents an opportunity to determine how much a mixture will shrink due only to moisture loss. Each Phase II mixture had three free shrinkage specimens that were kept in the temperature and moisture controlled shrinkage room, and three identical free shrinkage specimens kept outside on their respective LSBDs.

Measurement of the free shrinkage specimens kept outside was crucial to the consistency of the results. At least 1.5 hours of cooling or warming time was provided so that the shrinkage specimens could reach the shrinkage room's constant ambient temperature before measurement to avoid including any length change due to temperature effects.

Plots of each mixture's free shrinkage strain as a function of age are given below in Figures 5.24 through 5.28. It is important to point out that the CSA mixture actually made use of a restrained expansion test (ASTM C878 – Standard Test Method for Restrained Expansion of Shrinkage-Compensating Concrete) due to the expansive nature of the admixture. The results for the CSA mixture are included in the shrinkage graphs for convenience, even though the tests do not have a direct correspondence.

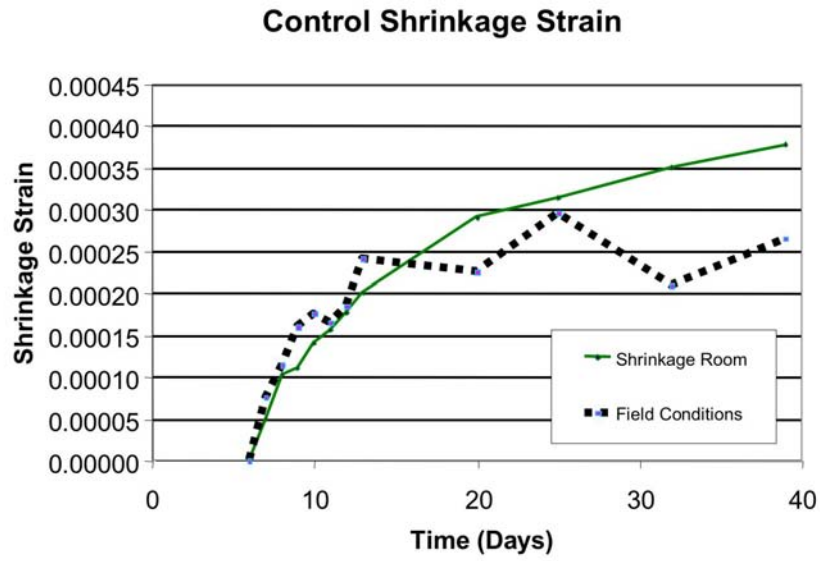


Figure 5.24 Free shrinkage strain for Phase II Control

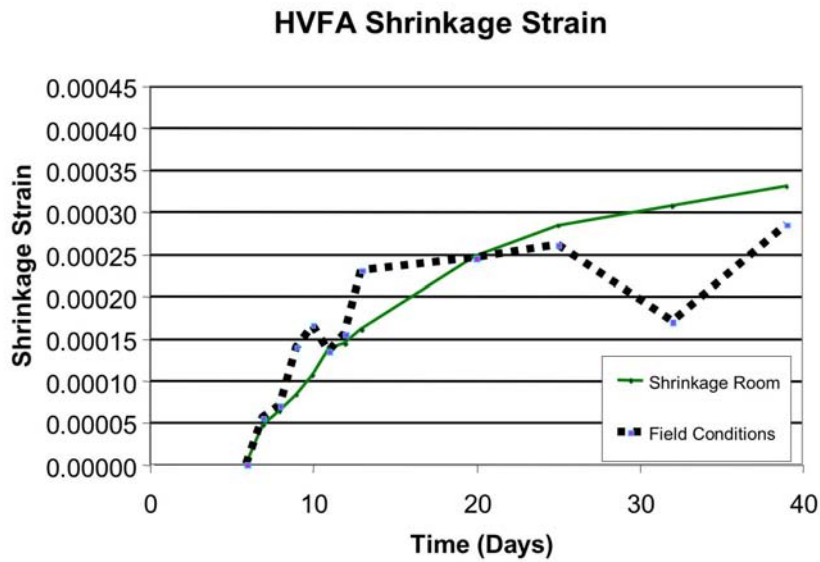


Figure 5.25 Free shrinkage strain for Phase II HVFA

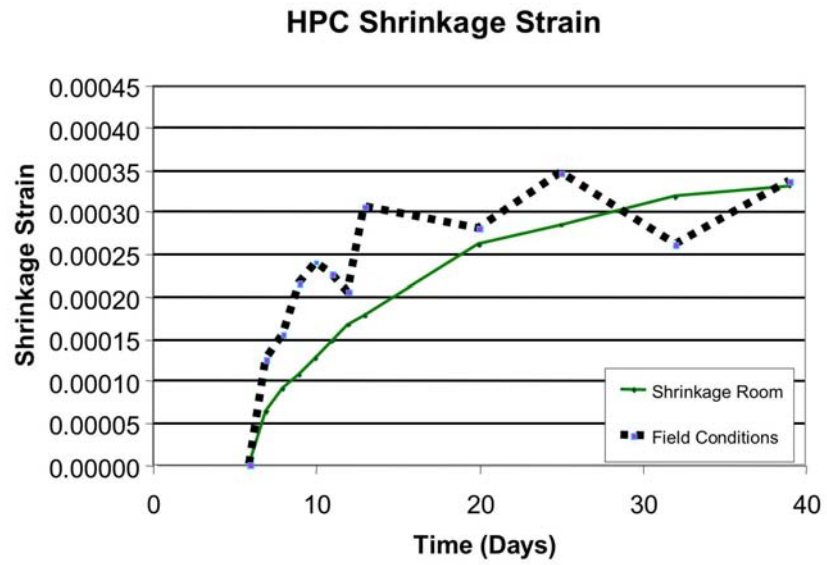


Figure 5.26 Free shrinkage strain for Phase II HPC

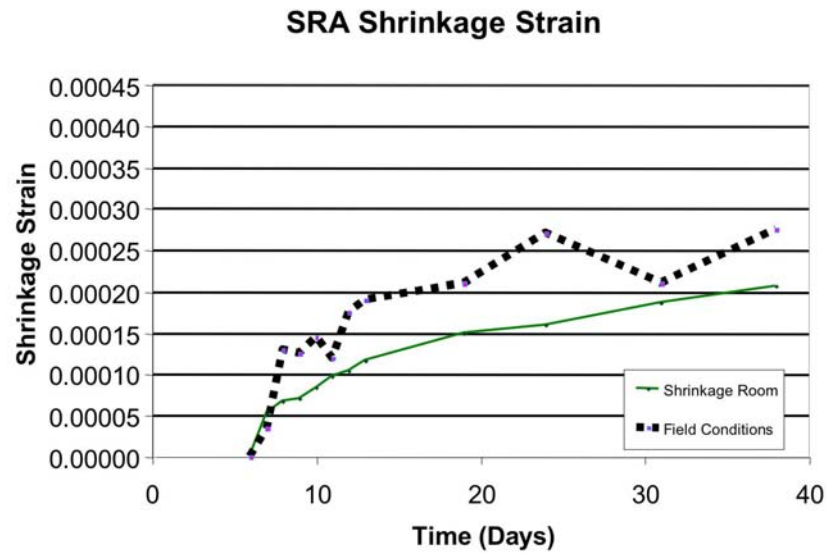


Figure 5.27 Free shrinkage strain for Phase II SRA

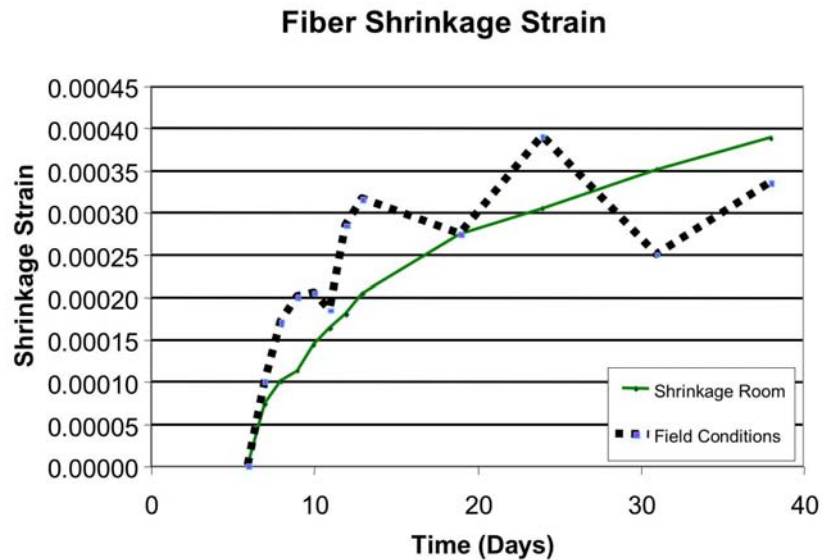


Figure 5.28 Free shrinkage strain for Phase II Fiber

The effect of the CSA expansive cement admixture is evident in both the field and shrinkage room exposure conditions. The fact that the CSA mixture has positive shrinkage values means that it has expanded from its original gage length. However, comparing the slope of the shrinkage versus time plot for the CSA mixture with the remaining five mixtures it is evident that the CSA mixture shrinks just as much as the other mixtures do. This illustrates the importance of ensuring proper curing methods are practiced, especially in the case of the CSA. The expansive nature of the CSA admixture will not occur as expected if improper curing methods are used, such as the failure to cure for an extended period of time or failure to maintain a constant level of curing.

The SRA mixture has a smaller overall shrinkage amount compared to the other mixtures, but only for the specimens kept in the moisture and temperature controlled shrinkage room. However, SRA failed to provide a lower shrinkage value when subjected to the field conditions. The discrepancy between the results is most likely a result of fluctuating moisture conditions such that water loss from the specimen is not as consistent,

nor as large, as that found in the shrinkage room since the average overall shrinkage for SRA was lower for the field condition specimens.

A clear pattern in the variability in shrinkage values between the field conditions and the shrinkage room conditions for each of the remaining specimens is difficult to identify. For some mixtures, such as the Control, HVFA, and CSA, the shrinkage associated with the field conditions is usually smaller than the shrinkage associated with the shrinkage room. However, for the HPC, SRA, and the Fibers mixtures the opposite is true so that the shrinkage room shrinkage values are smaller than for the field condition case specimens.

One general trend is true, however, between the field and the shrinkage room exposure conditions. The specimens exposed to field conditions shrink faster during the first 3 days of initial exposure, no matter what the mixture was. The shrinkage prism tests were conducted so that each shrinkage prism bar was given exactly 7 days of full limewater immersion curing. After this initial 7-day wet cure the specimens were either placed outside on the bridge decks (field conditions) or placed in the shrinkage room.

Overall, the free shrinkage results provided useful information for the shrinkage tendency of the various innovative mixtures and serve as a good relative comparison between the different mixtures. Knowing only the free shrinkage and nothing else will not provide adequate information to predict the shrinkage tendencies of various mixtures. Free shrinkage is just one of several hardened concrete tests that must be performed in order to obtain a clear picture of the probability for drying shrinkage cracking.

Restrained Shrinkage (Ring Method, AASHTO PP34-99)

The restrained shrinkage or “ring method” (AASHTO PP34-99 – Standard Practice for Estimating the Cracking Tendency of Concrete) was developed to estimate the cracking tendency of concrete. It serves only as a way to relatively compare the various mixture’s time-to-cracking. The test does not provide an absolute time to cracking value.

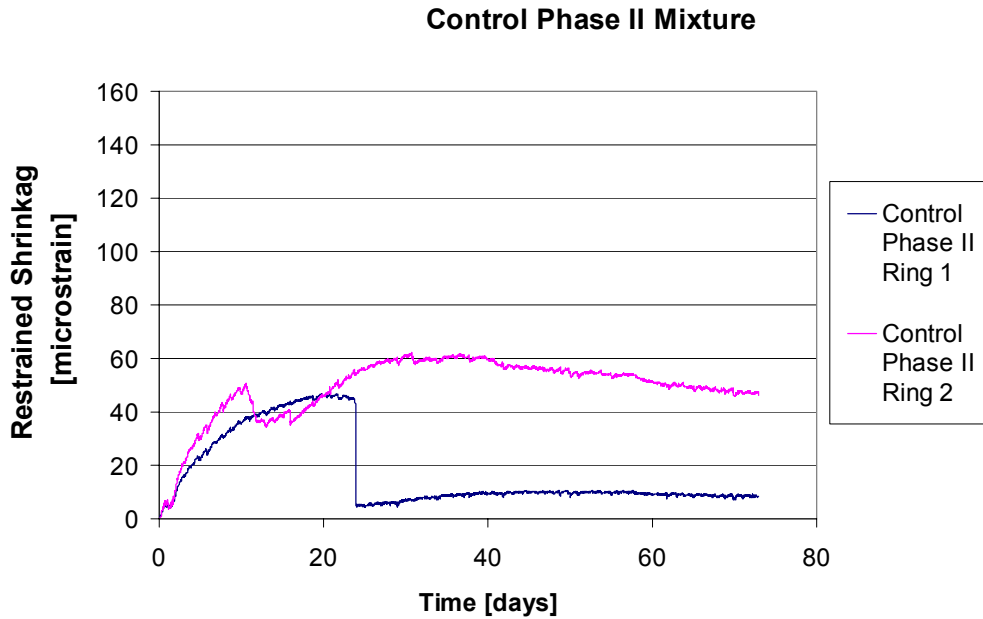


Figure 5.29 Restrained shrinkage strain gage output for Control Phase II

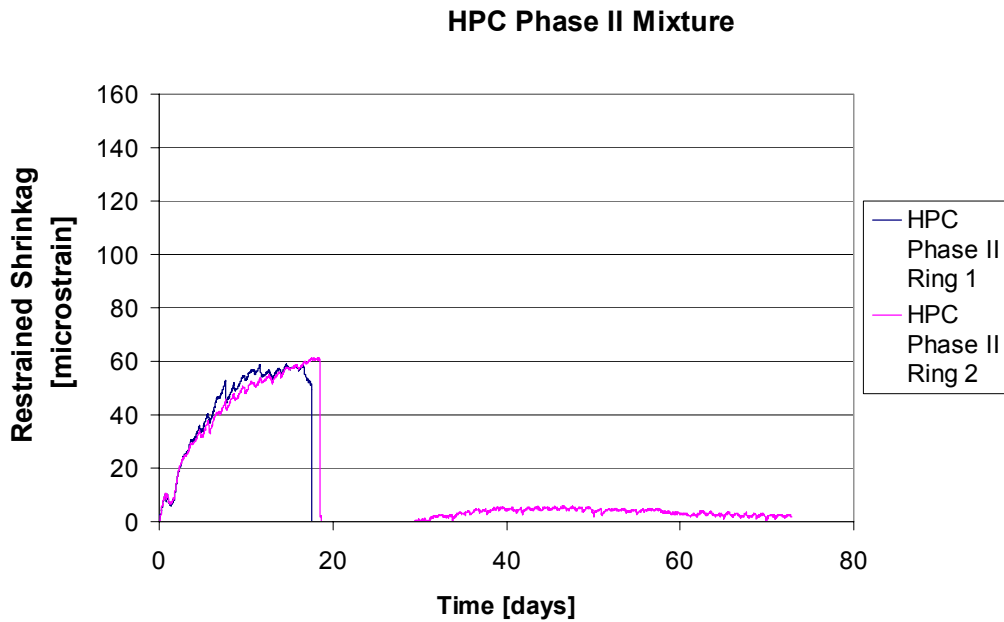


Figure 5.30 Restrained shrinkage strain gage output for HPC Phase II

The restrained shrinkage rings performed well during the Phase II portion of the project. Figure 5.29 and Figure 5.30 provide the strain gage output for both HPC and Control Phase II mixtures. For example, both HPC rings cracked within a day of each

other, an improvement in the repeatability of the shrinkage ring results compared to the laboratory program repeatability. Furthermore, the Control rings cracked within 8 days of each other. The remaining four mixtures, HVFA, CSA, SRA, and Fibers, did not crack up to the last measurement taken after 60 days and therefore the corresponding strain gage output is not shown.

Finally, the fact that both the HPC and Control were the only Phase II LSBDs to exhibit drying shrinkage cracking while the corresponding HPC and Control restrained shrinkage rings were the only restrained shrinkage rings to crack at all, is indicative of the potential of the restrained shrinkage ring test to successfully predict a mixture's potential for shrinkage cracking. The distinction here is the probability for cracking is higher. Nothing can be said with significant certainty when the crack will occur.

The key to using the restrained shrinkage ring test method successfully is to run as many ring tests simultaneously as possible while making sure that each ring specimen is consistent in its tolerances and uniform in the dimensions. Further study is still necessary to determine what factors of the ring construction and implementation significantly affect the results.

5.5.5 Instrumentation

The instrumentation of the Phase II LSBD was exactly like that of Phase I. However, instead of six temperature probes per bridge deck, only five temperature probes were used. The location of the five temperature probes were identical to the Phase I decks, with the probe on the right end of the deck being removed. Similarly, the initial heat of hydration was recorded for each bridge deck. The complete pour of all six LSBDs took place over two days. Control, HVFA, and HPC, in that order, were poured on the first day. CSA, SRA, and Fibers were poured on the second day, in that order. The temperature values for the first day of the Phase II LSBD pour are plotted in Figure 5.31 for one single point in the bridge deck. It was decided to use one point in the bridge deck instead of averaging all five locations of the temperature probes due to the effect of differing volumes of concrete surrounding the temperature probe. The temperature probe with the most volume of concrete surrounding it was used. Similarly, the temperature values for the second day of the Phase II LSBD pour are plotted in Figure 5.32. These second-day temperature values are also taken at a single point in the bridge deck for the reasons discussed previously.

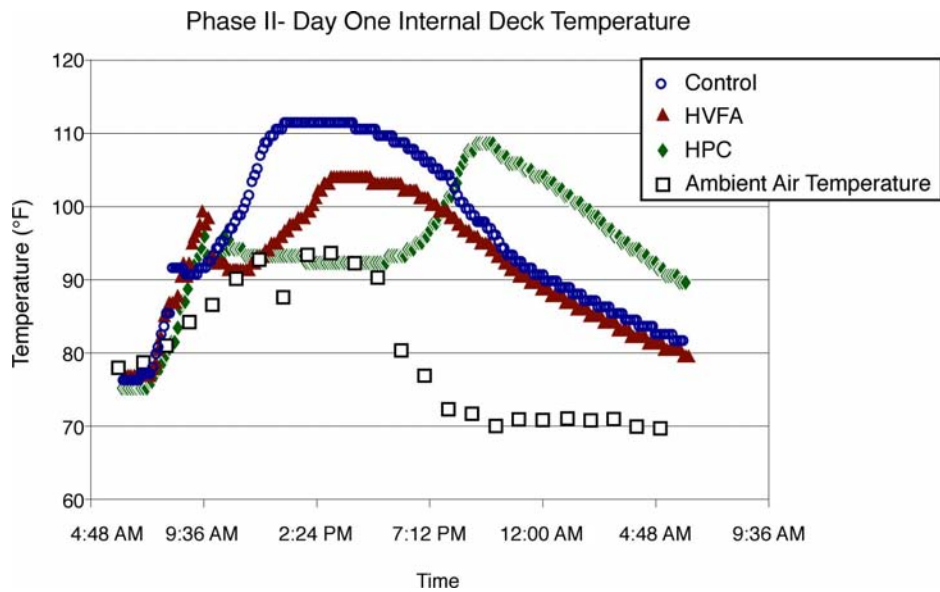


Figure 5.31 Internal deck temperature for Phase II LSBs on the first day of pouring from 6:00 a.m. on the day of the pour to 6:00 a.m. the next day

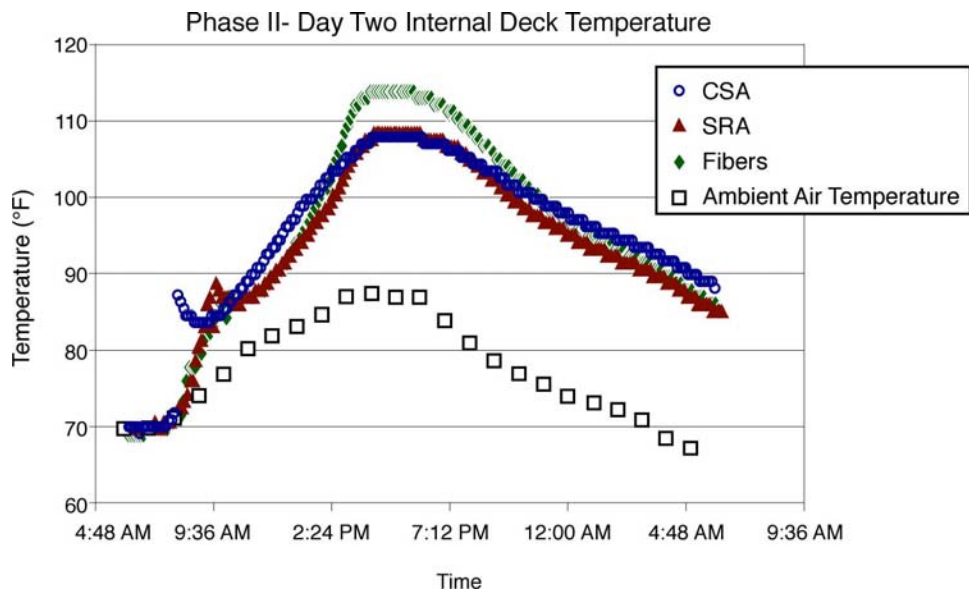


Figure 5.32 Internal deck temperature for Phase II LSBs on the second day of pouring from 6:00 a.m. on the day of the pour to 6:00 a.m. the next day

No unexpected or abnormal results were observed in terms of the temperature readings. The highest heat of hydration values occurred in the HPC, Control, and Fibers mixtures, as expected. The high heat of hydration for HPC, however, was delayed

compared to the other LSBD mixtures due to the high level of high range water reducers (HRWR) present in the mixture. HPC's high heat of hydration is due to the high cement content of the HPC mixture.

5.5.6 Cracking

The observed crack patterns appear in Figures 5.33 and 5.34 and represent the general crack pattern observed. The pictures do not represent the crack width nor do they account for every single crack that is present.

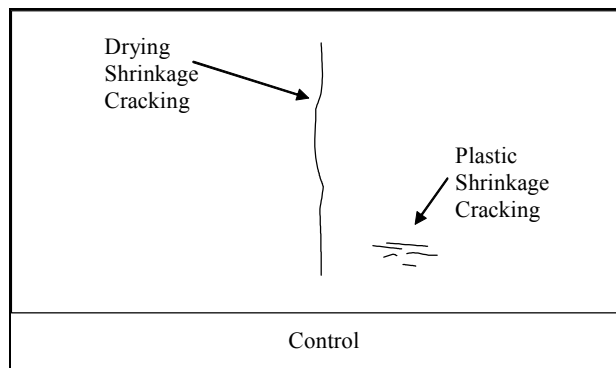


Figure 5.33 Observed cracking of Control LSBD

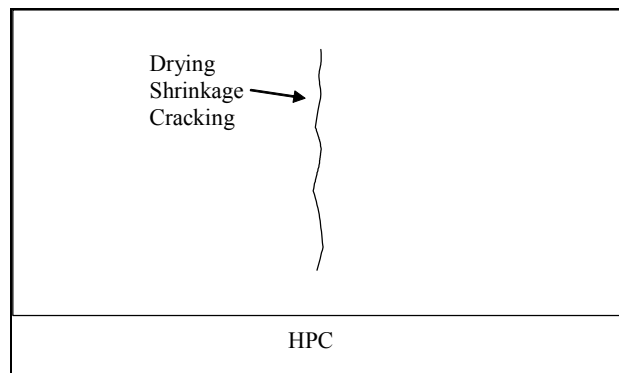


Figure 5.34 Observed cracking for HPC LSBD

Of the six bridge decks poured for the Phase II LSBD, two of them cracked in a manner representative of drying shrinkage cracking. These two decks, control and HPC, both cracked in the transverse direction within 16 days of the pour date. The first drying shrinkage cracks for both decks appeared at the center of the deck, right above where the two PCPs meet at the center. The cracking started in the center and propagated out over

the next few weeks along the transverse direction. This cracking location was expected for two reasons. First, there is an incongruity where the two PCP meet at the center. Because discontinuity causes a stress concentration cracking is more likely to appear in this area. Second, the distribution of restraint was design so that the least restraint is at the center of the deck and the most restraint is found at the ends.

It is obvious from the crack patterns on some of the bridge decks that plastic shrinkage cracking was a problem. Therefore, a discussion of plastic shrinkage cracking will be undertaken.

Plastic Shrinkage Cracking

Unfortunately, plastic shrinkage occurred in several of the Phase II bridge decks. This is most likely due to the lack of experience with the effects that various innovative materials have the initial set time, bleed rate, and subsequent moisture loss during the first 24 hours. Cotton curing mats were placed on the decks not more than 1.5 hours after the pour was completed for each bridge deck. Most likely, a lack of experience with the behavior of these innovative materials as to when to begin curing the decks caused the majority of the plastic shrinkage cracks. Luckily, these cracks are only surface cracks and are not expected to affect a bridge deck's affinity for drying shrinkage cracking. It does, however, introduce an avenue for further study, since the plastic shrinkage cracking of many of these materials has not been performed in depth and is relatively unknown.

5.5.7 Conclusions

The battle against early-age drying shrinkage cracking can be approached from many angles. Understanding the basic mechanics of drying shrinkage allows the researcher to hone in on the most promising methods of imparting drying shrinkage crack resistance into concrete bridge decks. Drying shrinkage can be approached from two basic perspectives: proactive or reactive. A proactive stance, such as that provided by shrinkage-reducing admixture, treats drying shrinkage before it even begins by impeding the actual mechanism of drying shrinkage: loss of water from smaller capillary pores.

A reactive stance, on the other hand, treats the symptoms of drying shrinkage, so that when drying shrinkage inevitably occurs it will not manifest itself into significant cracking and jeopardize the durability of the bridge deck. Mixtures such as the fibers, CSA, and

HVFA fall into this category since they do nothing to impede drying shrinkage, but rather impede the manifestation of cracking. Each reactive mixture does this in a unique way. For example, the CSA chemically prestresses the concrete so that the net shrinkage is negative and the relatively weak tensile strength of concrete is never exceeded. A fibers mixture will still allow shrinkage to occur but the resultant cracking is spread out, and reduces the manifesting of cracking by limiting crack size. Finally, the HVFA mixture imparts the properties of concrete that help to limit stress buildup, such as high creep, low early strength, and low modulus of elasticity, to the mixture so that stress concentrations around flaws are avoided and crack sizes are minimized.

Whether the problem is approached proactively or reactively, the end result should be the same: the mitigation of drying shrinkage cracking so that the durability of the concrete bridge decks is preserved. To this end, the innovative materials mixtures of SRA, CSA, fibers, and HVFA performed well, since they effectively limited cracking due to drying shrinkage. Specifying one innovative material over the other involves a holistic analysis of various other factors such as availability and cost of materials, handling precautions, and ease of use. However, to mitigate early-age drying shrinkage cracking in concrete bridge decks, it was determined that the use of SRA, fibers, HVFA, and CSA represents viable methods of reducing restrained drying shrinkage cracking.

6. Conclusions and Recommendations for Future Research

6.1 Conclusions

This report addresses all the major aspects of the entire project, including an in-depth state-of-the-art literature review, a comprehensive reporting and analysis of the final laboratory program test results, a description of the design and construction of the large-scale bridge decks (LSBDs) used to ascertain the drying shrinkage crack resistance of various innovative materials, and the analysis of the LSBD mixtures for drying shrinkage crack resistance.

As far as laboratory testing goes, free shrinkage of concrete (AASHTO T160), restrained shrinkage (AASHTO PP34-99), and early-age strength properties, specifically compression (AASHTO T22), tension (AASHTO T198), and modulus of elasticity (ASTM C469) testing are highly recommended for determining the propensity for drying shrinkage cracking of concrete. An individual test by itself will not provide sufficient information as to whether a certain concrete mixture will have a high or low propensity for drying shrinkage cracking. However, the combination of results from all of these laboratory tests will enable one to determine the relative susceptibility to drying shrinkage cracking. An ideal drying shrinkage resistant mixture is one in which no restrained rings crack, a relatively low free shrinkage strain, and extensible concrete strength properties such as a low initial modulus of elasticity value combined with low initial tensile and compressive strengths. Specific limits, such as how much free shrinkage is permissible or the highest modulus value possible, are difficult to prescribe due to the complexity of their interaction. Instead, the decision should be based on the overall outcome of the recommended tests.

In order to provide the best resistance to drying shrinkage cracking in concrete bridge decks it is recommended that a mixture proportioned similarly to that of SRA, fibers, CSA, or HVFA be used. No mixture from these four mixtures is an obvious first choice for mitigating restrained drying shrinkage cracking since an in-depth look at the other variables, such as cost, handling and use issues, or the availability of materials, were not performed.

6.2 Improvements in the Laboratory Program

From the perspective of the laboratory testing methods, several improvements can be made that would enhance the accuracy of the readings. These include better creep frames, improvement in the repeatability of the restrained shrinkage tests, and further investigation into the effect of moisture conditions on drying shrinkage.

Better creep frames are necessary to obtain more reliable creep results. The creep frame setup used during the laboratory program did not allow the researcher to measure the actual applied load values, nor did it permit readjustment of the applied load after the initial loading. Therefore, once the creep frame was hydraulically jacked to the correct load and locked in place, it was impossible to know what load the specimens in the creep frame were actually experiencing. To solve the load accuracy problem with the creep frames it is recommended that new creep frames be used in which small adjustments in load can be made while the specimen is in place and the current applied load can be determined easily.

To improve the repeatability of the restrained shrinkage test it is recommended that more attention be paid to the uniformity and placement of the shrinkage ring mold so that a uniform amount of concrete is present. It is also recommended that more than two ring specimens per concrete mixture be made so that a clearer trend in the time-to-cracking can be determined.

Further research into the effect of different moisture conditions (relative humidity) on the shrinkage tendencies of concrete is desired. For instance, in addition to having free shrinkage specimens in both an environmentally controlled chamber (shrinkage room) and the outside, it would be helpful to have specimens that are subjected to different values of relative humidity while all at the same temperature. Likewise, doing a similar thing with the restrained ring specimens would enable one to observe the effect that various values of relative humidity have on the time-to-cracking.

6.3 Improvements in the Large-Scale Bridge Decks

Improvements to the LSBDD setup include the use of strain gages within the concrete to get a picture of the strains occurring in the deck prior to cracking. This would permit the experimenter to get an idea of the strains involved before and after a drying shrinkage crack occurs.

The most promising avenue for further research using the LSBDD format is to investigate the effect of PCP placement and alignment on the drying shrinkage cracking of concrete. This would be an appropriate extension to this project, since the majority of drying shrinkage cracking observed on both the LSBDDs and the bridges considered during the shrinkage cracking survey exhibited drying shrinkage cracking that followed the outline of the PCP in a fairly regular pattern. The fact that the bridge deck cracking created a visible outline of the underlying PCP indicates that the shape or alignment of the PCP has an effect on the manifestation of drying shrinkage cracks.

6.4 Recommendation for Implementation

The next logical step after the large-scale bridge decks is to perform an implementation study in which each innovative material mixture is placed in a separate span of a multispan bridge deck. An ideal candidate for a bridge deck would consist of a multispan bridge deck that can be instrumented and monitored for the long-term. This would allow each of the innovative materials to be utilized and analyzed in a realistic environment. It is highly recommended that an implementation study be undertaken in which a multispan concrete bridge deck is constructed using all eight laboratory mixtures in order to evaluate their resistance to drying shrinkage cracking under actual conditions.

References

1. ACI Committee 209, "Prediction of Creep, Shrinkage, and Temperature Effects in Concrete Structures," ACI 209R-92, American Concrete Institute, 1999.
2. ACI Committee 223, "Standard Practice for the Use of Shrinkage Compensating Concrete," ACI 223-98, American Concrete Institute, 1998.
3. Altoubat, S. and Lange, D. "Early thermal changes," Report of RILEM Technical Committee 181-EAS, edited by A. Bentur, (RILEM Publications, France), 1 Vol., 1995.
4. Bloom, R., and Bentur, A., "Free and Restrained Shrinkage of Normal and High-Strength Concretes," ACI Materials Journal, Vol. 92, No. 2, March–April 1995.
5. Bouzoubaâ, N., Zhang, M.H., Bilodeau, A., and Malhotra, V.M., "Mechanical Properties and Durability of Concrete Made with High Volume Fly Ash Blended Cements," Fly-Ash, Silica Fume, and Slag, CANMET, Vol. I, pp. 449–474, 1998 (ed.: V.M. Malhotra).
6. Breitenbücher, R., "Investigation of Thermal Cracking with the Cracking Frame," Materials and Structures, Vol. 23, pp. 172–177, 1990.
7. Brown, Mike. "Evaluation of Innovative Materials to Control Restrained Drying Shrinkage Cracking in Concrete Bridge Decks." Masters Thesis. The University of Texas at Austin. August, 2002.
8. Burrows, R.D., The Visible and Invisible Cracking of Concrete, American Concrete Monograph No. 11, 1998.
9. Folliard, K.J., and Berke, N.S., "Properties of High-Performance Concrete Containing Shrinkage-Reducing Additives," Cement and Concrete Research, Vol. 24, No. 3, pp. 424–432, 1997.
10. Folliard, K.J., Ohta, M., Rathje, E., and Collins, P., "Influence of Mineral Admixtures on Expansive Cement Mortars," Cement and Concrete Research, Vol. 27, No. 3, pp. 424–432, 1994.
11. Folliard, K.J., and Simpson, B.T., "Low-Volume Polymeric Fiber-Reinforced Concrete Containing Shrinkage-Reducing Additives," Cement and Concrete Research, Vol. 27, No. 9, pp. 1357–1364, 1999.
12. Guo, X.H, and Gilbert, R.I., "The Effect of Specimen Size on the Fracture Energy and Softening Function of Concrete," Materials and Structures, Vol. 33, pp. 309-316, 2000.
13. Grzybowski, M., and Shah, S.P., "Shrinkage Cracking of Fiber-Reinforced Concrete," ACI Materials Journal, 138–147, March–April 1990.

REFERENCES

14. Kosmatka, Steven H., and Panarese, William C., "Design and Control of Concrete Mixtures," Portland Cement Association, Skokie, Ill. 1988.
15. Kovler, K., Sikuler, J., and Bentur, A., "Restrained Shrinkage Tests of Fibre-Reinforced Concrete Ring Specimens: Effect of Core Thermal Expansion," *Materials and Structures*, Vol. 26, pp. 231–237, 1993.
16. Krauss, P.D., and Rogalla, E.A., "Transverse Cracking in Newly Constructed Bridge Decks," National Cooperative Highway Research Program (NCHRP) Report 380, Transportation Research Board, 1996.
17. Mehta, P.K., and Monteiro, P., *Concrete – Structure, Properties, and Materials*, The McGraw-Hill Companies, Inc., New York, 1993.
18. Paillere, M., Buil, M., and Serrano, J.J., "Effect of Fiber Addition on the Autogenous Shrinkage of Silica Fume Concrete," *ACI Materials Journal*, Vol. 86, No. 2, March–April 1989.
19. Pittman, D.W., Ramey, G., Webster, G., and Carden, A., "Laboratory Evaluation of Concrete Mixture Designs Employing Type I and Type K Cement," *Journal of Materials in Civil Engineering*, Vol. 11, Issue 2, pp. 144–150, 1999.
20. Poston, R.W., Kesner, K.E., Emmons, P.H., and Vaysburd, A.M., "Performance Criteria for Concrete Repair Materials," Technical Report REMR-CS-57, U.S. Army Corps of Engineers, 1998.
21. Sellers, Greg. "The Use of Innovative Materials to Control Restrained Shrinkage Cracking in Concrete Bridge Decks." Masters Thesis. The University of Texas at Austin. May, 2002.
22. Shah, P.S., Marikunte, S., Yang, W., and Aldea, C., "Control of Cracking with Shrinkage-Reducing Admixtures," *Transportation Research Record*, 1574, pp. 25–36, 1997.
23. Springenschmid, R., *Thermal Cracking in Concrete at Early Ages*, E&FN Spon, London, 1994.
24. Tan, K., and Gjordv, O., "Performance of Concrete Under Different Curing Conditions," *Cement and Concrete Research*, Vol. 26, No. 3, pp. 355–361, 1996.
25. Weiss, W.J., Yang, W., and Shah, S.P., "Shrinkage Cracking – Can it be Prevented?" *Concrete International*, pp. 51–55, April 1998.
26. Weiss, W.J., Yang, W., and Shah, S.P., "Shrinkage Cracking of Restrained Concrete Slabs," *Journal of Engineering Mechanics*, Vol. 124, pp. 7–12, 1998.
27. Whiting, D., and Detwiler, R., "Silica Fume Concrete for Bridge Decks," NCHRP Report 410, Transportation Research Board, 1998.

28. Wiegrink, K., Marikunte, S., and Shah, S., "Shrinkage Cracking of High-Strength Concrete," *ACI Materials Journal*, Vol. 93, No. 2, September–October 1996.

